A COMBINATORIAL APPROACH TO KNOT THEORY: VOLUME BOUNDS FOR HYPERBOLIC SEMI-ADEQUATE LINK COMPLEMENTS

By

Adam Joseph Giambrone

A DISSERTATION

Submitted to
Michigan State University
in partial fulfillment of the requirements
for the degree of

Mathematics - Doctor of Philosophy

2014

ABSTRACT

A COMBINATORIAL APPROACH TO KNOT THEORY: VOLUME BOUNDS FOR HYPERBOLIC SEMI-ADEQUATE LINK COMPLEMENTS

By

Adam Joseph Giambrone

An interesting goal in knot theory is to discover how much geometric information about a link can be carried by a representative projection diagram of that link. To this end, we show that the volumes of certain hyperbolic semi-adequate links can be bounded above and below in terms of two diagrammatic quantities: the twist number and the number of special tangles in a semi-adequate diagram of the link. Given this result, we then narrow our focus to families of plat closures, families of closed braids, and families of links that have both plat and closed braid aspects. By more closely studying each of these families, we can often improve the lower bounds on volume provided by the main result. Furthermore, we show that the bounds on volume can be expressed in terms of a single stable coefficient of the colored Jones polynomial. By doing this, we provide new collections of links that satisfy a Coarse Volume Conjecture. The main approach of this entire work is to use a combinatorial perspective to study the connections among knot theory, hyperbolic geometry, and graph theory.

ACKNOWLEDGMENTS

I would like to begin by thanking my adviser, Efstratia Kalfagianni, for her unwavering support and guidance throughout my graduate career. I would also like to thank my mother, Diane Giambrone, for being a continual source of encouragement and perspective. Finally, I would like to thank my friends and colleagues David Bramer, Joshua Hallam, Faramarz Vafaee, and Luke Williams for joining me in this adventure.

TABLE OF CONTENTS

LIST OF FIGURES

KEY TO SYMBOLS AND ABBREVIATIONS

$\subseteq$	subset
K	a link
S^3	the 3-sphere
$D(K)$	a diagram of a link K
S^2	the 2-sphere
h_t	a homeomorphism from S^3 to itself
H_A	the all-A state associated to the link diagram $D(K)$
$\mathbb{G}_A$	the all-A graph associated to the link diagram $D(K)$
$\mathbb{G}'_A$	the reduced all-A graph associated to the link diagram $D(K)$
$v(\mathbb{G}'_A)$	the number of vertices in $\mathbb{G}'_A$
$e(\mathbb{G}_A)$	the number of edges in $\mathbb{G}_A$
$e(\mathbb{G}'_A)$	the number of edges in $\mathbb{G}'_A$
$\chi(\mathbb{G}'_A)$	the Euler characteristic, $v'_A - e'_A$, of $\mathbb{G}'_A$
$\chi_-(\cdot)$	the negative part, $\max\{-\chi(\cdot), 0\}$, of the Euler characteristic of $\cdot$
$t(D)$	the number of twist regions in $D(K)$
TELC	two-edge loop condition
$T(1, s)$	a tangle sum of a vertical one-crossing twist region and a vertical short twist region
$T(s_1, s_2)$	a tangle sum of two vertical short twist regions
$T(l, s)$	a tangle sum of a horizontal long twist region and a vertical short twist region
$st(D)$	the number of special tangles in $D(K)$

$S^3\backslash K$	the complement of the link K in S^3
S_A	the all-A surface of the link diagram $D(K)$
v_8	the volume, $3.6638\ldots$, of a regular ideal octahedron
v_3	the volume, $1.0149\ldots$, of a regular ideal tetrahedron
$\partial(\cdot)$	the boundary of $\cdot$
$\text{int}(\cdot)$	the interior of $\cdot$
M_A	the 3-manifold, $S^3\backslash\backslash S_A$, formed by cutting S^3 along S_A
$\text{guts}(M_A)$	the guts of M_A, which can be thought of as the "hyperbolic pieces" of the annular JSJ Decomposition of M_A
$J_K^n(t)$	the n^{th} colored Jones polynomial
β_n'	the penultimate coefficient of the n^{th} colored Jones polynomial of the link K
β_K'	the stable penultimate coefficient of the colored Jones polynomial of the link K
$t_1(D)$	the number of one-crossing twist regions in $D(K)$
$t_{\geq 2}^{\text{short}}(D)$	the number of short twist regions in $D(K)$
$t_{\geq 2}^{\text{long}}(D)$	the number of long twist regions in $D(K)$
$e_{\geq 2}^{\text{long}}(\mathbb{G}_A')$	the number of edges in $\mathbb{G}_A'$ coming from long twist regions
$\#\{\cdot\}$	the number of $\cdot$
SIC	small inner circle of the all-A state H_A
OC	other circle of the all-A state H_A
SC	special (other) circle of the all-A state H_A
B_n	the n-braid group
σ_i	the i^{th} generator of B_n

β	a braid
$a_{i,j}$	the number of crossings (counted with sign) in the i^{th} row and j^{th} column of twist regions in a plat diagram
$t^+(D)$	the number of positive twist regions in $D(K)$
$t^-(D)$	the number of negative twist regions in $D(K)$
$\widehat{\beta}$	the closure of the braid β
β'	a generic normal form $\beta' = C^k\sigma_1^{-p_1}\sigma_2^{q_1}\cdots\sigma_1^{-p_s}\sigma_2^{q_s}$ of β
k	a parameter from the generic Schreier normal form β' of β
s	a parameter from the generic Schreier normal form β' of β

Chapter 1

Introduction

This thesis centers around the study of knots and links, which have origins tracing back over one hundred years. A *knot* K is a smooth (or piecewise-linear) embedding of a circle into the 3-sphere S^3 and a *link*, which will also be denoted by K, is a disjoint but possibly intertwined collection of knots. Note that a knot can be viewed as a one-component link. We view two links K_1 and K_2 as *equivalent* if there is a one-parameter family h_t of homeomorphisms from S^3 to itself such that h_0 is the identity map and h_1 sends K_1 to K_2. A classical but difficult question in knot theory is to determine whether or not two links K_1 and K_2 are equivalent. For further details and a more thorough introduction to knot theory, see [19].

One approach to studying links is to project a link to the plane (or the 2-sphere S^2) in such a way that the only crossings are double crossings and in such a way that over- and under-crossing information is preserved by placing small gaps around the crossings of the projection. What results is called a *link diagram*. It should be noted that the study of links up to equivalence has been shown to be the same as the study of link diagrams up to a diagrammatic notion of equivalence ([24]).

Another approach to studying links is to associate a mathematical objects to links in such a way that equivalent links are associated to the exact same object. To be more precise, a function from the set of links to a set of mathematical objects is called a *link invariant* if it

is constant on equivalence classes of links. As a result, if $f(K_1) \neq f(K_2)$ for a link invariant f and links K_1 and K_2, then K_1 and K_2 cannot be equivalent links.

From the above two perspectives on the study of links, we can ask the following questions:

(1) What information can a link diagram provide about a link?

(2) What information can a link invariant provide about a link?

One of the main themes of this work is to investigate the conditions under which data extracted from a certain link diagram or data extracted from a quantum polynomial link invariant can be used to estimate geometric data for a given link. Tied to this theme is the goal of improving general estimates for this geometric data by studying the structure of specific families of links. Below we provide the background and framework needed for our investigation.

From a combinatorial and quantum perspective, a rich family of links to study is the family of semi-adequate (A- and B-adequate) links. By reflecting the diagram if needed, we may focus our attention on the collection of A-adequate links. To an A-adequate link diagram we can associate a loop-free graph. This graph, which can be cellularly embedded in a surface whose boundary is the link, is intimately related to the Jones polynomial of the link (a quantum link invariant). For example, the Jones polynomial of the link can be recovered from the Bollobás-Riordan polynomial of the associated graph ([5]). Additionally, Dasbach and Lin ([6]) have shown that the absolute value of the penultimate coefficient of the n^{th} colored Jones polynomial stabilizes to a value that is independent of $n > 1$ and only depends

on a reduction of the associated graph.

From a geometric perspective, a rich family of links to study is the family of hyperbolic links. Such links are characterized by having complements that admit a unique hyperbolic metric ([20], [23], [27]). By this uniqueness the volume, vol($S^3 \backslash K$), of the complement of a hyperbolic link K is a geometric link invariant.

Acting as a bridge between quantum and geometric invariants of links, the Volume Conjecture of Kashaev, Murakami, and Murakami ([7], [21]) predicts that the (asymptotic behavior of the) colored Jones polynomial can be used to determine the hyperbolic volume of the link complement. While it has been verified for a handful of hyperbolic links, the conjecture remains quite open in general.

Recently, Futer, Kalfagianni, and Purcell have related the colored Jones polynomial of an A-adequate link to both the topology of essential surfaces in the link complement and to bounds on the hyperbolic volume of the link complement. (See [11] for the complete work or [10] for a survey of results.) As an example, it was shown that, for sufficiently twisted negative (positive using their conventions) braid closures and for a large family of Montesinos links, the volume of the link complement can be bounded above and below in terms of the twist number of an A-adequate link diagram. For the class of alternating links, similar two-sided bounds were found by Lackenby ([18]), with the lower bound later improved by Agol, Storm and W. Thurston ([1]) and the upper bound later improved by Agol and D. Thurston ([18], Appendix).

The main result of this thesis, which builds upon the work mentioned above, is given below.

(The definitions of *connected*, *prime*, *A-adequate*, *twist region*, *special tangle*, and *the two-edge loop condition* will be provided in Section 2.1.) Let $t(D)$ denote the number of twist regions in $D(K)$, let $st(D)$ denote the number of special tangles in $D(K)$, let $v_8 = 3.6638\ldots$ denote the volume of a regular ideal octahedron, and let $v_3 = 1.0149\ldots$ denote the volume of a regular ideal tetrahedron.

Theorem 1.0.1 (Main Theorem)**.** *Let $D(K)$ be a connected, prime, A-adequate link diagram that satisfies the two-edge loop condition and contains $t(D) \geq 2$ twist regions. Then K is hyperbolic and the complement of K satisfies the following volume bounds:*

$$\frac{v_8}{3} \cdot [t(D) - st(D)] \leq \mathrm{vol}(S^3 \backslash K) < 10v_3 \cdot (t(D) - 1),$$

where $t(D) \geq st(D)$. If $t(D) = st(D)$, then $D(K)$ is alternating and the lower bound of $\frac{v_8}{2} \cdot (t(D) - 2)$ from Theorem 2.2 of [1] may be used.

To provide a family of links that satisfy the assumptions of the Main Theorem, we first restrict attention to A-adequate plat closures of certain braids. In particular, we study two families of plat diagrams: *negative plat diagrams* and *mixed-sign plat diagrams*. (See Section 4.1 for background on plat closures and more details about negative and mixed-sign plat diagrams.) By studying the structure of these two families of link diagrams, we are often able to improve the lower bounds on volume given by the Main Theorem above.

Theorem 1.0.2. *Let $D(K)$ be a negative plat diagram. Then K is hyperbolic and the complement of K satisfies the following volume bounds:*

$$\frac{4v_8}{5} \cdot (t(D) - 1) + \frac{v_8}{5} \leq \text{vol}(S^3 \backslash K) < 10v_3 \cdot (t(D) - 1) \,.$$

Theorem 1.0.3. *Let $D(K)$ be a mixed-sign plat diagram with at least as many negative twist regions as positive twist regions. Then K is hyperbolic and the complement of K satisfies the following volume bounds:*

$$\frac{v_8}{3} \cdot (t(D) - 1) - \frac{2v_8}{3} \leq \text{vol}(S^3 \backslash K) < 10v_3 \cdot (t(D) - 1) \,.$$

Furthermore, we are able to translate the volume bounds of the Main Theorem so that they may be expressed in terms of the number of special tangles, $st(D)$, and a stable coefficient, β'_K, of the colored Jones polynomial. (For more information concerning the colored Jones polynomial of an A-adequate link, see Section 2.3.)

Theorem 1.0.4. *Let $D(K)$ be a connected, prime, A-adequate link diagram that satisfies the two-edge loop condition and contains $t(D) \geq 2$ twist regions. Then K is hyperbolic and the complement of K satisfies the following volume bounds:*

$$v_8 \cdot \left(\left|\beta'_K\right| - 1\right) \leq \text{vol}(S^3 \backslash K) < 30v_3 \cdot \left(\left|\beta'_K\right| - 1\right) + 10v_3 \cdot (st(D) - 1) \,.$$

If we return to the family of plats considered in this work, then we are often able to improve the above upper bounds on volume.

Theorem 1.0.5. *Let $D(K)$ be a negative plat diagram. Then K is hyperbolic and the*

complement of K satisfies the following volume bounds:

$$v_8 \cdot \left(\left|\beta'_K\right| - 1\right) \leq \mathrm{vol}(S^3 \backslash K) < \frac{25v_3}{2} \cdot \left(\left|\beta'_K\right| - 1\right) - \frac{5v_3}{2}.$$

Theorem 1.0.6. *Let $D(K)$ be a mixed-sign plat diagram with at least as many negative twist regions as positive twist regions. Then K is hyperbolic and the complement of K satisfies the following volume bounds:*

$$v_8 \cdot \left(\left|\beta'_K\right| - 1\right) \leq \mathrm{vol}(S^3 \backslash K) < 30v_3 \cdot \left(\left|\beta'_K\right| - 1\right) + 20v_3.$$

The three results above can be viewed as providing families of links that satisfy a Coarse Volume Conjecture ([11], Section 10.4). A Coarse Volume Conjecture, roughly stated, says that the volume of the link complement can be bounded above and below by linear functions of the coefficients of the colored Jones polynomial. In the results above, we can actually bound the volume above and below in terms of a single coefficient, namely β'_K.

In the same spirit as above, we also show that a family of closed braids fits into the same volume bound framework. By studying the particular structure of these closed braid diagrams, we can often improve the bounds on volume. Since more can be said about closed 3-braids, we consider this case separately. (See Chapter 5 and Chapter 6 for further details. In particular, see Section 5.6 for the definition of *non-essential wandering circle*.)

Theorem 1.0.7. *Let $D(K)$ denote the closure of a certain n-braid. Then K is a hyperbolic*

link. In the case that $n = 3$, we get the following volume bounds:

$$\frac{v_8}{2} \cdot (t(D) - 1) - \frac{v_8}{2} \leq \mathrm{vol}(S^3 \backslash K) < 10v_3 \cdot (t(D) - 1).$$

Suppose, in the case that $n \geq 4$, that the all-A state contains m non-essential wandering circles. Then we get the following volume bounds:

$$\frac{v_8}{2} \cdot (t(D) - 1) - \frac{v_8}{2} \cdot (2(n + m) - 5) \leq \mathrm{vol}(S^3 \backslash K) < 10v_3 \cdot (t(D) - 1).$$

Theorem 1.0.8. *Let $D(K)$ denote the closure of a certain n-braid. Then K is a hyperbolic link. In the case that $n = 3$, we get the following volume bounds:*

$$v_8 \cdot (\left|\beta'_K\right| - 1) \leq \mathrm{vol}(S^3 \backslash K) < 20v_3 \cdot (\left|\beta'_K\right| - 1) + 10v_3.$$

Suppose, in the case that $n \geq 4$, that the all-A state contains m non-essential wandering circles. Then we get the following volume bounds:

$$v_8 \cdot (\left|\beta'_K\right| - 1) \leq \mathrm{vol}(S^3 \backslash K) < 20v_3 \cdot (\left|\beta'_K\right| - 1) + 10v_3 \cdot (2(n + m) - 5).$$

Additionally, for the closed 3-braids under consideration, we are able to bound the volume in terms of the parameter s from their Schreier normal form. (See Chapter 6 for further details.)

Theorem 1.0.9. *Let $D(K)$ denote the closure of a certain 3-braid. Then K is a hyperbolic*

link and K satisfies the following volume bounds:

$$v_8 \cdot (s-1) \leq \mathrm{vol}(S^3 \backslash K) < 4v_8 \cdot s.$$

Remark 1.0.1. It should be noted that volume bounds for closed 3-braids in terms of the parameter s were previously found by Futer, Kalfagianni, and Purcell in [12]. By using the results of their more recent work in [9] and [11], we are often able to improve their lower bound on volume from [12].

To conclude our study of link diagrams and volume bounds we investigate a third family of links, called *hybrid braid-plats*, which have both negative braid closure aspects and plat closure aspects. Again, we show that these link diagrams fit into the above volume bound framework.

Theorem 1.0.10. *For $D(K)$ a certain hybrid braid-plat diagram with negative plat diagram aspects, we have that K is hyperbolic and the complement of K satisfies the following volume bounds:*

$$\frac{2v_8}{3} \cdot (t(D)-1) + \frac{32v_8}{15} \leq \mathrm{vol}(S^3 \backslash K) < 10v_3 \cdot (t(D)-1)\,.$$

Similarly, for $D(K)$ a certain hybrid braid-plat diagram with mixed-sign plat diagram aspects, we have that K is hyperbolic and the complement of K satisfies the following volume bounds:

$$\frac{v_8}{3} \cdot (t(D)-1) + \frac{4v_8}{3} \leq \mathrm{vol}(S^3 \backslash K) < 10v_3 \cdot (t(D)-1)\,.$$

Translating these volume bounds to be expressed in terms of the coefficient β'_K of the colored

Jones polynomial, we get the following results:

Theorem 1.0.11. *For $D(K)$ a certain hybrid braid-plat diagram with negative plat diagram aspects, we have that K is hyperbolic and the complement of K satisfies the following volume bounds:*

$$v_8 \cdot \left(\left|\beta'_K\right| - 1\right) \leq \mathrm{vol}(S^3 \backslash K) < 15v_3 \cdot \left(\left|\beta'_K\right| - 1\right) - 32v_3.$$

Similarly, for $D(K)$ a certain hybrid braid-plat diagram with mixed-sign plat diagram aspects, we have that K is hyperbolic and the complement of K satisfies the following volume bounds:

$$v_8 \cdot \left(\left|\beta'_K\right| - 1\right) \leq \mathrm{vol}(S^3 \backslash K) < 30v_3 \cdot \left(\left|\beta'_K\right| - 1\right) - 40v_3.$$

Chapter 2

Preliminaries

2.1 Definitions

For the remainder of this thesis, we will let $D(K) \subseteq S^2$ denote a diagram of a link $K \subseteq S^3$. We call $D(K)$ *connected* if the projection graph formed by replacing all crossings of $D(K)$ with 4-valent vertices is path-connected. We call $D(K)$ *prime* if there does not exist a simple closed curve in the projection plane that both intersects $D(K)$ twice transversely (away from the crossings) and also contains crossings on both sides of the curve. For a schematic depiction of a non-prime diagram, see Figure 2.1.

To smooth a crossing of the link diagram $D(K)$, we may either *A-resolve* or *B-resolve* this crossing according to Figure 2.2. Note that interchanging overcrossings and undercrossings (called *reflecting* the link diagram) interchanges A-resolutions and B-resolutions. By A-

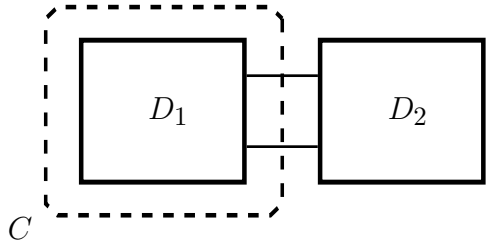

Figure 2.1: A schematic depiction of non-prime link diagram $D(K)$. The solid boxes, marked D_1 and D_2, contain the remainder of the link diagram. Each such box is assumed to contain at least one crossing of $D(K)$. The simple closed curve, C, exhibits the non-primeness of the diagram.

Figure 2.2: A crossing neighborhood of a link diagram (middle), along with its A-resolution (right) and B-resolution (left).

resolving each crossing of $D(K)$ we form the *all-A state* of $D(K)$, which we will denote by H_A. The all-A state H_A consists of a disjoint collection of *all-A circles* and a disjoint collection of dotted line segments, called *A-segments*, which are used record the locations of crossing resolutions. We will adopt the convention throughout this thesis that any unlabeled segments are assumed to be A-segments.

Definition 2.1.1. A link diagram $D(K)$ is called *A-adequate* if H_A does not contain any A-segments that join an all-A circle to itself. A link diagram is called *semi-adequate* if either it or its reflection is A-adequate. A link K is called *A-adequate* if it has a diagram that is A-adequate and is called *semi-adequate* if it has a diagram that is semi-adequate.

Remark 2.1.1. While we will focus exclusively on A-adequate links, our results can easily be extended to semi-adequate links by reflecting the link diagram $D(K)$ and obtaining the corresponding results for B-adequate links.

Definition 2.1.2. From H_A we may form the *all-A graph*, denoted $\mathbb{G}_A$, by contracting the all-A circles to vertices and reinterpreting the A-segments as edges. From this graph we can form the *reduced all-A graph*, denoted $\mathbb{G}'_A$, by replacing all multi-edges with a single edge. Said another way, we reduce the graph by removing all redundant parallel edges that join the same pair of vertices.

For an example of a diagram $D(K)$, its all-A resolution H_A, its all-A graph $\mathbb{G}_A$, and its reduced all-A graph $\mathbb{G}'_A$, see Figure 2.3.

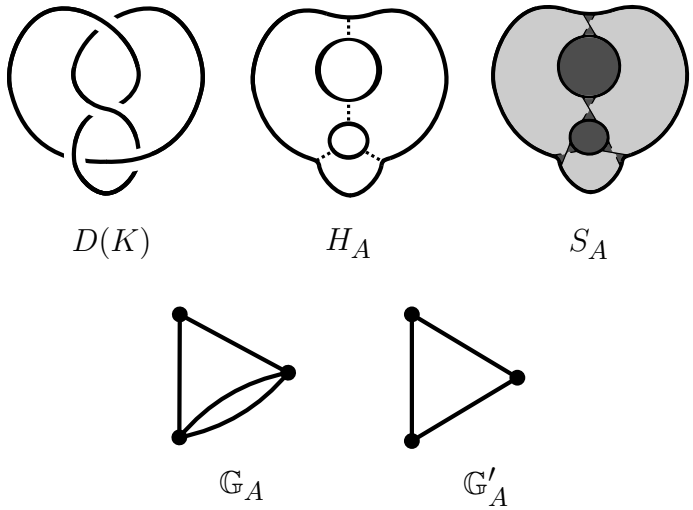

Figure 2.3: A link diagram $D(K)$, its all-A resolution H_A, its all-A surface S_A, its all-A graph $\mathbb{G}_A$, and its reduced all-A graph $\mathbb{G}'_A$.

Notation: Since reducing $\mathbb{G}_A$ to form $\mathbb{G}'_A$ leaves the vertices unchanged, then let $v(\mathbb{G}'_A)$ denote the number of vertices of either $\mathbb{G}'_A$ or $\mathbb{G}_A$. Let $e(\mathbb{G}_A)$ denote the number of edges of $\mathbb{G}_A$ and let $e(\mathbb{G}'_A)$ denote the number of edges of $\mathbb{G}'_A$. Let $-\chi(\mathbb{G}'_A) = e(\mathbb{G}'_A) - v(\mathbb{G}'_A)$ denote the negative Euler characteristic of $\mathbb{G}'_A$.

Remark 2.1.2. Note that $v(\mathbb{G}'_A)$ is the same as the number of all-A circles in H_A and that $e(\mathbb{G}_A)$ is the same as the number of A-segments in H_A. From a graphical perspective, A-adequacy of $D(K)$ can equivalently be defined by the condition that $\mathbb{G}_A$ (or $\mathbb{G}'_A$) contains no one-edge loops that connect a vertex to itself.

Definition 2.1.3. Define a *twist region* of $D(K)$ to be a longest possible string of crossings built from exactly two strands of $D(K)$. Denote the number of twist regions in $D(K)$ by $t(D)$ and call $t(D)$ the *twist number* of $D(K)$. See Figure 2.4 for an example.

Notice that it is potentially possible for a twist region to consist of a single crossing.

Definition 2.1.4. If a given twist region contains two or more crossings, then the A-

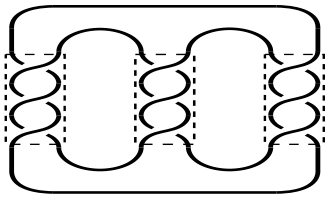

Figure 2.4: A link diagram with $t(D) = 3$ twist regions.

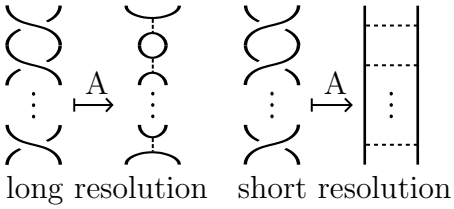

Figure 2.5: Long and short resolutions of a twist region of $D(K)$.

resolution of this twist region will consist of portions of two all-A circles that are either:

(1) joined by a path of A-segments and (small) all-A circles, or

(2) joined by a string of parallel A-segments.

Call a resolution in which (1) occurs a *long resolution* and call a resolution in which (2) occurs a *short resolution*. See Figure 2.5 for depictions of long and short resolutions. We will call a twist region *long* if its A-resolution is long and *short* if its A-resolution is short.

The following definition, which is very important, describes a key property of the link diagrams that will be considered in this work.

Definition 2.1.5. A link diagram $D(K)$ satisfies the *two-edge loop condition (TELC)* if, whenever two all-A circles share a pair of A-segments, these segments correspond to crossings from the same short twist region of $D(K)$.

Recall that the volume bounds from Theorem 1.0.1 are expressed in terms of two pieces of diagrammatic data, the first of which is the twist number $t(D)$. The second piece of

diagrammatic data, a count of specific types of alternating tangles in the diagram $D(K)$, is defined below.

Definition 2.1.6. Call an alternating tangle in $D(K)$ a *special tangle* if, up to planar isotopy, it consists of exactly one of the following:

(1) a tangle sum, $T(1, s)$, of a vertical one-crossing twist region and a vertical short twist region

(2) a tangle sum, $T(s_1, s_2)$, of two vertical short twist regions

(3) a tangle sum, $T(l, s)$, of a horizontal long twist region and a vertical short twist region

The values of $l, s, s_1, s_2 \geq 1$ denote the number of crossings in the relevant twist regions described above. To look for such tangles in $D(K) \subseteq S^2$, we look for simple closed curves in the plane that intersect $D(K)$ exactly four times (away from the crossings) and that contain a special tangle on one side of the curve. Equivalently, special tangles of $D(K)$ can be found in the all-A state H_A by looking for all-A circles that are incident to A-segments from a pair of twist regions from the tangle sums mentioned above. We will call these all-A circles *special circles* of H_A. See Figure 2.6 for depictions of special tangles and special circles. Let $st(D)$ denote the number of special tangles in $D(K)$ (or, equivalently, the number of special circles in H_A).

The advantage to looking for special circles in H_A, as opposed to looking for special tangles in $D(K)$, is that special circles are necessarily disjoint. Special tangles, on the other hand, can share one or both twist regions with another special tangle.

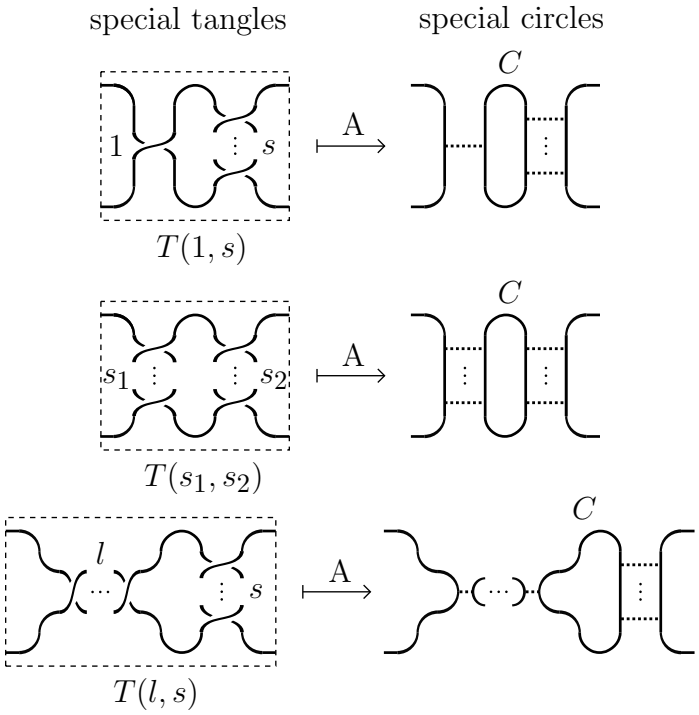

Figure 2.6: Special tangles of $D(K)$ and the corresponding special circles, C, of H_A.

2.2 Volume Bounds

The previous section provided the definitions of the terms involved in the statement of Theorem 1.0.1. We would now like to provide the mathematical background surrounding this theorem. First, to consider the hyperbolic volume of the link complement, we need to be able to ensure that our links are hyperbolic. The following result, due to Futer, Kalfagianni, and Purcell ([9]), does exactly this.

Proposition 2.2.1 ([9])**.** *Let $D(K)$ be a connected, prime, A-adequate link diagram that satisfies the TELC and contains $t(D) \geq 2$ twist regions. Then K is hyperbolic.*

Let $S^3 \backslash K$ denote the complement of the link K. Since the link complement is formed by removing a regular open neighborhood of the link K from S^3, then we have that $S^3 \backslash K$ is a 3-manifold with boundary a disjoint union of tori.

A common practice in 3-manifold theory is to study properly embedded surfaces in 3-manifolds. Our goal is now to find an essential surface in the complement $S^3\backslash K$. For what follows, let S be a compact surface that is properly embedded in a 3-manifold M, where being properly embedded means that $\partial S \subseteq \partial M$ and $\text{int}(S) \subseteq \text{int}(M)$. Let D be a disk in M with the property that $D \cap S = \partial D$. The disk D is called a *compressing disk* for S in M if ∂D does not bound a disk in S. If S does not contain compressing disks, then S is called *incompressible* in M. Let D' be a disk in M with the properties that $D' \cap S = \alpha$ and $D' \cap \partial M = \beta$, where α and β are arcs with $\alpha \cup \beta = \partial D'$ and $\alpha \cap \beta = \partial\alpha = \partial\beta$, and where α does not cobound a disk in S with another arc in ∂S. The disk D' is called a *boundary-compressing disk* for S. If S does not contain boundary-compressing disks, then S is called *boundary-incompressible* in M. The surface S is called *essential* in M if the boundary of a regular neighborhood of S is both incompressible and boundary-incompressible in M. We refer the reader to [13] for more details.

From the all-A state H_A of the link diagram $D(K)$ we form the *all-A surface* of $D(K)$, denoted S_A, by associating a disk to each all-A circle and a half-twisted band to each A-segment, doing this in such a way that the boundary of S_A is the link K and so that inner disks lie above outer disks. See the top right side of Figure 2.3 for an example of an all-A surface S_A. Notice that S_A is properly embedded in the 3-manifold $S^3\backslash K$. As it turns out, the A-adequacy of a connected link diagram $D(K)$ has a geometric interpretation that involves the all-A surface S_A. In [22], Ozawa showed that the A-adequacy of a connected link diagram $D(K)$ implies that the all-A surface S_A is essential in $S^3\backslash K$.

For a connected A-adequate link diagram $D(K)$ with essential all-A surface S_A in $S^3\backslash K$, we form the 3-manifold $M_A = (S^3\backslash K)\backslash\backslash S_A$ by cutting the the link complement along the

all-A surface. As proved in Lemma 2.4 of [11], the 3-manifold M_A is homeomorphic to a handlebody and therefore contains no essential tori. By the annulus version of the Jaco-Shalen-Johannson Decomposition Theorem ([14], [15]) and by Lemma 4.1 of [11], we can cut M_A along annuli (disjoint from the parabolic locus) to produce the following types of pieces:

(1) I-bundles over subsurfaces of S_A

(2) solid tori

(3) guts (which are the hyperbolic pieces with totally geodesic boundary)

Let $\chi_-(\text{guts}(M_A)) = \max\{-\chi(\text{guts}(M_A)), 0\}$. With the lower bound provided by Agol, Storm, and W. Thurston ([1]) and the upper bound provided by Agol and D. Thurston ([18], Appendix), we get the following volume bounds for the hyperbolic link complement.

Proposition 2.2.2 ([1], [18])**.** *Let $D(K)$ be a connected, prime, A-adequate diagram of a hyperbolic link K. Then:*

$$v_8 \cdot \chi_-(\text{guts}(M_A)) \leq \text{vol}(S^3 \backslash K) < 10v_3 \cdot (t(D) - 1),$$

where $v_8 = 3.6638\ldots$ denotes the volume of a regular ideal octahedron and $v_3 = 1.0149\ldots$ denotes the volume of a regular ideal tetrahedron.

Assumption: We will assume throughout this work that $\text{guts}(M_A)$ is nonempty. Otherwise, we would have that $\chi_-(\text{guts}(M_A)) = 0$ and, consequently, our lower bounds on volume would not be valuable.

By Remark 5.15 and Corollary 5.19 of [11], we get the following result:

Theorem 2.2.1. *Let $D(K)$ be a connected, prime, A-adequate link diagram that satisfies the TELC. Then:*

$$-\chi(\mathbb{G}'_A) = \chi_-(\text{guts}(M_A)).$$

By combining the above results together, we are able to state the theorem that will form the basis for our work. Specifically, Theorem 2.2.2 below forms a crucial foundation for Theorem 1.0.1.

Theorem 2.2.2. *Let $D(K)$ be a connected, prime, A-adequate link diagram that satisfies the TELC and contains $t(D) \geq 2$ twist regions. Then K is hyperbolic and:*

$$-v_8 \cdot \chi(\mathbb{G}'_A) \leq v_8 \cdot \chi_-(\text{guts}(M_A)) \leq \text{vol}(S^3 \backslash K) < 10v_3 \cdot (t(D) - 1).$$

Proof. By the combining Proposition 2.2.1 with Proposition 2.2.2 and Theorem 2.2.1, we get the desired results. □

Note that the above theorem uses the reduced all-A graph $\mathbb{G}'_A$ to get a lower bound on volume. This fact provides the key opportunity for a combinatorial perspective to be used.

2.3 A-Adequacy and the Colored Jones Polynomial

Now that the combinatorial and geometric approaches to the study of links have been investigated, we would like to introduce a third and final approach: quantum polynomial

invariants. To an oriented link we can associate a number of polynomial invariants, each of which can be used to distinguish links from each other. Some of the most recent such link polynomials are the Jones polynomial ([16], [17]) and the colored Jones polynomials ([28]), which form a sequence of Laurent polynomials indexed by the natural numbers.

Notation: Denote the n^{th} *colored Jones polynomial* of a link K by:

$$J_K^n(t) = \alpha_n t^{m_n} + \beta_n t^{m_n - 1} + \cdots + \beta'_n t^{r_n + 1} + \alpha'_n t^{r_n},$$

where $n \in \mathbb{N}$ and where the degree of each monomial summand decreases from left to right.

The following result, due to Dasbach and Lin and due to Stoimenow, relates the penultimate coefficient β'_n of the colored Jones polynomial of an A-adequate link to the reduced all-A graph $\mathbb{G}'_A$ associated to an A-adequate diagram of that link.

Theorem 2.3.1 ([6], [26])**.** *Let $D(K)$ be a connected, A-adequate link diagram. Then $\left|\beta'_n\right|$ is independent of n for $n > 1$. Specifically, for $n > 1$, we have that:*

$$\left|\beta'_K\right| := \left|\beta'_n\right| = 1 - \chi(\mathbb{G}'_A).$$

The above result has been and will be key in translating from volume bounds in terms of the twist number to volume bounds in terms of coefficients of the colored Jones polynomial.

Chapter 3

Volume Bounds for A-Adequate Links

Let $D(K)$ be a connected, A-adequate link diagram that satisfies the two-edge loop condition (TELC). We begin this chapter by closely investigating the twist regions of $D(K)$, the all-A state H_A of $D(K)$, and the reduction of the all-A graph $\mathbb{G}_A$ to the reduced all-A graph $\mathbb{G}'_A$. This is done in order to express $-\chi(\mathbb{G}'_A)$ in terms of the twist number $t(D)$ and the number of certain all-A circles. By studying the all-A circles and making use of graph theory, we are able to bound $-\chi(\mathbb{G}'_A)$ below in terms of the twist number $t(D)$ and the number, $st(D)$, of special circles in H_A (or the corresponding number of special tangles in $D(K)$). This lower bound, combined with Theorem 2.2.2, produces the Main Theorem (Theorem 1.0.1) of this work.

3.1 Twist Regions, State Circles, and $\mathbb{G}'_A$

We begin with a study of twist regions. Because long and short resolutions are not distinguishable when there is only one crossing in a twist region, we have defined long and short resolutions (Definition 2.1.4) as coming from twist regions that contain at least two crossings. Consequently, we will begin by considering the case of one-crossing twist regions.

See Figure 2.2 for a one-crossing twist region and its A-resolution. Let C_1 and C_2 denote the (portions of the) relevant all-A circles in H_A. Since $D(K)$ is A-adequate, then $C_1 \neq C_2$. Since $D(K)$ satisfies the TELC, then there can be no other additional A-segments between C_1 and C_2. Thus, the edge of $\mathbb{G}_A$ corresponding to this one-crossing twist region can never be a redundant parallel edge and, therefore, will always appear in $\mathbb{G}'_A$.

Notation: Let $t_1(D)$ denote the number of one-crossing twist regions in $D(K)$.

Remark 3.1.1. By what was said in the above paragraph, $t_1(D)$ is also the number of edges in $\mathbb{G}'_A$ that come from the one-crossing twist regions in $D(K)$.

Let us now consider twist regions that have at least two crossings. Such twist regions will either have a short resolution or a long resolution. See the right side of Figure 2.5 for a twist region and its short all-A resolution. Again using C_1 and C_2 to denote the (portions of the) the relevant all-A circles, the A-adequacy of $D(K)$ implies that $C_1 \neq C_2$ and the TELC implies that there can be no other A-segments between C_1 and C_2 (besides those of the short resolution). Furthermore, note that a short twist region will always create redundant parallel edges in $\mathbb{G}_A$ since the parallel A-segments of H_A join the same pair of state circles. Thus, all but one of these edges is removed when forming $\mathbb{G}'_A$. Said another way, there will be one edge of $\mathbb{G}'_A$ per short twist region of $D(K)$.

Notation: Let $t_s(D)$ denote the number of short twist regions in $D(K)$.

Remark 3.1.2. By what was said in the above paragraph, $t_s(D)$ is also the number of edges in $\mathbb{G}'_A$ that come from the short twist regions in $D(K)$.

See the left side of Figure 2.5 for a twist region and its long all-A resolution. We will use C_1 and C_2 to denote upper and lower (portions of the) relevant state circles. If there are three or more crossings in the twist region being considered, then it must necessarily be the case that none of the corresponding edges in $\mathbb{G}_A$ are lost in the reduction to form $\mathbb{G}'_A$. If there are two crossings in the twist region, then the TELC implies that $C_1 \neq C_2$ because, otherwise, we would have a two-edge loop in $\mathbb{G}_A$ coming from a long twist region. As a result, we have that no edges of $\mathbb{G}_A$ coming from long resolutions are removed when forming $\mathbb{G}'_A$.

Recall that a long resolution will consist of (portions of) two state circles joined by a path of A-segments and (small) all-A circles.

Definition 3.1.1. We call each (small) all-A circle in the interior of the long resolution a *small inner circle (SIC)*. The remaining all-A circles (coming from the all-A circle portions in the long resolutions, from the all-A circle portions in the short resolutions, and from the all-A circle portions in the A-resolutions of one-crossing twist regions) will simply be called *other circles (OCs)*.

Notation: Let $t_l(D)$ denote the number of long twist regions in $D(K)$ and let $e_l(\mathbb{G}'_A)$ denote the number of edges in $\mathbb{G}'_A$ coming from long twist regions.

By inspection, it can be seen that the number of A-segments in the long resolution is always one greater than the number of small inner circles in the long resolution. Since this phenomenon occurs for each long resolution, then we have that:

$$\#\{\text{SICs}\} = e_l(\mathbb{G}'_A) - t_l(D). \tag{3.1}$$

3.2 Computation of $-\chi(\mathbb{G}'_A)$

Lemma 3.2.1. *Let $D(K)$ be a connected, A-adequate link diagram that satisfies the TELC. Then we have that:*

$$-\chi(\mathbb{G}'_A) = t(D) - \#\{\text{OCs}\}.$$

Proof. By Remark 2.1.2 and Definition 3.1.1, we get:

$$\begin{aligned} -\chi(\mathbb{G}'_A) &= e(\mathbb{G}'_A) - v(\mathbb{G}'_A) \\ &= e(\mathbb{G}'_A) - \#\{\text{all} - \text{A state circles}\} \\ &= e(\mathbb{G}'_A) - \#\{\text{SICs}\} - \#\{\text{OCs}\}. \end{aligned} \tag{3.2}$$

Looking at how the twist regions of $D(K)$ were partitioned in Section 3.1, we get:

$$t(D) = t_1(D) + t_s(D) + t_l(D). \tag{3.3}$$

Next, Remark 3.1.1 and Remark 3.1.2 imply that:

$$e(\mathbb{G}'_A) = t_1(D) + t_s(D) + e_l(\mathbb{G}'_A). \tag{3.4}$$

By substituting Equation 3.4 and Equation 3.1 into Equation 3.2 and then using Equation 3.3, we get:

$$\begin{aligned} -\chi(\mathbb{G}'_A) &= e(\mathbb{G}'_A) - \#\{\text{SICs}\} - \#\{\text{OCs}\} \\ &= [t_1(D) + t_s(D) + e_l(\mathbb{G}'_A)] - [e_l(\mathbb{G}'_A) - t_l(D)] - [\#\{\text{OCs}\}] \\ &= t_1(D) + t_s(D) + t_l(D) - \#\{\text{OCs}\} \\ &= t(D) - \#\{\text{OCs}\}. \end{aligned}$$

□

By applying Lemma 3.2.1 to Theorem 2.2.2, we get the following corollary:

Corollary 3.2.1. *Let $D(K)$ be a connected, prime, A-adequate link diagram that satisfies the TELC and contains $t(D) \geq 2$ twist regions. Then K is hyperbolic and:*

$$v_8 \cdot [t(D) - \#\{\text{OCs}\}] \leq \text{vol}(S^3 \backslash K) < 10v_3 \cdot (t(D) - 1).$$

Rather than count the number, $\#\{\text{OCs}\}$, of other circles in H_A, we would instead like to find lower bounds on volume that have a more intrinsic and visual connection to the link diagram $D(K)$ itself. Consequently, our goal is now to bound $-\#\{\text{OCs}\}$ below in terms of quantities that can be read off of $D(K)$ directly.

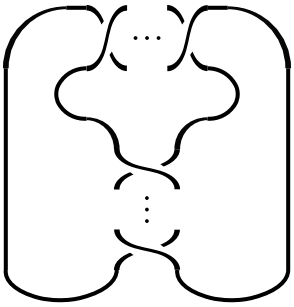

Figure 3.1: The exceptional link diagram consisting of two long twist regions, each of which must contain at least three crossings.

3.3 Special Circles and Special Tangles

As in the previous section, let $D(K)$ be a connected, A-adequate link diagram that satisfies the TELC. We will now also require that $D(K)$ is prime and contains $t(D) \geq 2$ twist regions. For such a link diagram $D(K)$, we are able to identify the simplest other circles of H_A with certain alternating tangles in $D(K)$.

Lemma 3.3.1. *Let $D(K)$ be a connected, prime, A-adequate link diagram that satisfies the TELC and contains $t(D) \geq 2$ twist regions. Furthermore, assume that $D(K)$ is not the link diagram depicted in Figure 3.1. Then:*

(1) there are no other circles of H_A that are incident to A-segments from one or fewer twist region resolutions, and

(2) the other circles of H_A that are incident to A-segments from exactly two twist region resolutions are the special circles of H_A.

Remark 3.3.1. In the case that $D(K)$ is the exceptional link diagram depicted in Figure 3.1, we have that $t(D) = 2$ and $st(D) = 0$. Therefore, by applying the Main Theorem

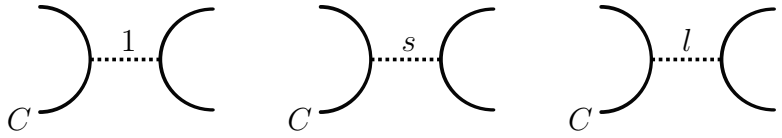

Figure 3.2: A schematic depiction of the A-resolutions of the three possible types of twist regions incident to an other circle C of H_A: one-crossing (left), short (middle), and long (right). The edge labels 1, s, and l are used not only to indicate the type of twist region resolution, but also to distinguish these edges from A-segments.

(Theorem 1.0.1), we get that the two-sided volume bounds for this link are:

$$\frac{2v_8}{3} \leq \text{vol}(S^3 \backslash K) < 10v_3.$$

Remark 3.3.2. In the future, it will be important to notice that $st(D) = 0$ for link diagrams whose other circles all have at least three incident twist region resolutions.

Proof of Lemma. See Figure 3.2 for schematic depictions of the A-resolutions of the twist regions of $D(K)$. Let C denote an other circle of the all-A state H_A. Such a circle must exist because, otherwise, we would have that H_A is a cycle of small inner circles and A-segments. Since this all-A state corresponds to the standard $(2, p)$-torus link diagram, then we would get a contradiction of the assumption that $t(D) \geq 2$.

Case 1: Suppose C is an other circle with no incident twist region resolutions. Then C corresponds to a standard unknotted component of $D(K)$. Thus, either $D(K)$ is not connected or $D(K)$ is the standard unknot diagram. In either case we get a contradiction, given the assumptions that $D(K)$ is connected and contains $t(D) \geq 2$ twist regions.

Case 2: Suppose C is an other circle with a single incident twist region resolution.

Subcase 1: Suppose the twist region resolution starts and ends at C. Similar to Case 1, this case is impossible given the assumptions that $D(K)$ is connected and contains $t(D) \geq 2$ twist regions.

Subcase 2: Suppose the twist region resolution joins C to a different state circle C'. Consider the portion of H_A corresponding to Figure 3.2 and recall that C and C' are closed curves. If C' is incident to no other additional twist region resolutions, then (as in Case 1) we get a contradiction of the assumptions that $D(K)$ is connected and contains $t(D) \geq 2$ twist regions. If C' is incident to additional twist region resolutions, then we get a contradiction of the primeness of the corresponding diagram $D(K)$.

Case 3: Suppose C is an other circle with exactly two incident twist region resolutions. If one of the twist region resolutions starts and ends at C, then (recalling Figure 2.2 and Figure 2.5 if needed) this twist region resolution can only correspond to a long resolution. This is because, otherwise, we would get a contradiction of the assumption that $D(K)$ is A-adequate.

Subcase 1: Suppose both (long) twist region resolutions start and end at C. The first three possibilities are depicted in Figure 3.3. As the rectangular dashed closed curves in the figure indicate, we get a contradiction of the primeness of the corresponding diagram $D(K)$. The fourth and final possibility is depicted in Figure 3.4. Translating back to $D(K)$, we get the exceptional link diagram depicted in Figure 3.1. Note that, by the TELC, it must be the case that there are at least three crossings per (long) twist region. This is because, otherwise, we would have a two-edge loop whose edges do not correspond to crossings of a short twist region. Recall that the link diagram of Figure 3.1 has been excluded from consideration.

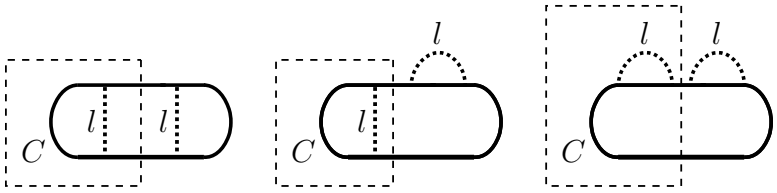

Figure 3.3: Three possibilities for an other circle C with two incident long resolutions that start and end at C.

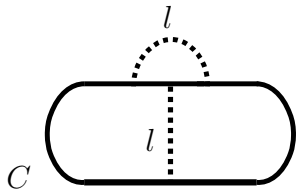

Figure 3.4: The fourth possibility for an other circle C with two incident long resolutions that start and end at C.

Subcase 2: Suppose one (long) twist region resolution starts and ends at $C = C_1$ and the other twist region resolution connects C_1 to another circle C_2. The three possibilities are depicted in Figure 3.5. As the rectangular dashed closed curves indicate, we get a contradiction of the primeness of the corresponding diagram $D(K)$.

Subcase 3: Suppose both twist region resolutions connect C to different other circles C_1 and C_2, where $C_1 = C_2$ is possible in some cases. The first possibility, that C_1 and C_2 are on opposite sides of C, is depicted in Figure 3.6. As the rectangular dashed closed curve indicates, we get a contradiction of the primeness of the corresponding diagram $D(K)$. Thus, both twist region resolutions incident to C must be on the same side of C. The choice of

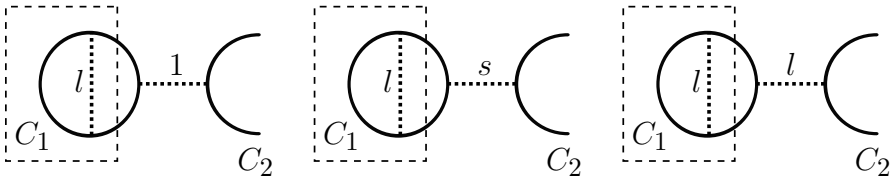

Figure 3.5: Three possibilities for an other circle C_1 with two incident twist region resolutions, one resolution from a long twist region that starts and ends at C_1 and the other resolution connecting to a different state circle C_2.

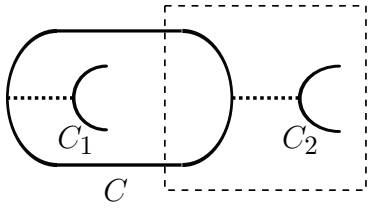

Figure 3.6: An other circle C with two incident twist region resolutions, one inside C and one outside C.

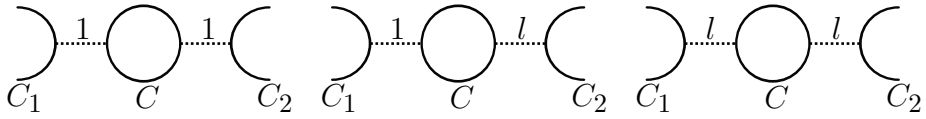

Figure 3.7: Three possibilities for an "other" circle C with two incident twist region resolutions, one connecting C to C_1 and the other connecting C to C_2.

side is irrelevant, however, since $D(K) \subseteq S^2$.

Given that both twist region resolutions must be on the same side of C, the first three possibilities are depicted in Figure 3.7. None of these cases are possible because, by translating back to $D(K)$ (and recalling Figure 2.2 and Figure 2.5 if needed), the two seemingly distinct twist region resolutions are actually part of the same long resolution. This makes C a small inner circle rather than an other circle, a contradiction.

The three remaining possibilities are depicted in Figure 3.8.

Remark 3.3.3. Note that by the TELC, it must be the case that $C_1 \neq C_2$ in the left and middle diagrams of Figure 3.8. However, because a long resolution involves a path of at least two A-segments, then it is possible that $C_1 = C_2$ in the right diagram of Figure 3.8. It is

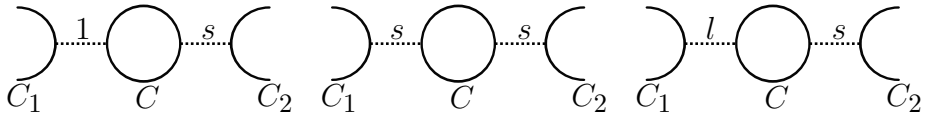

Figure 3.8: Three remaining possibilities for an other circle C with two incident twist region resolutions, one connecting C to C_1 and the other (a short twist region resolution) connecting C to C_2.

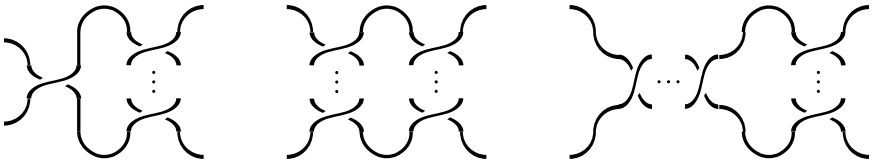

Figure 3.9: Three possible tangle subdiagrams of $D(K)$.

also important to note that, in all three diagrams, the remaining twist region resolutions and all-A circles (not depicted) must somehow join C_1 to C_2 in a second way. This is because, otherwise, there would exist a simple closed curve that cuts C in half and separates C_1 from C_2, a contradiction of the primeness of the corresponding diagram $D(K)$.

Assuming the conditions laid out in the above remark are satisfied, it is important to notice that the three possibilities in Figure 3.8 do not give a contradiction of the assumptions of Lemma 3.3.1. Equally as important, notice that these three possibilities correspond exactly to the special circles depicted on the right side of Figure 2.6.

□

Note that, by translating from the portions of H_A depicted in Figure 3.8 to the link diagram $D(K)$, we get the three special subdiagrams depicted in Figure 3.9. But these are exactly the three special tangles $T(1, s)$, $T(s_1, s_2)$, and $T(l, s)$ of the link diagram $D(K)$! Therefore, we have have shown that the special circles of H_A (which correspond to the special tangles in $D(K)$) are the least complicated other circles in H_A with respect to the number of incident twist region resolutions.

3.4 Volume Bounds in Terms of $t(D)$ and $st(D)$ (The Main Theorem)

In this section, we will shift perspective from the link diagram $D(K)$ and its all-A state H_A to the reduced all-A graph $\mathbb{G}'_A$. By combining some graph theory with both our previous computation of $-\chi(\mathbb{G}'_A)$ (Lemma 3.2.1) and our newly acquired knowledge about special circles (Lemma 3.3.1), we will prove the Main Theorem, which we restate below. Notice that the novel content of this theorem lies in the lower bound on volume.

Theorem 3.4.1 (Main Theorem)**.** *Let $D(K)$ be a connected, prime, A-adequate link diagram that satisfies the TELC and contains $t(D) \geq 2$ twist regions. Then K is hyperbolic and the complement of K satisfies the following volume bounds:*

$$\frac{v_8}{3} \cdot [t(D) - st(D)] \leq \text{vol}(S^3 \backslash K) < 10v_3 \cdot (t(D) - 1),$$

where $t(D) \geq st(D)$. If $t(D) = st(D)$, then $D(K)$ is alternating and the lower bound of $\frac{v_8}{2} \cdot (t(D) - 2)$ from Theorem 2.2 of [1] may be used.

Remark 3.4.1. Note that the coefficients of $t(D)$ in the upper and lower bounds differ by a multiplicative factor of $8.3102\ldots$, a factor that we would like to reduce by studying specific families of links.

Definition 3.4.1. Let G be a graph. We call G *simple* if it contains neither one-edge loops connecting a vertex to itself nor multiple edges connecting the same pair of vertices.

Notation: For G a simple graph, let $V(G)$ denote its vertex set and let $E(G)$ denote its

edge set. Furthermore, let $\deg(v)$ denote the degree of the vertex v, that is, the number of edges incident to v.

Proof of the Main Theorem. We will begin by using Theorem 2.1 of [4] which states that, for G a simple graph:

$$\sum_{v \in V(G)} \deg(v) = 2\,|E(G)|\,.$$

To see why this result is true, note that the edges of G are double counted as we sum the number of edges incident to the vertices. This is because each edge is shared by two distinct vertices (where we get distinct by the assumption that G is simple). Our strategy will be to apply this result to the reduced all-A graph $\mathbb{G}'_A$. We can do this because A-adequacy of $D(K)$ implies that $\mathbb{G}'_A$ will not contain any loops and the fact that $\mathbb{G}'_A$ is reduced implies that $\mathbb{G}'_A$ will not contain any multiple edges.

By Remark 2.1.2, Definition 3.1.1, and Lemma 3.3.1, we may partition $V(\mathbb{G}'_A)$ into three types of vertices:

(1) those corresponding to small inner circles (SICs),

(2) those corresponding to special circles (SCs), which are other circles that are incident to exactly two twist region resolutions, and

(3) those corresponding to the other circles (remaining OCs) that are incident to three or more twist region resolutions.

Recall that, as said in the paragraph following Remark 3.1.2, all edges corresponding to a long

resolution survive the reduction to $\mathbb{G}'_A$. Thus, we have that $\deg(v) = 2$ for v corresponding to a small inner circle. To visually verify this claim, see the left side of Figure 2.5. Also recall that, as said in the paragraph preceding Remark 3.1.1, the edge corresponding to a one-crossing twist region survives the reduction to $\mathbb{G}'_A$. Finally, as said in the paragraph following Remark 3.1.1, only a single edge coming from a short twist region survives the reduction to $\mathbb{G}'_A$. By applying this knowledge to Figure 3.8, we see that $\deg(v) = 2$ for v corresponding to a special circle. Similarly, we can see that $\deg(v) \geq 3$ for v corresponding to a remaining other circle. Therefore, translating Theorem 2.1 of [4] (stated above) to our setting, we get:

$$\begin{aligned} 2 \cdot e(\mathbb{G}'_A) &= \sum_{\text{SICs}} \deg(v) + \sum_{\text{SCs}} \deg(v) + \sum_{\substack{\text{remaining} \\ \text{OCs}}} \deg(v) \\ &= 2 \cdot [\#\{\text{SICs}\}] + 2 \cdot st(D) + \sum_{\substack{\text{remaining} \\ \text{OCs}}} \deg(v). \end{aligned} \tag{3.5}$$

Substituting Equation 3.4 into the left-hand side of Equation 3.5 gives:

$$2 \cdot t_1(D) + 2 \cdot t_s(D) + 2 \cdot e_l(\mathbb{G}'_A). \tag{3.6}$$

Substituting Equation 3.1 into the right-hand side of Equation 3.5 gives:

$$2 \cdot \left[e_l(\mathbb{G}'_A) - t_l(D)\right] + 2 \cdot st(D) + \sum_{\substack{\text{remaining} \\ \text{OCs}}} \deg(v). \tag{3.7}$$

By equating Expression 3.6 with Expression 3.7, canceling, rearranging terms, and using Equation 3.3, we end up with the following:

$$\begin{aligned} 2 \cdot st(D) + \sum_{\substack{\text{remaining} \\ \text{OCs}}} \deg(v) &= 2 \cdot t_1(D) + 2 \cdot t_s(D) + 2 \cdot t_l(D) \\ &= 2t(D). \end{aligned} \tag{3.8}$$

Recall that $\deg(v) \geq 3$ for v corresponding to a remaining other circle. Thus, we get:

$$2 \cdot st(D) + 3 \cdot [\#\{\text{remaining OCs}\}] \leq 2t(D).$$

Adding $st(D)$, the number of other circles that are not remaining other circles, to both sides allows us to write the above inequality in terms of the total number of other circles as:

$$3 \cdot [\#\{\text{OCs}\}] \leq 2t(D) + st(D).$$

This simplifies to:

$$\#\{\text{OCs}\} \leq \frac{2}{3} \cdot t(D) + \frac{1}{3} \cdot st(D).$$

Combining this inequality with Lemma 3.2.1 gives:

$$-\chi(\mathbb{G}'_A) = t(D) - \#\{\text{OCs}\} \geq \frac{1}{3} \cdot [t(D) - st(D)]. \tag{3.9}$$

Finally, by applying Inequality 3.9 to either Theorem 2.2.2 or Corollary 3.2.1, we get the desired volume bounds.

Furthermore, notice that Equation 3.8 implies that $t(D) \geq st(D)$. Thus, we have that the lower bound on volume is always nonnegative and is positive precisely when there exists at least one remaining other circle. Looking at Equation 3.8 from another perspective, note that if $t(D) = st(D)$, then there are can be no remaining other circles in the all-A state H_A. Hence, the only types of other circles in this case are special circles. Since each special circle is incident to exactly two twist region resolutions (and since the conditions mentioned in Remark 3.3.3 must be satisfied), then the all-A state H_A must form a cycle alternating between special circles and twist region resolutions. But recall that special tangles (which correspond to special circles) are alternating tangles. Hence, by cyclically fusing these tangles together, we form an alternating link diagram. Consequently, in the case that $t(D) = st(D)$ (which forces the lower bound of the Main Theorem to be zero), Theorem 2.2 of [1] can be used to provide a lower bound of $\frac{v_8}{2} \cdot (t(D) - 2)$ on volume.

□

Corollary 3.4.1. *Let $D(K)$ satisfy the hypotheses of the Main Theorem (Theorem 3.4.1). Furthermore, assume that each other circle of H_A has at least $m \geq 3$ incident twist region resolutions. Then $st(D) = 0$ and:*

$$-\chi(\mathbb{G}'_A) \geq \frac{m-2}{m} \cdot t(D).$$

Furthermore, K is hyperbolic and the complement of K satisfies the following volume bounds:

$$\frac{m-2}{m} \cdot v_8 \cdot t(D) \leq \text{vol}(S^3 \backslash K) < 10v_3 \cdot (t(D) - 1).$$

Remark 3.4.2. Notice that, as $m \to \infty$, the lower bound above approaches $v_8 \cdot t(D)$. Hence, the coefficients of $t(D)$ in the upper and lower bounds differ by a multiplicative factor of 2.7701 (in the limit).

Proof. We will prove this result by modifying what needs to be modified in the above proof of the Main Theorem. First, the assumption that each other circle has at least $m \geq 3$ incident twist region resolutions implies, by Lemma 3.3.1, that special circles cannot exist, so $st(D) = 0$. This assumption also implies that $\deg(v) \geq m$ for v corresponding to an other circle (which must be a remaining other circle). Consequently, this new assumption can be used to produce a sharper lower bound on volume. Specifically, by incorporating the conditions that $st(D) = 0$ and $\deg(v) \geq m$ into Equation 3.8, we get:

$$m \cdot \#\{\text{OCs}\} \leq 2 \cdot st(D) + \sum_{\substack{\text{remaining} \\ \text{OCs}}} \deg(v) = 2t(D).$$

Hence, we have that:

$$\#\{\text{OCs}\} \leq \frac{2}{m} \cdot t(D).$$

Combining this inequality with Lemma 3.2.1 gives:

$$-\chi(\mathbb{G}'_A) = t(D) - \#\{\text{OCs}\} \geq \frac{m-2}{m} \cdot t(D). \tag{3.10}$$

Finally, by applying the above inequality to either Theorem 2.2.2 or Corollary 3.2.1, we get the desired volume bounds.

□

3.5 Volume Bounds in Terms of the Colored Jones Polynomial

We will now express the volume bounds of the Main Theorem (Theorem 3.4.1) in terms of coefficients of the colored Jones polynomial (a quantum link invariant) and $st(D)$ rather than in terms of $t(D)$ (a diagrammatic quantity) and $st(D)$. In particular, when $st(D) = 0$ or when $st(D)$ can be bounded above by a positive constant, we will have volume bounds only in terms of coefficients of the colored Jones polynomial. In particular, our volume bounds will be in terms of the stable penultimate coefficient β'_K of the colored Jones polynomial. In doing this, we will show that such links satisfy a Coarse Volume Conjecture ([11], Section 10.4).

Theorem 3.5.1. *Let $D(K)$ be a connected, prime, A-adequate link diagram that satisfies the TELC and contains $t(D) \geq 2$ twist regions. Then K is hyperbolic and the complement of K satisfies the following volume bounds:*

$$v_8 \cdot \left(\left|\beta'_K\right| - 1\right) \leq \mathrm{vol}(S^3 \backslash K) < 30v_3 \cdot \left(\left|\beta'_K\right| - 1\right) + 10v_3 \cdot (st(D) - 1)\,.$$

Remark 3.5.1. As for $t(D)$ in the Main Theorem, note that the coefficients of $\left|\beta'_K\right|$ in the

upper and lower bounds above differ by a multiplicative factor of $8.3102\ldots$, a factor that we would like to reduce by studying specific families of links.

Proof of Theorem. Since $D(K)$ is connected and A-adequate, then Theorem 2.3.1 gives that $\left|\beta'_K\right| = 1 - \chi(\mathbb{G}'_A)$, which implies that $-\chi(\mathbb{G}'_A) = \left|\beta'_K\right| - 1$. Applying this to Theorem 2.2.2, we get the desired lower bound on volume. Theorem 2.2.2 also provides an upper bound of $10v_3 \cdot (t(D) - 1)$ on volume, which means that we will have proven the theorem once this quantity is bounded above in terms of $\left|\beta'_K\right|$ and $st(D)$. First, note that Inequality 3.9 gives:

$$\left|\beta'_K\right| - 1 = -\chi(\mathbb{G}'_A) \geq \frac{1}{3} \cdot [t(D) - st(D)]\,.$$

Solving for $t(D)$, we get:

$$t(D) \leq 3 \cdot (\left|\beta'_K\right| - 1) + st(D),$$

which implies that:

$$10v_3 \cdot (t(D) - 1) \leq 30v_3 \cdot (\left|\beta'_K\right| - 1) + 10v_3 \cdot (st(D) - 1).$$

□

Corollary 3.5.1. *Let $D(K)$ satisfy the hypotheses of the Main Theorem (Theorem 3.4.1). Furthermore, assume that each other circle of H_A has at least $m \geq 3$ incident twist region resolutions. Then K is hyperbolic and the complement of K satisfies the following volume*

bounds:

$$v_8 \cdot \left(\left|\beta'_K\right| - 1\right) \leq \mathrm{vol}(S^3 \backslash K) < \frac{m}{m-2} \cdot 10v_3 \cdot \left(\left|\beta'_K\right| - 1\right) - 10v_3.$$

Proof. First, notice that we get the lower bound on volume from Theorem 3.5.1. To get the upper bound on volume, we use the proof of Corollary 3.4.1. According to Inequality 3.10:

$$-\chi(\mathbb{G}'_A) = t(D) - \#\left\{\mathrm{OCs}\right\} \geq \frac{m-2}{m} \cdot t(D).$$

Combining this inequality with Theorem 2.3.1 gives:

$$\frac{m-2}{m} \cdot t(D) \leq -\chi(\mathbb{G}'_A) = \left|\beta'_K\right| - 1.$$

Since Theorem 2.2.2 provides an upper bound of $10v_3 \cdot (t(D) - 1)$ on volume, then our final step is to express this upper bound in terms of $\left|\beta'_K\right|$. Solving for $t(D)$, we get:

$$t(D) \leq \frac{m}{m-2} \cdot \left(\left|\beta'_K\right| - 1\right),$$

which implies that:

$$10v_3 \cdot (t(D) - 1) \leq \frac{m}{m-2} \cdot 10v_3 \cdot (\left|\beta'_K\right| - 1) - 10v_3.$$

□

Remark 3.5.2. Notice that, as $m \to \infty$, the upper bound above approaches:

$$10v_3 \cdot (\left|\beta'_K\right| - 1) - 10v_3.$$

Hence, the coefficients of $\left|\beta'_K\right|$ in the upper and lower bounds differ by a multiplicative factor of 2.7701 (in the limit).

Chapter 4

Volume Bounds for A-Adequate Plats

To provide a collection of links that satisfy the hypotheses of the Main Theorem (Theorem 3.4.1) and to seek to improve the lower bounds on volume, we now investigate a certain family of A-adequate plat diagrams. We begin by finding volume bounds solely in terms of the twist number $t(D)$. We then translate these volume bounds to be expressed in terms of the stable penultimate coefficient β'_K of the colored Jones polynomial, thus showing that the hyperbolic A-adequate plats under consideration satisfy a Coarse Volume Conjecture.

4.1 Background on Braids and Plat Closures

Recall that the braid group on n strings, called the *n-braid group* for short, has Artin presentation:

$$B_n = \left\langle \sigma_1, \cdots, \sigma_{n-1} \mid \sigma_i\sigma_j = \sigma_j\sigma_i \text{ and } \sigma_i\sigma_{i+1}\sigma_i = \sigma_{i+1}\sigma_i\sigma_{i+1} \right\rangle,$$

where the first relation (sometimes called *far commutativity*) occurs whenever $|i-j| \geq 2$ and the second relation occurs whenever $1 \leq i \leq n-2$.

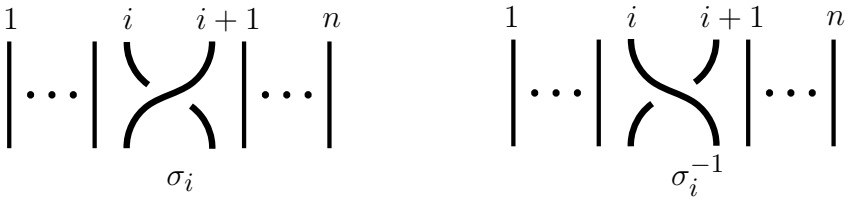

Figure 4.1: The generators σ_i and σ_i^{-1} of the n-braid group B_n, where $1 \leq i \leq n-1$.

The braid group and its generators can also be represented geometrically. See Figure 4.1. The multiplication operation in the braid group is concatenation. Furthermore, we will adopt the convention that a braid word, read from left to right, is visually represented by stacking the braid generators of Figure 4.1 vertically (reading the braid word visually from the top down).

In this chapter, we will work with braids that have an even number of strings. For clarity, we give the presentation for the even-stringed braid group B_{2n} below.

$$B_{2n} = \left\langle \sigma_1, \cdots, \sigma_{2n-1} \mid \sigma_i\sigma_j = \sigma_j\sigma_i \text{ and } \sigma_i\sigma_{i+1}\sigma_i = \sigma_{i+1}\sigma_i\sigma_{i+1} \right\rangle,$$

where the first relation occurs whenever $|i-j| \geq 2$ and the second relation occurs whenever $1 \leq i \leq 2n-2$. Within B_{2n}, define the following braid words:

- $\beta_e^j = \sigma_2^{r_2^j}\sigma_4^{r_4^j}\cdots\sigma_{2n-2}^{r_{2n-2}^j}$, where either $r_i^j \leq -3$ or $r_i^j \geq 1$.
- $\beta_o^j = \sigma_1^{r_1^j}\sigma_3^{r_3^j}\cdots\sigma_{2n-1}^{r_{2n-1}^j}$, where $r_i^j \leq -2$.

The types of $2n$-braids that we will consider in this chapter are of the form:

$$\beta = \beta_e^1\beta_o^1\beta_e^2\beta_o^2\cdots\beta_e^k\beta_o^k\beta_e^{k+1} \in B_{2n},$$

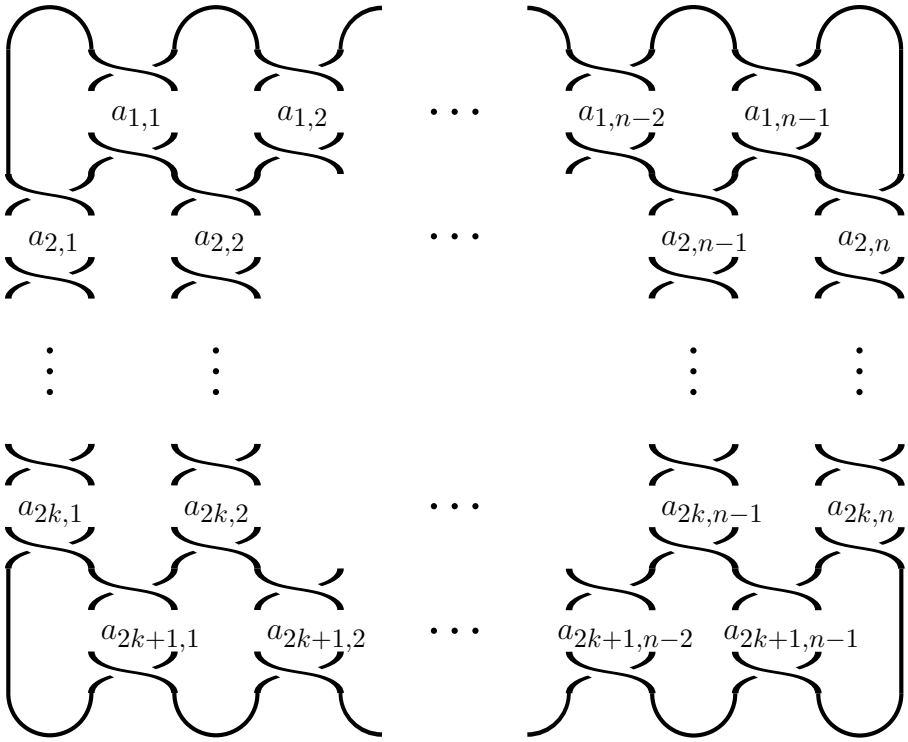

Figure 4.2: A schematic for a $2n$-plat diagram with $m = 2k + 1$ rows of twist regions, where the entry in the i^{th} row and j^{th} column is a twist region containing $a_{i,j}$ crossings (counted with sign). The twist regions depicted above are negative twist regions. Having $a_{i,j} > 0$ instead will reflect the crossings in the relevant twist region.

where $k \geq 1$ and $n \geq 3$. Call such a braid β of *negative-type* if $r_i^j < 0$ for all i and j in the braid word β and call β of *mixed-type* otherwise.

For an even-stringed braid $\beta \in B_{2n}$ of the type above, we form the *plat closure* of β (the result of which is called a *2n-plat*) by connecting the ends of consecutive braid strings by trivial semi-circular arcs. See Figure 4.2 for a schematic depiction of the plat closure of β.

Definition 4.1.1. A *negative plat diagram* is the plat closure of a negative-type braid and a *mixed-sign plat diagram* is the plat closure of a mixed-type braid. See the left side of Figure 4.3 for an example of a negative plat diagram and see the left side of Figure 4.4 for an example of a mixed-sign plat diagram.

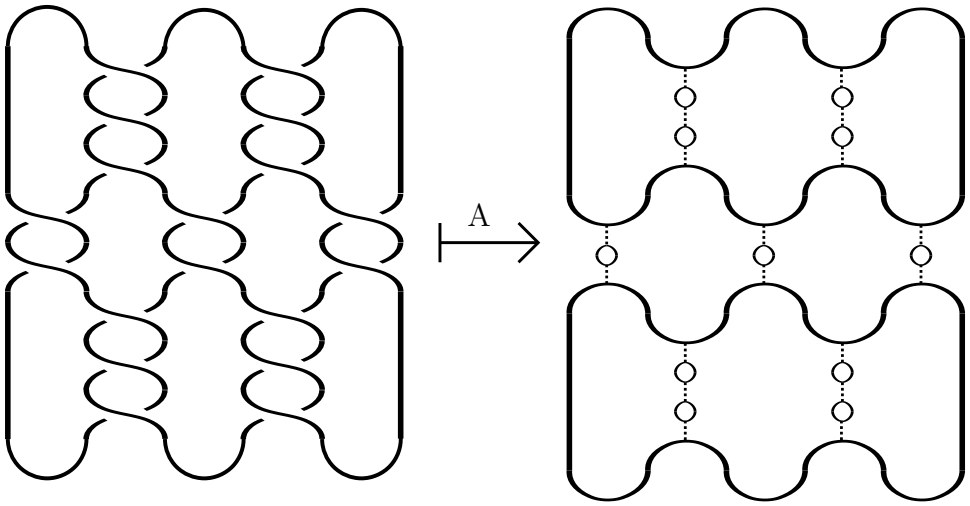

Figure 4.3: An example of a negative plat diagram and its all-A state.

Let $D(K)$ denote a negative or mixed-sign plat diagram. Furthermore, let $D(K)$ have $m = 2k + 1$ rows of twist regions. Specifically, if we number the rows of twist regions from the top down, then there are $k + 1$ odd-numbered rows, each of which contains $n - 1$ twist regions, and k even-numbered rows, each of which contains n twist regions. Index the twist regions according to row and column (where by column we really mean the left-to-right ordering of twist regions in a given row). Denote the number of twist regions in row i and column j (counted with sign) by $a_{i,j}$, where $1 \leq i \leq m$ and:

$$\begin{cases} 1 \leq j \leq n-1 & \text{if } i \text{ is odd} \\ 1 \leq j \leq n & \text{if } i \text{ is even.} \end{cases}$$

Refer back to Figure 4.2 to see this notation in use.

Remark 4.1.1. For the remainder of this chapter, the term "for all i and j" will be assumed to apply to i and j that satisfy the above conditions.

Remark 4.1.2. When $n = 1$ we have that $D(K)$ must be a (twisted) diagram of the

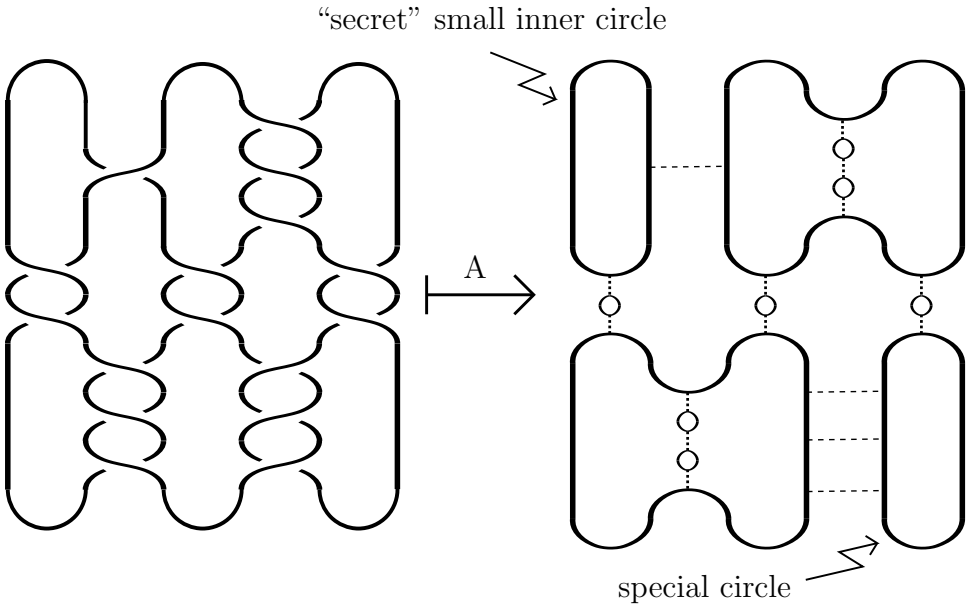

Figure 4.4: An example of a mixed-sign plat diagram and its all-A state. Note that the diagram above is obtained from the negative plat diagram of Figure 4.3 by changing the first negative twist region with three crossings to a positive twist region with a single crossing and changing the last negative twist region with three crossings to a positive twist region with three crossings. These changes create a "secret" small inner circle and a special circle, respectively.

unknot, which is not hyperbolic and will not be considered. When $n = 2$ we have that $D(K)$ represents a two-bridge link K. Using the fact that two-bridge links are alternating, let $D = D_{alt}(K)$ denote a reduced alternating diagram of K. It will be shown later that the plats considered in this work are all hyperbolic. Therefore, by Theorem B.3 of [8], we get the following volume bounds:

$$2v_3 \cdot t(D) - 2.7066 < \text{vol}(S^3 - K) < 2v_8 \cdot (t(D) - 1)\,.$$

Note that the coefficients of $t(D)$ in the upper and lower bounds above differ by a multiplicative factor of $3.6100\ldots$. Since we have the above volume bounds when $n = 2$, then will assume for the remainder of this chapter that $n \geq 3$.

Remark 4.1.3. When $k = 0$ (and $n \geq 3$) we have that $D(K)$ represents a connected sum of

two or more standard torus link diagrams, which is not hyperbolic and will not be considered. Hence, the assumption that $k \geq 1$ is a natural one to make.

4.2 Volume Bounds for Negative Plats in Terms of $t(D)$

In this section, we show that negative plat diagrams satisfy the assumptions of the Main Theorem (Theorem 3.4.1). By studying the specific structure of these diagrams, we are able to improve the lower bound on volume provided by the theorem.

Theorem 4.2.1. *Let $D(K)$ be a negative plat diagram (where $k \geq 1$, where $n \geq 3$, where $a_{i,j} \leq -3$ in odd-numbered rows, and where $a_{i,j} \leq -2$ in even-numbered rows). Then $D(K)$ is a connected, prime, A-adequate link diagram that satisfies the TELC, contains $t(D) \geq 7$ twist regions, and contains $st(D) = 0$ special tangles. Furthermore, K is hyperbolic and the complement of K satisfies the following volume bounds:*

$$\frac{4v_8}{5} \cdot (t(D) - 1) + \frac{v_8}{5} \leq \text{vol}(S^3 - K) < 10v_3 \cdot (t(D) - 1)\,.$$

For an example of a plat diagram that satisfies the assumptions above, see the left side of Figure 4.3. Having such a figure in mind will help when considering the proof of Theorem 4.2.1 (which is given below).

Proof of Theorem 4.2.1. Since $a_{i,j} \neq 0$ for all i and j, then $D(K)$ must be a connected link diagram. See Figure 4.2 for visual support.

Since we have that $k \geq 1$, that $n \geq 2$, and that $a_{i,j} \neq 0$ for all i and j, then by careful and methodical inspection we get that $D(K)$ is prime. To see this, let C denote a simple closed curve in the projection plane that intersects $D(K)$ twice transversely (away from the crossings) and let p be an arbitrary base point for C. Considering the possible locations of p in $S^2 \backslash D(K)$ (perhaps using Figure 4.3 to assist in visualization), it can be seen that it is impossible for C to both close up and contain crossings on both sides. Thus, $D(K)$ is indeed a prime link diagram.

By inspecting H_A, we get that $D(K)$ is A-adequate since $a_{i,j} \leq -2$ in odd-numbered rows. To see this, first notice that the vertical A-segments between (the necessarily distinct) other circles can never contribute to non-A-adequacy. Second, notice that the vertical A-segments within a given other circle either connect distinct small inner circles or connect an other circle to a small inner circle. Therefore, since no A-segment connects a circle to itself, then $D(K)$ is A-adequate.

The assumptions that $a_{i,j} \leq -3$ in odd-numbered rows and $a_{i,j} \leq -2$ in even-numbered rows guarantee that $D(K)$ satisfies the TELC. To be specific, having $a_{i,j} \leq -2$ in even-numbered rows forces there to always be at least one small inner circle to act as a buffer between adjacent other circles, making it is impossible for two given other circles to share any (let alone two) A-segments. Furthermore, notice that a small inner circle from an even-numbered row must always connect to a pair of distinct circles. Next, having $a_{i,j} \leq -3$ in odd-numbered rows guarantees that there are at least two inner circles for each odd-rowed twist region, which prevents an other circle from connecting to an interior small inner circle and then back to itself along another A-segment. Finally, by construction, it is impossible for a pair of small inner circles to share more than one A-segment. Since we have just shown

that no two all-A circles share more than one A-segment, then the TELC is trivially satisfied.

By inspection, we have that $D(K)$ contains $t(D) \geq 7 \geq 2$ regions. Combining this fact with what was shown above and using Proposition 2.2.1, we can conclude that K is hyperbolic. Inspection also shows that $st(D) = 0$, because each other circle is incident to at least five twist region resolutions.

It remains to show that K satisfies the desired volume bounds. Since there is one other circle (OC) of H_A corresponding to each odd row of twist regions in $D(K)$, then we have that:

$$\#\{\text{OCs}\} = k + 1.$$

Applying Lemma 3.2.1 gives:

$$-\chi(\mathbb{G}'_A) = t(D) - \#\{\text{OCs}\} = t(D) - k - 1.$$

We would now like to eliminate the dependence of $-\chi(\mathbb{G}'_A)$ on k. Expand $t(D)$ as:

$$\begin{aligned} t(D) &= \#(\text{odd-numbered rows}) \cdot \#(\text{twist regions per odd row}) \\ &\quad + \#(\text{even-numbered rows}) \cdot \#(\text{twist regions per even row}) \\ &= (k+1)(n-1) + kn. \end{aligned}$$

Since $n \geq 3$, then:

$$t(D) = (k+1)(n-1) + kn = 2kn - k + n - 1 \geq 5k + 2,$$

which implies that:

$$k \leq \frac{t(D) - 2}{5}.$$

Thus, we get the following:

$$-\chi(\mathbb{G}'_A) = t(D) - k - 1 \geq t(D) - \left(\frac{t(D) - 2}{5}\right) - 1 = \frac{4}{5} \cdot (t(D) - 1) + \frac{1}{5}. \tag{4.1}$$

By applying Theorem 2.2.2, we have the desired volume bounds.

□

4.3 Applying the Main Theorem to Negative Plats

In this section, we apply the Main Theorem (actually we apply Corollary 3.4.1) to obtain volume bounds for the family of negative plats considered in this work. Furthermore, we compare these volume bounds to those found in Theorem 4.2.1.

Proposition 4.3.1. *Applying Corollary 3.4.1 to the negative plats of Theorem 4.2.1, we get that:*

$$\frac{3v_8}{5} \cdot t(D) \leq \mathrm{vol}(S^3 \backslash K) < 10v_3 \cdot (t(D) - 1)$$

Proof. By the conclusions of Theorem 4.2.1, we see that we can apply Theorem 3.4.1. In fact, inspection of the all-A state H_A shows that each other circle is incident to at least $m \geq 5$ twist region resolutions. Using either this observation or using Theorem 4.2.1, we have that $st(D) = 0$ for $D(K)$ a negative plat diagram. Therefore, by applying Corollary 3.4.1, we get the desired volume bounds. □

Let us now compare the lower bounds of Proposition 4.3.1 to those of Theorem 4.2.1. We would like to determine exactly when the lower bounds given by our study of negative plats are an improvement over those that result from applying Corollary 3.4.1 (using Proposition 4.3.1).

For the negative plats considered in this thesis, we have that:

$$\frac{4v_8}{5} \cdot (t(D) - 1) + \frac{v_8}{5} \geq \frac{3v_8}{5} \cdot t(D)$$

is equivalent to the condition that $t(D) \geq 3$. But this condition is always satisfied because we have shown in the proof of Theorem 4.2.1 that $t(D) \geq 7$. Therefore, the lower bound found in Theorem 4.2.1 is always sharper than the lower bound provided by applying Corollary 3.4.1 (using Proposition 4.3.1).

4.4 Volume Bounds for Mixed-Sign Plats in Terms of $t(D)$

In this section, we first show that we can alter the negative plat diagrams considered in this work to get new plat diagrams that enjoy the same nice properties as the original negative plat diagrams. Specifically, we show that our new plat diagrams (which will be mixed-sign plat diagrams) satisfy the assumptions of the Main Theorem (Theorem 3.4.1). By studying the specific structure of these diagrams, we are often able to improve the lower bound on volume provided by the theorem.

Beginning with a negative plat diagram that satisfies the hypotheses of Theorem 4.2.1, we may iteratively change any of the negative twist regions in the odd-numbered rows to positive twist regions. Furthermore, the positive twist regions need only contain at least one crossing. For an example of this process, see Figure 4.3 and Figure 4.4.

Notation: Let $t^+(D)$ and $t^-(D)$ denote the number of positive and negative twist regions in $D(K)$, respectively.

Remark 4.4.1. Changing an arbitrary negative twist region of an odd-numbered row to a positive twist region will break the relevant other circle into two all-A circles. This is because a long twist region is changed to a one-crossing or short twist region. In the relevant part of the new all-A state, all but one of the new horizontal A-segments correspond to redundant parallel edges of $\mathbb{G}_A$. Thus, this entire new positive twist region corresponds to a single edge of $\mathbb{G}'_A$. These remarks hold true during every iteration of the procedure mentioned above.

Theorem 4.4.1. *Let $D(K)$ be a mixed-sign plat diagram (where $k \geq 1$, where $n \geq 3$, where $a_{i,j} \leq -3$ or $a_{i,j} \geq 1$ in odd-numbered rows, and where $a_{i,j} \leq -2$ in even-numbered rows). Then $D(K)$ is a connected, prime, A-adequate link diagram that satisfies the TELC, contains $t(D) \geq 3$ twist regions, and contains $st(D) \leq 4$ special tangles. Furthermore, K is hyperbolic and the complement of K satisfies the following volume bounds:*

$$\frac{v_8}{3} \cdot \left(2t^-(D) - 1\right) - \frac{2v_8}{3} \leq \text{vol}(S^3 \backslash K) < 10v_3 \cdot (t(D) - 1)\,.$$

If we also have that $D(K)$ contains at least as many negative twist regions as it does positive twist regions, then:

$$\frac{v_8}{3} \cdot (t(D) - 1) - \frac{2v_8}{3} \leq \text{vol}(S^3 \backslash K) < 10v_3 \cdot (t(D) - 1)\,.$$

Proof of Theorem. The proofs of the connectedness and primeness of $D(K)$ are the same as those found in the proof of Theorem 4.2.1 and the proof that $D(K)$ is A-adequate is very similar. The only new observation that is needed is that any horizontal A-segments coming from positive twist regions necessarily connect distinct all-A circles. The proof that $D(K)$ satisfies the TELC is also similar to that found in the proof of Theorem 4.2.1, but two-edge loops may now exist. The new possibility that $a_{i,j} \geq 1$ in odd-numbered rows will give rise to two-edge loops whenever $a_{i,j} \geq 2$. These two-edge loops come from the same short twist region and are, therefore, allowed by the TELC.

Inspection of H_A shows that the mixed-sign plat diagrams under consideration contain at least $7 - 4 = 3$ twist regions. This is because having $a_{i,j} = 1$ in any of the four corners

of $D(K)$ means that the corresponding state circles of H_A in those corners will be "secret" small inner circles rather than other circles and, consequently, we may have that potentially different twist regions are actually part of a single twist region. See Figure 4.4 for an example.

Using what was shown above, we can apply Proposition 2.2.1 to conclude that K is hyperbolic. Furthermore, inspection of H_A shows that, unlike for negative plat diagrams, special circles can actually occur in mixed-sign plat diagrams. However, special circles can only possibly occur at the four corners of the link diagram. This is because, by the assumption that $a_{i,j} \neq 0$ for all i and j, all but at most the four corner other circles must be incident to three or more twist region resolutions. See Figure 4.4 for an example. Therefore, we have that $st(D) \leq 4$. It remains to show that K satisfies the desired volume bounds.

Recall the observation that we may start with a negative plat diagram and iteratively change any of the negative twist regions in the odd-numbered rows to positive twist regions. Specifically, such an alteration creates either a new other circle (OC) or a new "secret" small inner circle. Thus, after changing some or all of the allowed negative twist regions to positive twist regions, we have that:

$$\#\{\text{OCs}\} \leq k + 1 + t^+(D).$$

Applying Lemma 3.2.1 gives:

$$-\chi(\mathbb{G}'_A) = t(D) - \#\{\text{OCs}\} \geq t(D) - k - 1 - t^+(D) = t^-(D) - k - 1.$$

Recall that, by construction, we can only have positive twist regions in odd-numbered rows.

Thus, all of the even-numbered rows must still contain only negative twist regions. Said another way:

$$\begin{aligned} t^-(D) &\geq \#(\text{even-numbered rows}) \cdot \#(\text{twist regions per even row}) \\ &= k \cdot n. \end{aligned} \tag{4.2}$$

We would now like to eliminate the dependence of $-\chi(\mathbb{G}'_A)$ on k. Since $t^-(D) \geq kn$, then the assumption that $n \geq 3$ gives:

$$k \leq \frac{t^-(D)}{n} \leq \frac{t^-(D)}{3}.$$

Therefore, we get:

$$-\chi(\mathbb{G}'_A) \geq t^-(D) - k - 1 \geq t^-(D) - \frac{t^-(D)}{3} - 1 = \frac{1}{3} \cdot (2t^-(D) - 1) - \frac{2}{3}.$$

Now suppose that $D(K)$ contains at least as many negative twist regions as it does positive twist regions, so that we have $t^-(D) \geq t^+(D)$. This implies that:

$$2t^-(D) = t^-(D) + t^-(D) \geq t^-(D) + t^+(D) = t(D),$$

which then implies that:

$$-\chi(\mathbb{G}'_A) \geq \frac{1}{3} \cdot (2t^-(D) - 1) - \frac{2}{3} \geq \frac{1}{3} \cdot (t(D) - 1) - \frac{2}{3}. \tag{4.3}$$

By applying Theorem 2.2.2, we have the desired volume bounds.

□

Remark 4.4.2. Note that the lower bounds on volume in terms of $t^-(D)$ will be sharper than those in terms of $t(D)$ in the case that $D(K)$ is a mixed-sign plat with more negative twist regions than positive twist regions. Furthermore, as the disparity between the number of negative and positive twist regions increases, the lower bound on volume in terms of $t^-(D)$ will become increasingly sharper than the lower bound on volume in terms of $t(D)$.

Remark 4.4.3. To conclude our study of mixed-sign plats, we would like to find a sufficient condition to guarantee that the mixed-sign plats considered in this work also contain at least as many negative twist regions as positive twist regions.

For negative plats, recall that Equation 4.1 gives that $t(D) = (k+1)(n-1) + kn$. Since (as mentioned in the above proof of Theorem 4.4.1) the process to change a negative plat into a mixed-sign plat may create a situation where potentially different twist regions are actually part of a single twist region, then Equation 4.1 becomes the inequality:

$$t(D) \leq (k+1)(n-1) + kn$$

for mixed-sign plats. Also, since the even-numbered rows of a mixed-sign plat must contain only negative twist regions, then Inequality 4.2 gives that $t^-(D) \geq kn$. Combining this

information, we get:

$$t^-(D) + t^+(D) = t(D) \leq (k+1)(n-1) + kn \leq (k+1)(n-1) + t^-(D),$$

which implies that:

$$t^+(D) \leq (k+1)(n-1) = kn + n - k - 1 \leq t^-(D) + n - k - 1.$$

Thus, to guarantee that $t^-(D) \geq t^+(D)$, we need that $n - k - 1 \leq 0$. But this condition is equivalent to $k \geq n - 1$ is equivalent to $m = 2k + 1 \geq 2n - 1$. Therefore, to guarantee that the mixed-sign plats considered in this work contain at least as many negative twist regions as positive twist regions, we need that the mixed-sign plats must contain at least $2n-1$ rows of twist regions.

4.5 Applying the Main Theorem to Mixed-Sign Plats

In this section, we apply the Main Theorem (Theorem 3.4.1) to obtain volume bounds for the family of mixed-sign plats considered in this work. Furthermore, we compare these volume bounds to those found in Theorem 4.4.1 (at least for the mixed-sign plats that contain at least as many negative twist regions as positive twist regions).

Proposition 4.5.1. *Applying Theorem 3.4.1 to the mixed-sign plats of Theorem 4.4.1, we get that:*

$$\frac{v_8}{3} \cdot (t(D) - 4) \leq \text{vol}(S^3 \backslash K) < 10v_3 \cdot (t(D) - 1)$$

Proof. By the conclusions of Theorem 4.4.1, we see that we can apply Theorem 3.4.1. Theorem 4.4.1 also shows that $st(D) \leq 4$ for $D(K)$ a mixed-sign plat diagram. Therefore, by applying Theorem 3.4.1, we get the desired volume bounds. □

Let us now compare the lower bounds of Proposition 4.5.1 to those of Theorem 4.4.1, at least for the mixed-sign plats that contain at least as many negative twist regions as positive twist regions. We would like to determine exactly when the lower bounds given by our study of such mixed-sign plats are an improvement over those that result from applying Theorem 3.4.1 (using Proposition 4.5.1).

For the mixed-sign plats considered in this work (that contain at least as many negative twist regions as positive twist regions), we have that:

$$\frac{v_8}{3} \cdot (t(D) - 1) - \frac{2v_8}{3} \geq \frac{v_8}{3} \cdot (t(D) - 4)$$

is equivalent to the condition that $-1 \geq -\frac{4}{3}$. But this condition is always satisfied. Therefore, the lower bound found in Theorem 4.4.1 is always (slightly) sharper than the lower bound provided by applying Theorem 3.4.1 (using Proposition 4.5.1).

4.6 Volume Bounds for Plats in Terms of the Colored Jones Polynomial

To conclude our study of volume bounds for hyperbolic A-adequate plats, we will translate our diagrammatic volume bounds (in terms of $t(D)$) to volume bounds in terms of the stable penultimate coefficient β'_K of the colored Jones polynomial. We shall prove the following theorems:

Theorem 4.6.1. *Let $D(K)$ be a negative plat diagram (where $n \geq 3$). Then $D(K)$ is a connected, prime, A-adequate link diagram that satisfies the TELC, contains $t(D) \geq 7$ twist regions, and contains $st(D) = 0$ special tangles. Furthermore, K is hyperbolic and the complement of K satisfies the following volume bounds:*

$$v_8 \cdot \left(\left|\beta'_K\right| - 1\right) \leq \text{vol}(S^3 - K) < \frac{25v_3}{2} \cdot \left(\left|\beta'_K\right| - 1\right) - \frac{5v_3}{2}.$$

Theorem 4.6.2. *Let $D(K)$ be a mixed-sign plat diagram (where $n \geq 3$) that contains at least as many negative twist regions as it does positive twist regions. Then $D(K)$ is a connected, prime, A-adequate link diagram that satisfies the TELC, contains $t(D) \geq 3$ twist regions, and contains $st(D) \leq 4$ special tangles. Furthermore, K is hyperbolic and the complement of K satisfies the following volume bounds:*

$$v_8 \cdot \left(\left|\beta'_K\right| - 1\right) \leq \text{vol}(S^3 - K) < 30v_3 \cdot \left(\left|\beta'_K\right| - 1\right) + 20v_3.$$

Combined Proof of Both Theorems. To begin, note that Theorem 4.2.1 and Theorem 4.4.1

combine to give all but the volume bounds. Theorem 3.5.1 gives the desired lower bounds on volume. Since Theorem 2.2.2 provides $10v_3 \cdot (t(D) - 1)$ as an upper bound on volume, then we will have written the volume bounds in terms of the coefficients of the colored Jones polynomial (specifically, in terms of $\left|\beta'_K\right|$) if we are able to bound $t(D)$ above by a function of $\left|\beta'_K\right|$.

By Theorem 2.3.1 and Inequality 4.1 for negative plat diagrams, we get that:

$$\left|\beta'_K\right| - 1 = -\chi(\mathbb{G}'_A) \geq \frac{4}{5} \cdot (t(D) - 1) + \frac{1}{5},$$

which implies that:

$$t(D) - 1 \leq \frac{5}{4} \cdot (\left|\beta'_K\right| - 1) - \frac{1}{4},$$

which implies that:

$$10v_3 \cdot (t(D) - 1) \leq \frac{25v_3}{2} \cdot (\left|\beta'_K\right| - 1) - \frac{5v_3}{2}.$$

This gives the desired result for negative plats.

Now assume that $D(K)$ is a mixed-sign plat diagram with at least as many negative twist regions as positive twist regions. By Theorem 2.3.1 and Inequality 4.3 for mixed-sign plat diagrams, we get:

$$\left|\beta'_K\right| - 1 = -\chi(\mathbb{G}'_A) \geq \frac{1}{3} \cdot (t(D) - 1) - \frac{2}{3},$$

which implies that:

$$t(D) - 1 \leq 3 \cdot (\left|\beta'_K\right| - 1) + 2,$$

which implies that:

$$10v_3 \cdot (t(D) - 1) \leq 30v_3 \cdot (\left|\beta'_K\right| - 1) + 20v_3.$$

This gives the desired result for mixed-sign plats with at least as many negative twist regions as positive twist regions.

□

Chapter 5

Volume Bounds for A-Adequate Closed Braids

To provide a second collection of links that satisfy the hypotheses of the Main Theorem (Theorem 3.4.1) and to seek to improve the lower bounds on volume, we now investigate a certain family of A-adequate closed braid diagrams. We begin by finding volume bounds solely in terms of the twist number $t(D)$. We then translate these volume bounds to be expressed in terms of the penultimate coefficient β'_K of the colored Jones polynomial, thus showing that the hyperbolic A-adequate closed braids under consideration satisfy a Coarse Volume Conjecture.

5.1 Braid Closure and Cyclic Reduction of Braid Words

We now return to n-braids and consider a second type of closure operation (viewing the the plat closure of even-stringed braids as the first type of closure). Let $\beta \in B_n$ denote an n-braid. To form the *braid closure* of β means that, for all braid string positions $1 \leq i \leq n$, we identify the top of the string in the i^{th} position with the bottom of string in the i^{th} position. We denote the braid closure of β by $\widehat{\beta}$. See Figure 5.1 for a schematic depiction of a braid closure.

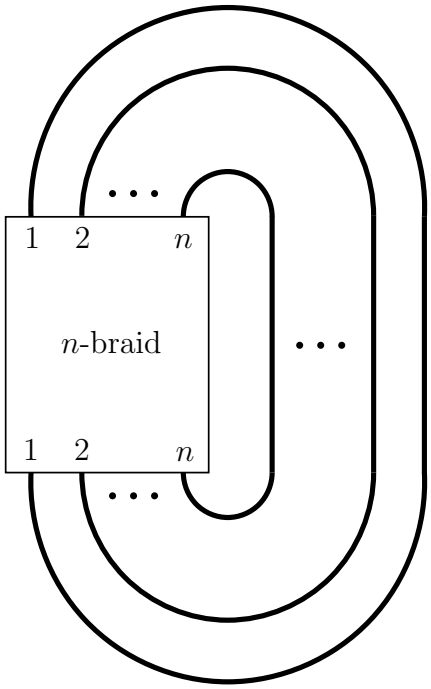

Figure 5.1: The closure of an n-braid.

Definition 5.1.1. Call a subword γ of $\beta \in B_n$ *(cyclically) induced* if the letters of γ are all adjacent up to cyclic permutation of the braid word β and if these letters appear in the same order as in the braid word β.

As an example, given the braid word:

$$\beta = \sigma_1^3\sigma_2^{-3}\sigma_1^2\sigma_3^{-2}\sigma_2\sigma_3 = \sigma_1^3\sigma_2^{-1}(\sigma_2^{-2}\sigma_1^2\sigma_3^{-1})\sigma_3^{-1}\sigma_2\sigma_3,$$

the subword $\gamma = \sigma_2^{-2}\sigma_1^2\sigma_3^{-1}$ is an induced subword of β but the subword $\gamma' = \sigma_2^{-2}\sigma_1^2\sigma_2$ is not an induced subword of β.

Because conjugate braids have isotopic braid closures and because our focus will ultimately be on links that are braid closures, we will work within conjugacy classes of braids. Furthermore, note that cyclic permutation is a special case of conjugation.

Definition 5.1.2. As in [26], call a braid $\beta = \sigma_{m_1}^{r_1}\sigma_{m_2}^{r_2}\cdots\sigma_{m_l}^{r_l} \in B_n$ *cyclically reduced into syllables* if the following hold:

(1) for all j, we have that $r_j \neq 0$

(2) for all j, (looking up to cyclic permutation) we have that there are no occurrences of cyclically induced subwords of the form $\sigma_j\sigma_j^{-1}$ or $\sigma_j^{-1}\sigma_j$

(3) for all j (modulo l), we have that $m_j \neq m_{j+1}$

Definition 5.1.3. Let $\beta = \sigma_i^{r_1}\sigma_j^{r_2}\cdots\sigma_i^{r_{2l-1}}\sigma_j^{r_{2l}}$ denote a 3-braid that has been cyclically reduced into syllables, where $\{i, j\} = \{1, 2\}$. As was done in [26], form the *exponent vector* $(r_1, r_2, \ldots, r_{2l})$ of β.

Definition 5.1.4. Call an n-braid $\beta \in B_n$ *positive* if all of its exponents are positive and call β *negative* if all of its exponents are negative.

5.2 A-Adequacy for Closed 3-Braids

We now present Stoimenow's ([26]) classification of A-adequate closed 3-braids. We also present the proof of this result (which was left to the reader) since the methodology and perspective will be useful in what follows.

Proposition 5.2.1 ([26], Lemma 6.1)**.** *Let $D(K) = \widehat{\beta}$ denote the closure of a 3-braid $\beta = \sigma_i^{r_1}\sigma_j^{r_2}\cdots\sigma_i^{r_{2l-1}}\sigma_j^{r_{2l}}$, where $\{i, j\} = \{1, 2\}$ and where β has been cyclically reduced into syllables. Furthermore, assume that $l \geq 2$ (which says that the exponent vector has length at least four). Then $D(K)$ is A-adequate if and only if either:*

(1) β is positive, or

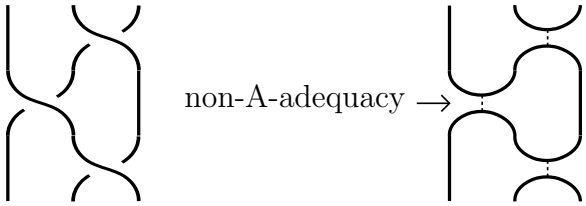

Figure 5.2: The subdiagram of a closed 3-braid diagram corresponding to a subword $\sigma_2^{-1}\sigma_1^{-1}\sigma_2^{-1}$ (left) and the corresponding portion of the all-A state that exhibits the non-A-adequacy of $D(K)$ (right).

(2) β does not contain $\sigma_1^{-1}\sigma_2^{-1}\sigma_1^{-1} = \sigma_2^{-1}\sigma_1^{-1}\sigma_2^{-1}$ as a cyclically induced subword and β also has the property that all positive entries of the exponent vector are cyclically isolated (meaning they must be adjacent to negative entries on both sides).

Remark 5.2.1. The condition that positive entries of the exponent vector be cyclically isolated can equivalently be phrased as the condition that *positive syllables* in the braid word (of the form σ_i^p for $p > 0$) must be cyclically adjacent to *negative syllables* (of the form $\sigma_j^{n'}$ for $n' < 0$) on both sides, where $\{i, j\} = \{1, 2\}$.

Proof of Proposition. ($\Rightarrow$) We shall proceed by contraposition.

Case 1: Suppose β is not positive and that β contains $\sigma_1^{-1}\sigma_2^{-1}\sigma_1^{-1} = \sigma_2^{-1}\sigma_1^{-1}\sigma_2^{-1}$ as a cyclically induced subword. From the portion of the all-A state H_A corresponding to this subword, it can be seen that $D(K)$ is not A-adequate. (See Figure 5.2.)

Case 2: Suppose β is not positive and that there exist cyclically adjacent positive syllables in the braid word. Since β is not positive, then there must exist at least one negative syllable in the braid word. Choose a pair of cyclically adjacent positive syllables that are are immediately followed by a negative syllable. Hence, β must have a subword of the form $\sigma_i^{p_1}\sigma_j^{p_2}\sigma_i^{n'}$, where $p_1, p_2 > 0$ are positive integers, where $n' < 0$ is a negative integer, and

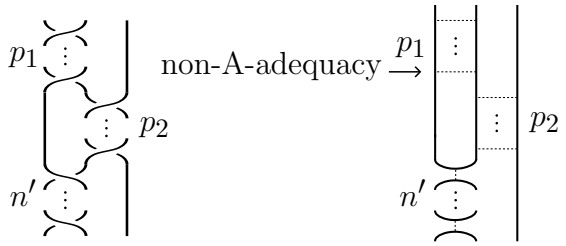

Figure 5.3: The subdiagram of a closed 3-braid diagram corresponding to a subword $\sigma_1^{p_1}\sigma_2^{p_2}\sigma_1^{n'}$, where the p_i are positive integers and n' is a negative integer (left), and the corresponding portion of the all-A state that exhibits the non-A-adequacy of $D(K)$ (right).

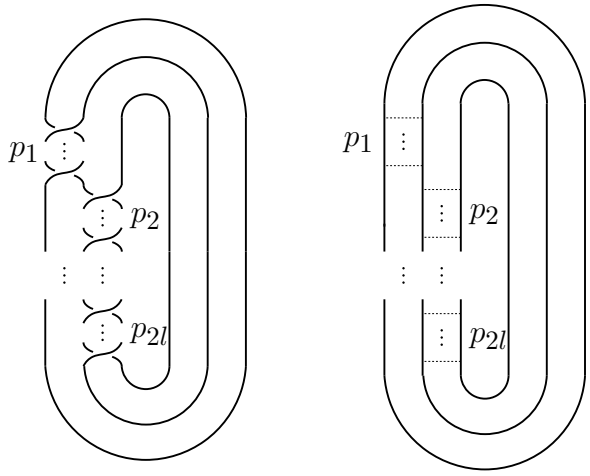

Figure 5.4: A positive closed 3-braid diagram (left) and the corresponding all-A state that exhibits the A-adequacy of $D(K)$ (right).

where $\{i, j\} = \{1, 2\}$. From the portion of the all-A state H_A corresponding to this subword, it can be seen that $D(K)$ is not A-adequate. (See Figure 5.3.)

($\Leftarrow$)

Case 1: Assume $D(K)$ is a positive closed 3-braid. From the corresponding all-A state H_A it can be seen that $D(K)$ is A-adequate. (See Figure 5.4.)

Case 2: Assume β does not contain $\sigma_1^{-1}\sigma_2^{-1}\sigma_1^{-1} = \sigma_2^{-1}\sigma_1^{-1}\sigma_2^{-1}$ as a cyclically induced subword and assume β has the property that all positive entries of the exponent vector are cyclically isolated (which implies that β cannot be positive). For a contradiction, suppose

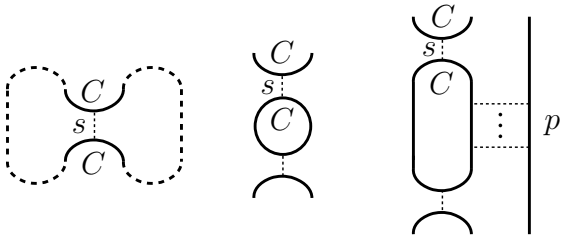

Figure 5.5: Potential non-A-adequacy coming from σ_1^{-1}. From the perspective of the all-A state H_A, the vertical segment s coming from σ_1^{-1} is assumed to join a state circle C to itself (left). Also depicted are the case where σ_1^{-1} is followed by another copy of σ_1^{-1} (center) and the case where σ_1^{-1} is followed a positive syllable σ_2^p, which must then be followed by the letter σ_1^{-1} (right).

$D(K)$ is not A-adequate.

Subcase 1: Suppose non-A-adequacy comes from the occurrence of σ_1^{-1} (or, symmetrically, σ_2^{-1}) in the braid word. Since the argument is very similar, we will not consider the symmetric case. Having non-A-adequacy in this setting means that when we A-resolve the crossing of $D(K)$ corresponding to σ_1^{-1}, the corresponding vertical A-segment of H_A, call it s, will connect an all-A circle, call it C, to itself. (See the left side of Figure 5.5.) Let us now consider what other letters can surround σ_1^{-1} in the braid word.

First, notice that σ_1^{-1} cannot be surrounded by other copies of σ_1^{-1} on either side, as this will contradict how C must close up. (See the center of Figure 5.5.) Second, σ_1^{-1} cannot be surrounded on both sides by σ_2^{-1}, as this would imply the existence of a forbidden subword $\sigma_2^{-1}\sigma_1^{-1}\sigma_2^{-1}$, a contradiction. Thus, it must be the case that σ_1^{-1} is surrounded on at least one side by a positive syllable σ_2^p. Furthermore, since the exponent vector is assumed to have length at least four and since positive entries are assumed to be cyclically isolated, then the next adjacent letter after the positive syllable σ_2^p must be σ_1^{-1}. But then it can be seen that the A-resolution of the subword $\sigma_1^{-1}\sigma_2^p\sigma_1^{-1}$ contradicts how C must close up. (See the right side of Figure 5.5.)

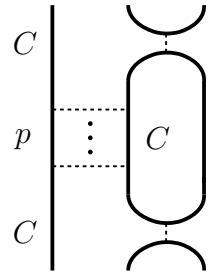

Figure 5.6: Potential non-A-adequacy coming from a positive syllable σ_1^p. From the perspective of the all-A state H_A, the horizontal A-segments coming from σ_1^p are assumed to join a state circle C to itself.

Subcase 2: Suppose non-A-adequacy comes from the occurrence of a positive syllable σ_1^p (or, symmetrically, σ_2^p) in the braid word. Since the argument is very similar, we will not consider the symmetric case. Having non-A-adequacy in this setting means that when we A-resolve the twist region of $D(K)$ corresponding to σ_1^p, the corresponding horizontal A-segments will connect a state circle, call it C, to itself. Since the exponent vector is assumed to have length at least four and since positive entries are assumed to be cyclically isolated, then σ_1^p must be surrounded by the same letter σ_2^{-1} on both sides. But then it can be seen that the A-resolution of the subword $\sigma_2^{-1}\sigma_1^p\sigma_2^{-1}$ contradicts how C must close up. (See Figure 5.6.)

□

5.3 State Circles of A-Adequate Closed 3-Braids

The goal of this section is to classify the possible types of all-A circles that can arise in the all-A state of an A-adequate closed 3-braid.

Proposition 5.3.1. *Let $\beta = \sigma_i^{r_1}\sigma_j^{r_2}\cdots\sigma_i^{r_{2l-1}}\sigma_j^{r_{2l}}$ denote a 3-braid that has been cyclically reduced into syllables, where $l \geq 2$ and $\{i,j\} = \{1,2\}$. Assume that $D(K) = \widehat{\beta}$ is an A-adequate closed 3-braid. Then we may categorize the all-A circles of H_A into the following*

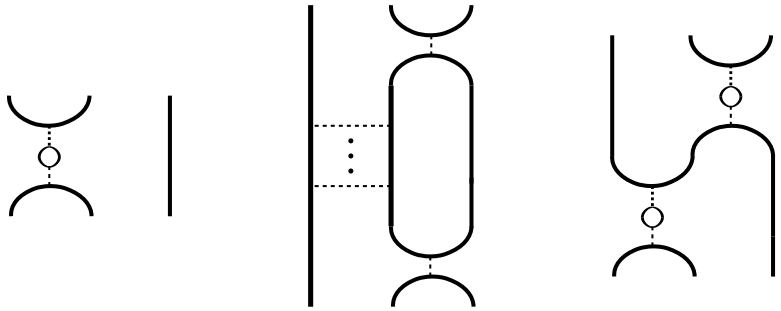

Figure 5.7: An example of a small inner circle coming from a σ_1^{-2} subword (left), an example of a medium inner circle and a potential nonwandering circle portion coming from a $\sigma_2^{-1}\sigma_1^p\sigma_2^{-1}$ subword where $p > 0$ (center), and an example of a wandering circle portion coming from a $\sigma_2^{-2}\sigma_1^{-2} = \sigma_2^{-1}(\sigma_2^{-1}\sigma_1^{-1})\sigma_1^{-1}$ subword (right).

types:

(1) small inner circles *that come from negative exponents $r_i \leq -2$ in the braid word β*

(2) medium inner circles *that come from cyclically isolated positive syllables in the braid word β*

(3) wandering circles *whose wandering arises from adjacent negative syllables in the braid word β*

(4) nonwandering circles *that come from the case when a given generator σ_i occurs with only positive exponents in the braid word β*

For depictions of the types of circles mentioned above (or portions of the types of circles mentioned above), see Figure 5.7.

Remark 5.3.1. From the 3-braid perspective, it will be important to note that the left half of Figure 2.5 depicts the A-resolution of a negative syllable (excluding a portion of a third trivial braid string). Similarly, the right half of Figure 2.5 depicts the A-resolution of a positive syllable (excluding a portion of a third trivial braid string).

Proof of Proposition. Recall that A-adequate closed 3-braids $D(K) = \widehat{\beta}$ were classified by Proposition 5.2.1 into two main types.

Case 1: Suppose β is positive. Then each all-A circle in the all-A state H_A of $D(K)$ is a nonwandering circle. (See Figure 5.4.)

Case 2: Suppose β does not contain $\sigma_1^{-1}\sigma_2^{-1}\sigma_1^{-1} = \sigma_2^{-1}\sigma_1^{-1}\sigma_2^{-1}$ as a cyclically induced subword and suppose β also has the property that all positive syllables are cyclically isolated. Since positive syllables of β are cyclically isolated, then (using cyclic permutation if needed) we may decompose β as $\beta = N_1$ (in the case that β is a negative braid) or $\beta = P_1N_1 \cdots P_tN_t$, where P_i denotes a positive syllable of β and N_i denotes a maximal length negative induced subword of β.

Small Inner Circles: Let $\sigma_i^{n'}$ denote a negative syllable. Then, except for the additional vertical trivial braid string portion to the right or left (depending on whether $i = 1$ or $i = 2$), the A-resolution of this syllable will look like the left side of Figure 5.7 if $n' = -2$ and look like the left side of Figure 2.5 in general. In particular, having $n' \leq -2$ is equivalent to the existence of small inner circles.

Wandering Circles: Let $\sigma_i^{n_1}\sigma_j^{n_2} = \sigma_i^{n_1+1}\left(\sigma_i^{-1}\sigma_j^{-1}\right)\sigma_j^{n_2+1}$ denote a pair of adjacent negative syllables, where $\{i, j\} = \{1, 2\}$. Then the corresponding portion of H_A will resemble the right side of Figure 5.7 (except that the long resolutions may possibly consist of longer paths of A-segments and small inner circles). The key feature of this figure is the fact that we see a portion of a wandering circle, where the wandering behavior corresponds to the existence of the $\sigma_i^{-1}\sigma_j^{-1}$ induced subword.

Medium Inner Circles and Nonwandering Circles: Let $\sigma_i^{-1}\sigma_j^p\sigma_i^{-1}$ denote a positive syllable that is cyclically surrounded by negative letters, where $\{i,j\} = \{1,2\}$. Then the corresponding portion of H_A will resemble the center of Figure 5.7. In particular, the existence of a (cyclically isolated) positive syllable corresponds to the existence of a medium inner circle. Furthermore, a generator σ_1 or σ_2 occurring with only positive exponents (again, see the center of Figure 5.7) will correspond to a nonwandering circle.

Since the A-resolutions of all portions of the closure of $\beta = N_1$ and $\beta = P_1N_1 \cdots P_tN_t$ have been considered locally and since gluing such portions together joins wandering and potential nonwandering circle portions together, then we have the desired result.

□

5.4 Primeness, Connectedness, and Twistedness for Closed Braid Diagrams

Assume that an n-braid $\beta \in B_n$ has been cyclically reduced into syllables and let $D(K) = \widehat{\beta}$. The main goal of this section is to find sufficient conditions for the diagram $D(K)$ to be prime.

Definition 5.4.1. Call two induced subwords γ_1 and γ_2 of a given braid word β *disjoint* if the subwords share no common letters when viewed as part of β.

As an example, given the braid word:

$$\beta = \sigma_1^3\sigma_2^{-3}\sigma_1^2\sigma_3^{-2}\sigma_2\sigma_3 = \sigma_1^2(\sigma_1\sigma_2^{-3}\sigma_1)\sigma_1(\sigma_3^{-2}\sigma_2)\sigma_3,$$

the subwords $\gamma_1 = \sigma_1\sigma_2^{-3}\sigma_1$ and $\gamma_2 = \sigma_3^{-2}\sigma_2$ are disjoint induced subwords of β.

Definition 5.4.2. Call a subword $\gamma \in B_n$ of a braid word $\beta \in B_n$ *complete* if it contains, at some point, each of the generators $\sigma_1, \ldots, \sigma_{n-1}$ of B_n.

It is important to note that the generators $\sigma_1, \ldots, \sigma_{n-1}$ need not occur in any particular order and that repetition of some or all of these generators is allowed.

Proposition 5.4.1. *Let $\beta \in B_n$ be cyclically reduced into syllables. If β contains two disjoint induced complete subwords γ_1 and γ_2, then $D(K) = \widehat{\beta}$ is a prime link diagram.*

Remark 5.4.1. Note that, in the case when $n = 3$, the condition that β contains two disjoint induced complete subwords is equivalent to the condition that σ_1 and σ_2 each occur at least twice nontrivially in the braid word β is equivalent to the condition that the exponent vector of β has length at least four.

Proof of Proposition. Let γ_1 and γ_2 be two disjoint induced complete subwords of $\beta \in B_n$. See Figure 5.8 for a schematic depiction of this situation. Let C be a simple closed curve that intersects $D(K) = \widehat{\beta}$ exactly twice (away from the crossings). We need to show that C cannot contain crossings of $D(K)$ on both sides. Note that we may view a closed braid diagram as lying in an annular region of the plane. (See Figure 5.1.)

Suppose C contains a point p that lives outside of this annular region. Since C only intersects $D(K)$ twice and must start and end at p, then it must be the case that C intersects $D(K)$

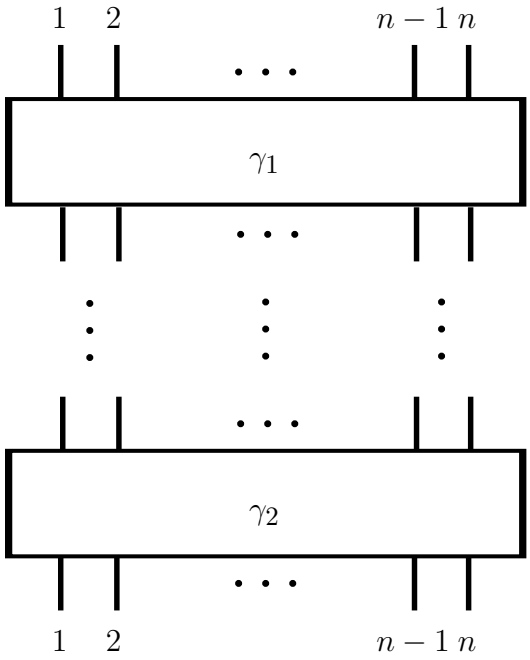

Figure 5.8: A schematic depiction of a braid $\beta \in B_n$ that contains two disjoint induced complete subwords γ_1 and γ_2.

twice in braid string position 1 or twice in braid string position n. In either case, it is impossible for such a closed curve C to contain crossings on both sides. This is because C would need to intersect $D(K)$ more than twice to be able to close up and surround crossings on both sides, and this would contradict the assumption that C intersects $D(K)$ exactly twice.

Suppose C contains a point p between braid string positions i and $i+1$ for some $1 \leq i \leq n-1$. See Figure 5.9. Since C intersects $D(K)$ exactly twice and since C is a simple closed curve, then it must be the case that C either intersects $D(K)$ twice in braid string position i or twice in braid string position $i+1$. Since β contains two disjoint induced complete subwords, then the generator σ_i, the generator σ_{i-1} (if it exists), and the generator σ_{i+1} (if it exists) must each occur at least twice, once cyclically before p and once cyclically after p. Since σ_{i-1} and σ_{i+1} occur both before and after p, then it is impossible for C to both close up and

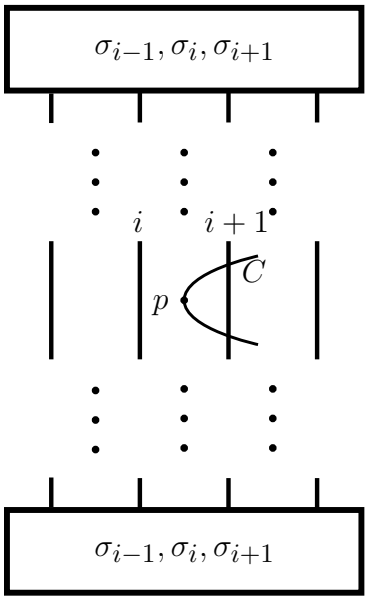

Figure 5.9: A schematic depiction of the fact that a simple closed curve C containing a point p (between braid string positions i and $i+1$) cannot contain crossings on both sides. Each box in the figure represents the eventual occurrence of the generator σ_i, the generator σ_{i-1} (if it exists), and the generator σ_{i+1} (if it exists). No assumptions are made about the order in which these generators appear or the frequency with which these generators appear.

contain crossings on both sides. This is because C is forced to cross a braid string position before encountering $\sigma_i^{\pm 1}$ (cyclically above and below), and because the occurrences of $\sigma_{i-1}^{\pm 1}$ and $\sigma_{i+1}^{\pm 1}$ (cyclically above and below) block C from being able to close up in a way that will contain crossings on both sides.

□

The assumptions about subwords of β in Proposition 5.4.1 also force $D(K)$ to have other desired properties, as seen in the proposition below.

Proposition 5.4.2. *Let $\beta \in B_n$ be cyclically reduced into syllables. If β contains two disjoint induced complete subwords γ_1 and γ_2, then $D(K) = \widehat{\beta}$ is a connected link diagram with $t(D) \geq 2(n-1)$ twist regions.*

Proof. Recall that $D(K)$ is connected if and only if the projection graph of $D(K)$ is connected. Since $\beta \in B_n$ contains a complete subword, then each generator of B_n (each of which corresponds to a crossing of $D(K)$ between adjacent braid string positions) must occur at least once. This fact implies that the closed n-braid diagram $D(K)$ must be connected. (See Figure 5.1.)

Since β contains two disjoint complete subwords, then it must be that each of the generators $\sigma_1, \ldots, \sigma_{n-1}$ of B_n must occur at least twice in (two distinct syllables of) the braid word. Since syllables of the cyclically reduced braid word β correspond to twist regions of $D(K)$, then we have that $t(D) \geq 2(n-1)$.

□

Because the majority of the braids considered in this paper will satisfy the same set of assumptions, we make the following definition.

Definition 5.4.3. Call a braid $\beta \in B_n$ *nice* if the following hold:

(1) β is cyclically reduced into syllables.

(2) β contains two disjoint induced complete subwords γ_1 and γ_2.

5.5 The Foundational Theorem for Closed Braids

Theorem 5.5.1. *Let $D(K) = \widehat{\beta}$ denote the closure of a nice n-braid $\beta = \sigma_{m_1}^{r_1} \cdots \sigma_{m_l}^{r_l}$, where $1 \leq m_1, \ldots, m_l \leq n-1$. If β satisfies the conditions:*

(1) all negative exponents $r_i < 0$ in β satisfy the stronger requirement that $r_i \leq -3$, and

(2) when $r_i > 0$, we have that $r_{i-1} < 0$ and $r_{i+1} < 0$ and either $m_{i-1} = m_{i+1} = m_i + 1$ or $m_{i-1} = m_{i+1} = m_i - 1$,

then $D(K)$ is a connected, prime, A-adequate link diagram that satisfies the TELC and contains $t(D) \geq 2(n-1)$ twist regions. Furthermore, we have that K is a hyperbolic link.

Remark 5.5.1. Condition (2) above says that positive syllables in the letter σ_{m_i} are cyclically adjacent to negative syllables in the same adjacent letter (either σ_{m_i+1} or σ_{m_i-1}). This condition extends to n-braids Stoimenow's 3-braid condition (see Proposition 5.2.1) that positive entries in the exponent vector are cyclically isolated. Condition (2) also implies that β cannot be a positive braid. Furthermore, Condition (1) above trivially satisfies Stoimenow's condition that the 3-braid does not contain $\sigma_1^{-1}\sigma_2^{-1}\sigma_1^{-1} = \sigma_2^{-1}\sigma_1^{-1}\sigma_2^{-1}$ as an induced subword. Hence, to conclude A-adequacy (among other things) for braids with $n \geq 3$ strings, we generalize one of Stoimenow's two conditions and impose further restrictions on the other.

Definition 5.5.1. Since $\beta \in B_n$ is cyclically reduced into syllables, then the positive syllables σ_i^p of β (where $p > 0$) correspond to what we will call *positive twist regions* of $D(K)$ and the negative syllables $\sigma_i^{n'}$ of β (where $n' < 0$) correspond to what we will call *negative twist regions* of $D(K)$.

Proof of Theorem. From Proposition 5.4.1 and Proposition 5.4.2, we have already seen that $D(K)$ is connected and prime with $t(D) \geq 2(n-1)$ twist regions. Furthermore, once it is shown that $D(K)$ is A-adequate and satisfies the TELC, then the conclusion that K is hyperbolic will follow from Proposition 2.2.1.

To see that $D(K)$ is A-adequate, it suffices to show that no A-segment of the all-A state H_A joins an all-A circle to itself. Note that positive syllables in β (positive twist regions of

$D(K)$) A-resolve to give horizontal segments and that negative syllables in β (negative twist regions of $D(K)$) A-resolve to give vertical segments. Suppose, for a contradiction, that an A-segment joins an all-A circle to itself.

Case 1: Suppose the A-segment is a vertical segment. Condition (1), that negative exponents are at least three in absolute value, implies that it is impossible for a vertical A-segment to join an all-A circle to itself. This is because all vertical A-segments either join distinct small inner circles or join a small inner circle to a medium or a wandering circle. (See the left side of Figure 2.5.)

Case 2: Suppose the A-segment is a horizontal segment. Condition (2), that positive syllables are cyclically surrounded by negative syllables in the same adjacent generator, implies that it is impossible for a horizontal A-segment to join an all-A circle to itself. This is because all horizontal A-segments join a medium inner circle to either a wandering circle or a nonwandering circle. (See Figure 5.6.)

We will now show that $D(K)$ satisfies the TELC. Let C_1 and C_2 be two distinct all-A circles that share a pair of distinct A-segments, call them s_1 and s_2.

Case 1: Suppose one of s_1 and s_2 is a horizontal segment. By Conditions (1) and (2), it is impossible for the other segment to be a vertical segment. This is because, as in Figure 5.6, one of C_1 and C_2 must be a medium inner circle. Let us say that C_1 is a medium inner circle. This circle is adjacent, via horizontal A-segments, to the second circle C_2, which will either be a wandering circle or a nonwandering circle. The circle C_1 is also adjacent to small inner circles above and below. Therefore, since a small inner circle is neither wandering nor

nonwandering, then the second segment cannot be vertical. Thus, if one of the segments s_1 and s_2 is horizontal, then the other segment must also be horizontal. Since the horizontal segments incident to the medium inner circle C_1 necessarily belong to the same short twist region of $D(K)$, then the TELC is satisfied.

Case 2: Suppose both s_1 and s_2 are vertical segments. Since all vertical A-segments either join distinct small inner circles or join a small inner circle to a medium inner circle or a wandering circle, then one of C_1 and C_2 must be a small inner circle. But, by construction, it is impossible for a small inner circle to share more than one A-segment with another circle. Therefore, this case cannot occur.

□

5.6 State Circles of A-Adequate Closed n-Braids (where $n \geq 4$)

The goal of this section is to classify the possible types of all-A circles that can arise in the all-A state of an A-adequate closed n-braid, where $n \geq 4$ and where the braid is of the type described in Theorem 5.5.1.

Proposition 5.6.1. *Let $D(K) = \widehat{\beta}$ denote the closure of a nice n-braid $\beta = \sigma_{m_1}^{r_1} \cdots \sigma_{m_l}^{r_l}$, where $1 \leq m_1, \ldots, m_l \leq n-1$. Furthermore, assume that β satisfies the assumptions of Theorem 5.5.1 and assume that $n \geq 4$. View $D(K)$ as lying in an annular region of the plane. Then we may categorize the all-A circles of H_A into the following types:*

(1) small inner circles *that come from negative exponents $r_i \leq -2$ in the braid word β*

(2) medium inner circles *that come from cyclically isolated positive syllables in the braid word* β

(3a) essential wandering circles *that are essential in the annulus and have wandering that arises from adjacent negative syllables in the braid word* β

(3b) non-essential wandering circles *that are non-essential (contractible) in the annulus and have wandering that arises from adjacent negative syllables in the braid word* β

(4) nonwandering circles *that come from the cases when* σ_1 *or* σ_{n-1} *or an adjacent pair of generators* σ_i *and* σ_{i+1} *for* $2 \leq i \leq n-3$ *occur with only positive exponents in the braid word* β*.*

Remark 5.6.1. Note that, as compared with the $n = 3$ case of Section 5.3, we now have that a new type of wandering circle, called a non-essential wandering circle, is possible. Also note that neither the pair of generators σ_1 and σ_2 nor the pair of generators σ_{n-2} and σ_{n-1} can occur with only positive exponents. This is due to Condition (2) of Theorem 5.5.1 (the condition that positive syllables are cyclically surrounded by negative syllables in the same adjacent generator).

Proof of Proposition. With some exceptions, this proof is similar to the proof of Proposition 5.3.1. Recall that, as noted in Remark 5.5.1, β cannot be positive. Because positive syllables of β are cyclically isolated, we may decompose β as $\beta = N_1$ (in the case that β is a negative braid) or $\beta = P_1 N_1 \cdots P_t N_t$, where P_i denotes a positive syllable of β and N_i denotes a maximal length negative induced subword of β.

Small Inner Circles: Let $\sigma_i^{n'}$ denote a negative syllable. Then, except for the additional

$n-2$ vertical trivial braid string portions to the right and/or left of the twist region, the A-resolution of this syllable will look like the left side of Figure 5.7 if $n' = 2$ and look like the left side of Figure 2.5 in general. In particular, having $n' \leq -2$ is equivalent to the existence of small inner circles.

Wandering Circles: Let $\sigma_i^{n_1}\sigma_j^{n_2} = \sigma_i^{n_1+1}(\sigma_i^{-1}\sigma_j^{-1})\sigma_j^{n_2+1}$ denote a pair of adjacent negative syllables.

Suppose $\{i,j\} = \{m_q, m_{q+1}\}$. Then the pair of adjacent negative syllables involve adjacent letters (generators of B_n). Consequently, the corresponding portion of H_A will resemble the right side of Figure 5.7 (except that the long resolutions may possibly consist of longer paths of A-segments and small inner circles). The key feature of this figure is the fact that we see a portion of a wandering circle, where the wandering behavior corresponds to the existence of the $\sigma_i^{-1}\sigma_j^{-1}$ induced subword.

Suppose $\{i,j\} = \{m_q, m_{q+r}\}$, where $r \geq 2$. In this case, the pair of adjacent negative syllables involve far commuting generators of B_n. Then, except for the additional $n-4$ vertical trivial braid string portions around the two negative twist regions, we get that the A-resolution will look like two copies of the left side of Figure 2.5.

Medium Inner Circles and Nonwandering Circles: Let $\sigma_i^{-1}\sigma_j^{p}\sigma_i^{-1}$ denote a positive syllable of β that is cyclically surrounded by negative letters, where $\{i,j\} = \{m_q, m_{q+1}\}$. Note that the letters involved in this induced subword are adjacent generators of B_n. Consequently, by adding $n-3$ trivial braid string portions, the corresponding portion of H_A will resemble the center of Figure 5.7. In particular, the existence of an isolated positive syllable corresponds

to the existence of a medium inner circle. Furthermore, a nonwandering circle will occur in H_A precisely when σ_1 or σ_{n-1} or an adjacent pair of generators σ_i and σ_{i+1} for $2 \leq i \leq n-3$ occur with only positive exponents.

Note that we may classify the wandering circles in the annulus into essential and nonessential circles. Since the A-resolutions of all portions of the closure of $\beta = N_1$ and $\beta = P_1 N_1 \cdots P_t N_t$ have been considered locally and since gluing such portions together joins wandering and potential nonwandering circle portions together, then we have the desired result.

□

5.7 Computation of $-\chi(\mathbb{G}'_A)$

Recall that an other circle (OC) is an all-A circle that is not a small inner circle (so it must be a medium inner circle, a wandering circle, or a nonwandering circle). Also, recall that $t^+(D)$ denotes the number of positive (short) twist regions in $D(K)$ and $t^-(D)$ denotes the number of negative (long) twist regions in $D(K)$. To compute $-\chi(\mathbb{G}'_A)$, we will consider the cases $n = 3$ and $n \geq 4$ separately. This is because it is only in the case that $n \geq 4$ that non-essential wandering circles can exist.

Case 1: Suppose $n = 3$.

Lemma 5.7.1. *Let $D(K) = \widehat{\beta}$ denote the closure of a nice 3-braid $\beta \in B_3$. Furthermore, assume that the positive syllables of β are cyclically isolated. Then the all-A state, H_A, of $D(K)$ satisfies precisely one of the following two properties:*

(1) H_A contains exactly one nonwandering circle and no wandering circles.

(2) H_A contains exactly one wandering circle and no nonwandering circles.

Proof. Either β is alternating or β is nonalternating.

Suppose β is alternating. Then one of the braid generators must always occur with positive exponents and the other generator must always occur with negative exponents. Hence, by Proposition 5.6.1, since a generator occurs with only positive exponents, then there will be a nonwandering circle. Since only one generator occurs with only positive exponents, then there is only one such nonwandering circle. Also, since adjacent negative syllables cannot occur in β, then wandering circles cannot occur in H_A.

Suppose β is nonalternating. Since positive syllables are cyclically isolated, then the nonalternating behavior of β must come from a pair of adjacent negative syllables. This implies the existence of a wandering circle in H_A and prevents the existence of a nonwandering circle (since both generators occur once with negative exponent). Finally, since a wandering circle (which is always essential in the case that $n = 3$) "uses up" a braid string from the braid closure and since a wandering circle must wander from braid string position 1 to braid string position 3 and back before closing up, then the existence of a second such wandering circle is impossible.

□

Theorem 5.7.1. *Let $D(K) = \widehat{\beta}$, where $\beta \in B_3$ satisfies the assumptions of Theorem 5.5.1. Then:*

$$-\chi(\mathbb{G}'_A) = t^-(D) - 1 \geq \frac{1}{2} \cdot (t(D) - 1) - \frac{1}{2}.$$

Proof. Since Theorem 5.5.1 guarantees that $D(K)$ is connected, A-adequate, and satisfies the TELC, then by Lemma 3.2.1 we have that $-\chi(\mathbb{G}'_A) = t(D) - \#\{\text{OCs}\}$. By Proposition 5.3.1, we have classified the types of all-A circles. By Condition (2) of Theorem 5.5.1 (that positive syllables are cyclically isolated) and by inspecting the A-resolution of a positive twist region (see Figure 5.6), we see that the number of medium inner circles in H_A is exactly the number of positive twist regions in $D(K)$, which we have denoted by $t^+(D)$. By Lemma 5.7.1, we know that the total number of wandering circles and nonwandering circles is one. Again using the assumption that positive syllables are cyclically isolated, we have that at least half of the twist regions in $D(K)$ must be negative twist regions. Therefore, using all of what was said above (in order) gives:

$$\begin{aligned}
-\chi(\mathbb{G}'_A) &= t(D) - \#\{\text{OCs}\} \\
&= t(D) - \#\{\text{medium inner circles}\} - \#\{\text{wandering circles}\} \\
&\qquad\qquad -\#\{\text{nonwandering circles}\} \\
&= t(D) - t^+(D) - 1 \\
&= t^-(D) - 1 \\
&\geq \frac{t(D)}{2} - 1 \\
&= \frac{1}{2} \cdot (t(D) - 1) - \frac{1}{2}.
\end{aligned}$$

□

Case 2: Suppose $n \geq 4$.

Theorem 5.7.2. *For $n \geq 4$, let $D(K) = \widehat{\beta}$, where $\beta \in B_n$ satisfies the assumptions of Theorem 5.5.1. Let m denote the number of non-essential wandering circles in the all-A state H_A of $D(K)$. Then:*

$$-\chi(\mathbb{G}'_A) \geq t^-(D) - (n+m-2) \geq \frac{1}{2} \cdot (t(D)-1) - \frac{1}{2} \cdot (2(n+m)-5).$$

Proof. By applying Lemma 3.2.1, we have that:

$$-\chi(\mathbb{G}'_A) = t(D) - \#\{\text{OCs}\}.$$

By Proposition 5.6.1, we have classified the types of all-A circles. As discussed in the proof of Theorem 5.7.1, the number of medium inner circles in H_A is exactly the number of positive twist regions in $D(K)$ and at least half of the twist regions in $D(K)$ must be negative twist regions. Since Condition (2) of Theorem 5.5.1 implies that β is not a positive braid, then there must be at least one negative syllable in the braid word. Also, note that both essential wandering circles and nonwandering circles "use up" a braid string from the braid closure. The previous two facts imply that:

$$\#\{\text{essential wandering circles}\} + \#\{\text{nonwandering circles}\} \leq n-2.$$

Therefore, using all of what was said above gives:

$$
\begin{aligned}
-\chi(\mathbb{G}'_A) &= t(D) - \#\{\text{OCs}\} \\
&= t(D) - \#\{\text{medium inner circles}\} - \#\{\text{non-essential wandering circles}\} \\
&\qquad -\#\{\text{essential wandering circles}\} - \#\{\text{nonwandering circles}\} \\
&\geq t(D) - t^{+}(D) - m - (n-2) \\
&= t^{-}(D) - (n+m-2) \\
&\geq \frac{t(D)}{2} - (n+m-2) \\
&= \frac{1}{2} \cdot (t(D)-1) - \frac{1}{2} \cdot (2(n+m)-5).
\end{aligned}
$$

□

Remark 5.7.1. Recall that, by Proposition 5.4.2, we have that $t(D) \geq 2(n-1)$. Since at least half of the twist regions of $D(K)$ are negative, then:

$$t^{-}(D) \geq \frac{t(D)}{2} \geq n-1,$$

which gives that:

$$-\chi(\mathbb{G}'_A) \geq t^{-}(D) - (n+m-2) \geq 1-m.$$

Note in particular that, for $m = 0$, we are able to conclude that the lower bound, $-v_8 \cdot \chi(\mathbb{G}'_A)$, on volume given by Theorem 2.2.2 will be positive.

5.8 Applying the Main Theorem to Closed Braids

In this section, we apply the Main Theorem (Theorem 3.4.1) to obtain volume bounds for the family of closed braids considered in Theorem 5.5.1.

Proposition 5.8.1. *Applying Theorem 3.4.1 to the closed braids of Theorem 5.5.1, we get that:*

$$\frac{v_8}{3} \cdot (t(D) - 1) \leq \text{vol}(S^3 \backslash K) < 10v_3 \cdot (t(D) - 1)$$

in the case that $n = 3$ and get that:

$$\frac{v_8}{3} \cdot (t(D) - 1) - \frac{v_8}{3} \leq \text{vol}(S^3 \backslash K) < 10v_3 \cdot (t(D) - 1)$$

in the case that $n \geq 4$.

Proof. Recall that special circles in the all-A state H_A are other circles that are incident to A-segments from one of three possible pairs of twist region resolutions. (See Definition 2.1.6 and Figure 2.6.) Given the assumptions of Theorem 5.5.1, the all-A state circles of H_A have been classified by Proposition 5.3.1 and Proposition 5.6.1. Furthermore, we claim that medium circles, essential wandering circles, and non-essential wandering circles (which can only exist if the number of braid strings is $n \geq 4$) must all be incident to A-segments from three or more distinct twist region resolutions. To see why this is true for medium inner circles, see the center of Figure 5.7. To see why this is true for wandering circles, note that wandering circles must wander at least twice (wandering and wandering back) to be able to

return to the same braid string position and close up. Therefore, the image on the right side of Figure 5.7 occurs at least twice per wandering circle and the claim can now seen to be true for wandering circles. Thus, we have that medium inner circles and wandering circles cannot be special circles. It is possible, however, for a nonwandering circle to be a special circle. Given the classification of nonwandering circles in Proposition 5.3.1 and Proposition 5.6.1, we see that there are two main cases to consider.

Case 1: Suppose that σ_1 (or, symmetrically, σ_{n-1}) occurs in the braid word with only positive exponents. Then braid string 1 (or, symmetrically, braid string n) is a nonwandering circle. If this is the case, to be a special circle, the generator σ_1 (or, symmetrically, σ_{n-1}) must appear exactly twice (as a positive syllable) in the braid word.

Case 2: Suppose that an adjacent pair of generators σ_i and σ_{i+1} for $2 \leq i \leq n-3$ occur with only positive exponents. Then braid string $i+1$ is a nonwandering circle. To be a special circle, this braid string must be incident to A-segments from exactly two (positive) twist regions of $D(K)$ (which are positive syllables in β). Since β is nice, then each generator must occur at least twice nontrivially in the braid word. Therefore, since we need to have two positive syllables in σ_i and two positive syllables in σ_{i+1}, then we get a total of at least four positive twist region resolutions incident to braid string $i+1$. This prevents the nonwandering circle (braid string $i+1$) from being a special circle.

To summarize, we have shown that at most two special circles (namely braid string 1 and braid string n) are possible, so $st(D) \leq 2$. In the case that $n = 3$, Lemma 5.7.1 gives that there can only be at most one nonwandering circle and, therefore, at most one special circle. Thus, $st(D) \leq 1$ when $n = 3$. Notice that the conclusions of Theorem 5.5.1 allow us to

apply Theorem 3.4.1. Applying Theorem 3.4.1 in the case that $n = 3$, we get that:

$$\frac{v_8}{3} \cdot (t(D) - 1) \leq \text{vol}(S^3 \backslash K) < 10v_3 \cdot (t(D) - 1).$$

Applying Theorem 3.4.1 in the case that $n \geq 4$, we get that:

$$\frac{v_8}{3} \cdot (t(D) - 1) - \frac{v_8}{3} \leq \text{vol}(S^3 \backslash K) < 10v_3 \cdot (t(D) - 1).$$

□

5.9 Volume Bounds in Terms of $t(D)$ (and $t^-(D)$)

We will now use our study of A-adequate closed braids to obtain bounds on volume. Additionally, we will compare the lower bounds on volume we find to those that were found in Proposition 5.8.1 by applying Theorem 1.0.1). In doing this, we show that studying the specific structure of the closed braids considered in this paper often provides sharper lower bounds on volume.

Theorem 5.9.1. *Let $D(K) = \widehat{\beta}$ denote the closure of a nice n-braid $\beta = \sigma_{m_1}^{r_1} \cdots \sigma_{m_l}^{r_l}$, where $1 \leq m_1, \ldots, m_l \leq n - 1$. If β satisfies the conditions:*

(1) all negative exponents $r_i < 0$ in β satisfy the stronger requirement that $r_i \leq -3$, and

(2) when $r_i > 0$, we have that $r_{i-1} < 0$ and $r_{i+1} < 0$ and either $m_{i-1} = m_{i+1} = m_i + 1$ or $m_{i-1} = m_{i+1} = m_i - 1$,

then $D(K)$ is a connected, prime, A-adequate link diagram that satisfies the TELC and contains $t(D) \geq 2(n-1)$ twist regions. Furthermore, we have that K is a hyperbolic link. In the case that $n = 3$, we get the following volume bounds:

$$\frac{v_8}{2} \cdot (t(D) - 1) - \frac{v_8}{2} \leq v_8 \cdot (t^-(D) - 1) \leq \mathrm{vol}(S^3 \backslash K) < 10v_3 \cdot (t(D) - 1).$$

Suppose, in the case that $n \geq 4$, that the all-A state H_A contains m non-essential wandering circles. Then we get the following volume bounds:

$$\frac{v_8}{2} \cdot (t(D) - 1) - \frac{v_8}{2} \cdot (2(n+m) - 5) \leq v_8 \cdot (t^-(D) - (n+m-2)) \leq \mathrm{vol}(S^3 \backslash K) < 10v_3 \cdot (t(D) - 1).$$

Proof. By combining the results of Theorem 5.5.1, Theorem 2.2.2, Theorem 5.7.1, and Theorem 5.7.2, we get the desired results.

□

Let us now compare the lower bounds of Proposition 5.8.1 to those of Theorem 5.9.1. We would like to determine exactly when the lower bounds given by our study of A-adequate closed braids are an improvement over those that result from applying Theorem 3.4.1 (using Proposition 5.8.1).

In the case that $n = 3$, we have that:

$$\frac{v_8}{2} \cdot (t(D) - 1) - \frac{v_8}{2} \geq \frac{v_8}{3} \cdot (t(D) - 1)$$

is equivalent to the condition that $t(D) \geq 4 = 2(3 - 1) = 2(n - 1)$. But this condition is always satisfied because the assumption that β is nice allows us to use Proposition 5.4.2. Therefore, the lower bound found in Theorem 5.9.1 is always the same or sharper than the lower bound provided by applying Proposition 5.8.1.

In the case that $n \geq 4$, we have that:

$$\frac{v_8}{2} \cdot (t(D) - 1) - \frac{v_8}{2} \cdot (2(n + m) - 5) \geq \frac{v_8}{3} \cdot (t(D) - 1) - \frac{v_8}{3}$$

is equivalent to the condition that $t(D) \geq 6(n + m) - 16$. Therefore, the lower bound found in Theorem 5.9.1 is the same or sharper than the lower bound provided by Proposition 5.8.1 effectively when the number of twist regions is large compared to the sum, $n + m$, of the number of braid strings and number of non-essential wandering circles.

Remark 5.9.1. It is also worth mentioning that, at the cost of keeping track of both twist regions and negative twist regions, there is further potential to improve the lower bounds on volume by using the lower bounds of Theorem 5.9.1 that are expressed in terms of $t^-(D)$. This improvement will be especially noticeable when $t^-(D) - t^+(D) \geq 0$ is large.

5.10 Volume Bounds in Terms of the Colored Jones Polynomial

To conclude our study of volume bounds for hyperbolic A-adequate closed braids, we will translate our diagrammatic volume bounds (in terms of $t(D)$) to volume bounds in terms of the stable penultimate coefficient β'_K of the colored Jones polynomial.

Theorem 5.10.1. *Let $D(K) = \widehat{\beta}$ denote the closure of a nice n-braid $\beta = \sigma_{m_1}^{r_1} \cdots \sigma_{m_l}^{r_l}$, where $1 \leq m_1, \ldots, m_l \leq n-1$. If β satisfies the conditions:*

(1) all negative exponents $r_i < 0$ in β satisfy the stronger requirement that $r_i \leq -3$, and

(2) when $r_i > 0$, we have that $r_{i-1} < 0$ and $r_{i+1} < 0$ and either $m_{i-1} = m_{i+1} = m_i + 1$ or $m_{i-1} = m_{i+1} = m_i - 1$,

then $D(K)$ is a connected, prime, A-adequate link diagram that satisfies the TELC and contains $t(D) \geq 2(n-1)$ twist regions. Furthermore, we have that K is a hyperbolic link. In the case that $n = 3$, we get the following volume bounds:

$$v_8 \cdot (|\beta'_K| - 1) \leq \mathrm{vol}(S^3 \backslash K) < 20v_3 \cdot (|\beta'_K| - 1) + 10v_3.$$

Suppose, in the case that $n \geq 4$, that the all-A state H_A contains m non-essential wandering circles. Then we get the following volume bounds:

$$v_8 \cdot (|\beta'_K| - 1) \leq \mathrm{vol}(S^3 \backslash K) < 20v_3 \cdot (|\beta'_K| - 1) + 10v_3 \cdot (2(n+m) - 5).$$

Proof. The first conclusions of the theorem follow from Theorem 5.5.1. Combining Theorem 2.3.1 with Theorem 2.2.2, we get that (for all $n \geq 3$):

$$v_8 \cdot (\left|\beta'_K\right| - 1) = -v_8 \cdot \chi(\mathbb{G}'_A) \leq \text{vol}(S^3 \backslash K).$$

Consider the case when $n = 3$. Combining Theorem 2.3.1 with Theorem 5.7.1 gives:

$$\left|\beta'_K\right| = 1 - \chi(\mathbb{G}'_A) \geq 1 + \frac{1}{2} \cdot (t(D) - 1) - \frac{1}{2} = \frac{t(D)}{2},$$

which implies that:

$$t(D) - 1 \leq 2 \cdot (\left|\beta'_K\right| - 1) + 1.$$

Applying this inequality to Theorem 2.2.2, we get:

$$\text{vol}(S^3 \backslash K) < 10v_3 \cdot (t(D) - 1) \leq 20v_3 \cdot (\left|\beta'_K\right| - 1) + 10v_3.$$

This gives the first desired set of volume bounds. Now consider the case when $n \geq 4$. Combining Theorem 2.3.1 with Theorem 5.7.2 gives:

$$\left|\beta'_K\right| = 1 - \chi(\mathbb{G}'_A) \geq 1 + \frac{1}{2} \cdot (t(D) - 1) - \frac{1}{2} \cdot (2(n+m) - 5) = \frac{t(D) - 2(n+m) + 6}{2},$$

which implies that:

$$t(D) - 1 \leq 2 \cdot (\left|\beta'_K\right| - 1) + 2(n+m) - 5.$$

Applying this inequality to Theorem 2.2.2, we get:

$$\text{vol}(S^3 \backslash K) < 10v_3 \cdot (t(D) - 1) \leq 20v_3 \cdot (\left|\beta'_K\right| - 1) + 10v_3 \cdot (2(n+m) - 5).$$

This gives the second desired set of volume bounds.

□

Chapter 6

Volume Bounds for A-Adequate Closed 3-Braids in Terms of the Schreier Normal Form

6.1 The Schreier Normal Form for 3-Braids

A useful development in the history of 3-braids was the solution to the Conjugacy Problem (and, as a corollary, the Word Problem) for the 3-braid group ([25]). As it turns out, there is an explicit algorithm that produces from an arbitrary 3-braid word β a conjugate 3-braid word β' which is called the *Schreier normal form* of β. This new braid word β' is the unique representative of the conjugacy class of β. See below (or see Section 7.1 of [3]) for a modern exposition of the algorithm.

Given such an algorithm, Birman and Menasco ([3]) gave a complete classification of links that can be represented as 3-braid closures. To be more specific they showed that, up to an explicit list of exceptions, each 3-braid closure comes from a single conjugacy class. Hence, up to some exceptions, the normal form of the braid β determines the unique link type of the closed braid $\widehat{\beta}$.

Because it will be needed in what follows, we now present the algorithm (adapted from Section 7.1 of [3]) that, given a 3-braid $\beta \in B_3$, produces the Schreier normal form β' of β.

Remark 6.1.1. It is important to note that cyclic permutation (a special case of conjugacy) may be needed during the steps of this algorithm.

Schreier Normal Form Algorithm:

(1) Let $\beta \in B_3 = \langle \sigma_1, \sigma_2 \mid \sigma_1\sigma_2\sigma_1 = \sigma_2\sigma_1\sigma_2 \rangle$ be cyclically reduced into syllables.

Introduce new variables $x = (\sigma_1\sigma_2\sigma_1)^{-1}$ and $y = \sigma_1\sigma_2$. Thus we have that:

- $\sigma_1 = y^2x$
- $\sigma_2 = xy^2$
- $\sigma_1^{-1} = xy$
- $\sigma_2^{-1} = yx$

Possibly using cyclic permutation, rewrite β as a cyclically reduced word that is positive in x and y.

(2) Introduce $C = x^{-2} = y^3 \in Z(B_3)$, where $Z(B_3)$ denotes the center of the 3-braid group B_3.

By using these relations and commutativity of C as much as possible, group all powers of C at the beginning of the braid word and reduce the exponents of x and y as much as possible.

Rewrite β as:

$$\beta = C^k \eta,$$

where $k \in \mathbb{Z}$ and where η is a subword whose syllables in x have exponent at most one and whose syllables in y have exponent at most two. To be more precise, by possibly using cyclic permutation:

$$\eta = \begin{cases} (xy)^{p_1}\left(xy^2\right)^{q_1} \cdots (xy)^{p_s}\left(xy^2\right)^{q_s} & \text{for some } s, p_i, q_i \geq 1 \\ (xy)^p & \text{for some } p \geq 1 \\ \left(xy^2\right)^q & \text{for some } q \geq 1 \\ y & \\ y^2 & \\ x & \\ 1 & \end{cases}$$

(3) Possibly using cyclic permutation and the commutativity of C, rewrite β back in terms of σ_1 and σ_2 as $\beta' = C^k \eta'$, where:

$$\eta' = \begin{cases} \sigma_1^{-p_1}\sigma_2^{q_1} \cdots \sigma_1^{-p_s}\sigma_2^{q_s} & \text{for some } s, p_i, q_i \geq 1 \\ \sigma_1^p & \text{for some } p \in \mathbb{Z} \\ \sigma_1\sigma_2 & \\ \sigma_1\sigma_2\sigma_1 & \\ \sigma_1\sigma_2\sigma_1\sigma_2 & \end{cases}$$

Definition 6.1.1. We call $\beta' \in B_3$ the *Schreier normal form* of $\beta \in B_3$. The braid word β' is the unique representative of the conjugacy class of β.

Definition 6.1.2. Following [12], we will call a braid β *generic* if it has Schreier normal form

$$\beta' = C^k \sigma_1^{-p_1} \sigma_2^{q_1} \cdots \sigma_1^{-p_s} \sigma_2^{q_s}.$$

6.2 Hyperbolicity for Closed 3-Braids and Volume Bounds

Using the Schreier normal form of a 3-braid, Futer, Kalfagianni, and Purcell ([12]) classified the hyperbolic 3-braid closures. Furthermore, given such a hyperbolic closed 3-braid, they gave two-sided bounds on the volume of the link complement, expressing the volume in terms of the parameter s from the Schreier normal form of the 3-braid. Because we will compare the lower bounds on volume of this paper to those of [12], we give precise statements of the relevant results from [12] below.

Proposition 6.2.1 ([12], Theorem 5.5)**.** *Let $D(K) = \widehat{\beta}$ denote the closure of a 3-braid $\beta \in B_3$. Then K is hyperbolic if and only if:*

(1) β is generic, and

(2) β is not conjugate to $\sigma_1^p \sigma_2^q$ for any integers p and q.

Proposition 6.2.2 ([12], Theorem 5.6)**.** *Let $D(K) = \widehat{\beta}$ denote the closure of a 3-braid $\beta \in B_3$ and let β' denote the Schreier normal form of β. Then, assuming that K is hyperbolic, we have that:*

$$4v_3 \cdot s - 276.6 < \mathrm{vol}(S^3 - K) < 4v_8 \cdot s.$$

By using the more recent machinery built by the same authors in [11], we will often obtain a sharper lower bound on volume.

6.3 Volume Bounds in Terms of the Schreier Normal Form

In this section, we study the Schreier normal form of the 3-braids β given in Theorem 5.5.1.

Theorem 6.3.1. *Let $D(K) = \widehat{\beta}$ denote the closure of a nice 3-braid β, which we denote by $\beta = \sigma_i^{r_1}\sigma_j^{r_2}\cdots\sigma_i^{r_{2l-1}}\sigma_j^{r_{2l}}$, where $\{i,j\} = \{1,2\}$. Assume that β satisfies the conditions:*

(1) all negative exponents $r_i < 0$ in β satisfy the stronger requirement that $r_i \leq -3$.

(2) positive syllables are cyclically isolated.

Then β is generic with Schreier normal form $\beta' = C^k\sigma_1^{-p_1}\sigma_2^{q_1}\cdots\sigma_1^{-p_s}\sigma_2^{q_s}$, where $k \in \mathbb{Z}$ and $s, p_i, q_i \geq 1$. Furthermore, we are able to express the parameters k and s of the Schreier normal form β' in terms of the original braid β as follows:

(a) $k = -\#\left\{\text{induced products } \sigma_2^{n_2}\sigma_1^{n_1} \text{ of negative syllables of } \beta, \text{ where } n_1, n_2 \leq -3\right\}$.

(b) $s = t^-(D) = \#\{\text{negative syllables in } \beta\}$.

Note that, when looking for the induced products $\sigma_2^{n_2}\sigma_1^{n_1}$ of negative syllables of β to find k, one must look cyclically in the braid word. As an example computation, consider the

3-braid:

$$\beta = \sigma_1^3\sigma_2^{-3}\sigma_1^{-5}\sigma_2^{-3}.$$

Applying the Schreier Normal Form Algorithm, we get:

$$\begin{aligned}
\beta &= \sigma_1^3\sigma_2^{-3}\sigma_1^{-5}\sigma_2^{-3} \\
&= (y^2x)^3(yx)^3(xy)^5(yx)^3 \\
&= y^2(xy^2)^2(xy)^3(x^2)y(xy)^3(xy^2)(xy)^2x \\
&= y^2(xy^2)^2(xy)^3(C^{-1})y(xy)^3(xy^2)(xy)^2x \\
&\cong C^{-1}y^2(xy^2)^2(xy)^2(xy^2)(xy)^3(xy^2)(xy)^2x \\
&\cong C^{-1}(xy^2)^3(xy)^2(xy^2)(xy)^3(xy^2)(xy)^2 \\
&\cong C^{-1}(xy)^2(xy^2)^3(xy)^2(xy^2)(xy)^3(xy^2) \\
&= C^{-1}\sigma_1^{-2}\sigma_2^3\sigma_1^{-2}\sigma_2\sigma_1^{-3}\sigma_2 \\
&= \beta',
\end{aligned}$$

where $\cong$ denotes that either cyclic permutation or the fact that $C \in Z(B_3)$ has been used. Thus, we see that:

$$k = -1 = -\#\left\{\text{induced products } \sigma_2^{n_2}\sigma_1^{n_1} \text{ of negative syllables of } \beta, \text{ where } n_1, n_2 \leq -3\right\}$$

and:

$$s = 3 = \#\{\text{negative syllables in } \beta\}.$$

Remark 6.3.1. As a special case of the above theorem, notice that if $\beta = \sigma_i^{p_1}\sigma_j^{n_1}\cdots\sigma_i^{p_l}\sigma_j^{n_l}$ is an alternating 3-braid where $\{i,j\} = \{1,2\}$, then $k = 0$ and $s = l$.

Deferring the proof of the above theorem to the next section, we now relate s to the colored Jones polynomial of a hyperbolic A-adequate closed 3-braid from Theorem 5.5.1. In particular, we relate s to the stable penultimate coefficient β_K' of the colored Jones polynomial.

Corollary 6.3.1. *Given the assumptions of Theorem 6.3.1, we have that:*

$$s = t^-(D) = |\beta_K'|.$$

Thus, $t^-(D)$ and s are actually link invariants.

Proof. To begin, note that the assumptions of Theorem 6.3.1 are the same as those of Theorem 5.5.1 because Condition (2) of Theorem 5.5.1 can be expressed more simply for 3-braids. Theorem 5.7.1 also relies on the assumptions of Theorem 5.5.1. Using the conclusions of Theorem 5.5.1, we can apply Theorem 2.3.1, Theorem 5.7.1, and Theorem 6.3.1 respectively to get that:

$$\begin{aligned} |\beta'_K| &= 1 - \chi(\mathbb{G}'_A) \\ &= 1 + (t^-(D) - 1) \\ &= t^-(D) \\ &= s. \end{aligned}$$

Since the colored Jones polynomial and therefore its coefficients are link invariants, then we can conclude that $t^-(D)$ and s are link invariants.

□

Theorem 6.3.2. *Let $D(K) = \widehat{\beta}$ denote the closure of a nice 3-braid β, which we denote by $\beta = \sigma_i^{r_1}\sigma_j^{r_2}\cdots\sigma_i^{r_{2l-1}}\sigma_j^{r_{2l}}$, where $\{i,j\} = \{1,2\}$. Assume that β satisfies the conditions:*

(1) all negative exponents $r_i < 0$ in β satisfy the stronger requirement that $r_i \leq -3$.

(2) positive syllables are cyclically isolated.

Then $D(K)$ is a connected, prime, A-adequate link diagram that satisfies the TELC and contains $t(D) \geq 2$ twist regions. Furthermore, we have that K is a hyperbolic link and β is generic. Moreover, we get the following volume bounds:

$$v_8 \cdot (s-1) \leq \mathrm{vol}(S^3 \backslash K) < 4v_8 \cdot s.$$

Proof. By combining Theorem 5.10.1, Proposition 6.2.1, Corollary 6.3.1, and Proposition 6.2.2,

we get the desired result.

□

Remark 6.3.2. Comparing the lower bound on volume of Theorem 6.3.2 to that of Proposition 6.2.2, we get that $v_8 \cdot (s-1) \geq 4v_3 \cdot s - 276.6$ is equivalent to the condition that $s \leq \dfrac{276.6 - v_8}{4v_3 - v_8} < 689$. Therefore, the lower bound found in Theorem 6.3.2 is sharper than the lower bound provided by Proposition 6.2.2 unless the parameter s from the Schreier normal form is very large.

6.4 The Proof of Theorem 6.3.1.

Proof. By Theorem 5.5.1, we have that K is hyperbolic. By Proposition 6.2.1, this implies that β is generic. Consider the following two cases.

Case 1: Suppose β is a negative braid. Then, possibly using cyclic permutation, we may write β as $\beta = \sigma_1^{n_1}\sigma_2^{n_2}\cdots\sigma_1^{n_{2m-1}}\sigma_2^{n_{2m}}$, where $n_i \leq -3$ and the fact that β is nice forces the condition that $m \geq 2$. Applying the Schreier Normal Form Algorithm, we get:

$$\begin{aligned}
\beta &= \sigma_1^{n_1}\sigma_2^{n_2}\cdots\sigma_1^{n_{2m-1}}\sigma_2^{n_{2m}} \\
&= (xy)^{-n_1}(yx)^{-n_2}\cdots(xy)^{-n_{2m-1}}(yx)^{-n_{2m}} \\
&= (xy)^{-n_1-1}(xy^2)(xy)^{-n_2-1}(x^2)y\cdots(x^2)y(xy)^{-n_{2m-1}-2}(xy^2)(xy)^{-n_{2m}-1}x \\
&= (xy)^{-n_1-1}(xy^2)(xy)^{-n_2-1}(C^{-1})y\cdots(C^{-1})y(xy)^{-n_{2m-1}-2}(xy^2)(xy)^{-n_{2m}-1}x \\
&\cong (C^{-1})^{m-1}(xy)^{-n_1-1}(xy^2)(xy)^{-n_2-2}(xy^2)\cdots
\end{aligned}$$

$$
\begin{aligned}
& \cdots (xy^2)(xy)^{-n_{2m-1}-2}(xy^2)(xy)^{-n_{2m}-1}x \\
\cong\ & (C^{-1})^{m-1}x(xy)^{-n_1-1}(xy^2)(xy)^{-n_2-2}(xy^2)\cdots \\
& \cdots (xy^2)(xy)^{-n_{2m-1}-2}(xy^2)(xy)^{-n_{2m}-1} \\
=\ & (C^{-1})^{m-1}(x^2)y(xy)^{-n_1-2}(xy^2)(xy)^{-n_2-2}(xy^2)\cdots \\
& \cdots (xy^2)(xy)^{-n_{2m-1}-2}(xy^2)(xy)^{-n_{2m}-1} \\
=\ & (C^{-1})^{m}y(xy)^{-n_1-2}(xy^2)(xy)^{-n_2-2}(xy^2)\cdots \\
& \cdots (xy^2)(xy)^{-n_{2m-1}-2}(xy^2)(xy)^{-n_{2m}-1} \\
\cong\ & (C^{-1})^{m}(xy)^{-n_1-2}(xy^2)(xy)^{-n_2-2}(xy^2)\cdots \\
& \cdots (xy^2)(xy)^{-n_{2m-1}-2}(xy^2)(xy)^{-n_{2m}-1}y \\
=\ & (C^{-1})^{m}(xy)^{-n_1-2}(xy^2)(xy)^{-n_2-2}(xy^2)\cdots \\
& \cdots (xy^2)(xy)^{-n_{2m-1}-2}(xy^2)(xy)^{-n_{2m}-2}(xy^2) \\
=\ & (C^{-1})^{m}\sigma_1^{n_1+2}\sigma_2\sigma_1^{n_2+2}\sigma_2\cdots \\
& \cdots \sigma_2\sigma_1^{n_{2m-1}+2}\sigma_2\sigma_1^{n_{2m}+2}\sigma_2 \\
=\ & \beta',
\end{aligned}
$$

where $\cong$ denotes that cyclic permutation or the fact that $C \in Z(B_3)$ has been used. Thus, we see that:

$$k = -m = -\#\left\{\text{induced products } \sigma_2^{n_2}\sigma_1^{n_1} \text{ of negative syllables of } \beta, \text{ where } n_1, n_2 \leq -3\right\}$$

and:

$$s = 2m = \#\{\text{negative syllables in } \beta\}.$$

Recall that, when looking for the induced products $\sigma_2^{n_2}\sigma_1^{n_1}$ of negative syllables of β to find k, one must look cyclically in the braid word.

Case 2: Suppose β is not a negative braid. Then, possibly using cyclic permutation, we may write β as $\beta = P_1N_1 \cdots P_tN_t$, where P_i denotes a positive syllable of β and where N_i denotes a maximal length negative induced subword of β. Note that this decomposition arises as a result of the fact that positive syllables are assumed to be cyclically isolated.

Our strategy for the proof of this case is to apply the Schreier Normal Form Algorithm to the subwords P_iN_i, show that the theorem is locally satisfied for the P_iN_i, show that cyclic permutation is never needed in applying the algorithm to the P_iN_i, and to finally show that juxtaposing the subwords P_iN_i to form β allows the local conclusions of the theorem for the P_iN_i to combine to give the global conclusion of the theorem for β.

To begin, we list the possible subwords P_iN_i. For each subword, we consider the two possible subtypes. Let $p > 0$ be a positive exponent and let the $n_i \leq -3$ be negative exponents.

List of Types of Induced Subwords P_iN_i of β:

(1a) $\sigma_2^p\sigma_1^{n_1}$

(1b) $\sigma_1^p\sigma_2^{n_1}$

(2a) $\sigma_2^p\sigma_1^{n_1}\sigma_2^{n_2}$

(2b) $\sigma_1^p\sigma_2^{n_1}\sigma_1^{n_2}$

(3a) $\sigma_2^p \sigma_1^{n_1} \sigma_2^{n_2} \sigma_1^{n_3}$

(3b) $\sigma_1^p \sigma_2^{n_1} \sigma_1^{n_2} \sigma_2^{n_3}$

(4a) $\sigma_2^p \sigma_1^{n_1} \sigma_2^{n_2} \cdots \sigma_1^{n_{2m-1}} \sigma_2^{n_{2m}}$, where $m \geq 2$

(4b) $\sigma_1^p \sigma_2^{n_1} \sigma_1^{n_2} \cdots \sigma_2^{n_{2m-1}} \sigma_1^{n_{2m}}$, where $m \geq 2$

(5a) $\sigma_2^p \sigma_1^{n_1} \sigma_2^{n_2} \cdots \sigma_1^{n_{2m-1}} \sigma_2^{n_{2m}} \sigma_1^{n_{2m+1}}$, where $m \geq 2$

(5b) $\sigma_1^p \sigma_2^{n_1} \sigma_1^{n_2} \cdots \sigma_2^{n_{2m-1}} \sigma_1^{n_{2m}} \sigma_2^{n_{2m+1}}$, where $m \geq 2$

We now apply the Schreier Normal Form Algorithm to each (sub)type of induced subword above, implicitly showing along the way that cyclic permutation is never used during the application of the algorithm. Let k_i denote the exponent of C in the normal form for the subword $P_i N_i$. We also explicitly show that:

$$k_i = -\#\left\{\text{induced products } \sigma_2^{n_j}\sigma_1^{n_{j+1}} \text{ of negative syllables of } P_iN_i \text{ (where } n_j, n_{j+1} \leq -3)\right\}.$$

The Algorithm for Type (1a):

$$\begin{aligned} P_i N_i &= \sigma_2^p \sigma_1^{n_1} \\ &= (xy^2)^p (xy)^{-n_1} \\ &= \sigma_2^p \sigma_1^{n_1} \end{aligned}$$

Thus we get that:

$$k_i = 0$$

$$= \quad -\#\left\{\text{induced products } \sigma_2^{n_j}\sigma_1^{n_{j+1}} \text{ of negative syllables of } P_iN_i\right\}.$$

The Algorithm for Type (1b):

$$\begin{aligned} P_iN_i &= \sigma_1^p\sigma_2^{n_1} \\ &= (y^2x)^p(yx)^{-n_1} \\ &= y^2(xy^2)^{p-1}(xy)^{-n_1}x \\ &= y^2\sigma_2^{p-1}\sigma_1^{n_1}x \end{aligned}$$

Thus we get that:

$$\begin{aligned} k_i &= 0 \\ &= -\#\left\{\text{induced products } \sigma_2^{n_j}\sigma_1^{n_{j+1}} \text{ of negative syllables of } P_iN_i\right\}. \end{aligned}$$

The Algorithm for Type (2a):

$$\begin{aligned} P_iN_i &= \sigma_2^p\sigma_1^{n_1}\sigma_2^{n_2} \\ &= (xy^2)^p(xy)^{-n_1}(yx)^{-n_2} \\ &= (xy^2)^p(xy)^{-n_1-1}(xy^2)(xy)^{-n_2-1}x \\ &= \sigma_2^p\sigma_1^{n_1+1}\sigma_2\sigma_1^{n_2+1}x \end{aligned}$$

Thus we get that:

$$\begin{aligned} k_i &= 0 \\ &= -\#\left\{\text{induced products } \sigma_2^{n_j}\sigma_1^{n_{j+1}} \text{ of negative syllables of } P_iN_i\right\}. \end{aligned}$$

The Algorithm for Type (2b):

$$\begin{aligned} P_iN_i &= \sigma_1^p\sigma_2^{n_1}\sigma_1^{n_2} \\ &= (y^2x)^p(yx)^{-n_1}(xy)^{-n_2} \\ &= y^2(xy^2)^{p-1}(xy)^{-n_1}(x^2)y(xy)^{-n_2-1} \\ &= y^2(xy^2)^{p-1}(xy)^{-n_1}(C^{-1})y(xy)^{-n_2-1} \\ &\cong C^{-1}y^2(xy^2)^{p-1}(xy)^{-n_1-1}(xy^2)(xy)^{-n_2-1} \\ &= C^{-1}y^2\sigma_2^{p-1}\sigma_1^{n_1+1}\sigma_2\sigma_1^{n_2+1} \end{aligned}$$

Thus we get that:

$$\begin{aligned} k_i &= -1 \\ &= -\#\left\{\text{induced products } \sigma_2^{n_j}\sigma_1^{n_{j+1}} \text{ of negative syllables of } P_iN_i\right\}. \end{aligned}$$

The Algorithm for Type (3a):

$$\begin{aligned} P_iN_i &= \sigma_2^p\sigma_1^{n_1}\sigma_2^{n_2}\sigma_1^{n_3} \\ &= (xy^2)^p(xy)^{-n_1}(yx)^{-n_2}(xy)^{-n_3} \end{aligned}$$

$$
\begin{aligned}
&= (xy^2)^p(xy)^{-n_1-1}(xy^2)(xy)^{-n_2-1}(x^2)y(xy)^{-n_3-1} \\
&= (xy^2)^p(xy)^{-n_1-1}(xy^2)(xy)^{-n_2-1}(C^{-1})y(xy)^{-n_3-1} \\
&\cong C^{-1}(xy^2)^p(xy)^{-n_1-1}(xy^2)(xy)^{-n_2-2}(xy^2)(xy)^{-n_3-1} \\
&= C^{-1}\sigma_2^p\sigma_1^{n_1+1}\sigma_2\sigma_1^{n_2+2}\sigma_2\sigma_1^{n_3+1}
\end{aligned}
$$

Thus we get that:

$$
\begin{aligned}
k_i &= -1 \\
&= -\#\left\{\text{induced products } \sigma_2^{n_j}\sigma_1^{n_{j+1}} \text{ of negative syllables of } P_iN_i\right\}.
\end{aligned}
$$

The Algorithm for Type (3b):

$$
\begin{aligned}
P_iN_i &= \sigma_1^p\sigma_2^{n_1}\sigma_1^{n_2}\sigma_2^{n_3} \\
&= (y^2x)^p(yx)^{-n_1}(xy)^{-n_2}(yx)^{-n_3} \\
&= y^2(xy^2)^{p-1}(xy)^{-n_1}(x^2)y(xy)^{-n_2-2}(xy^2)(xy)^{-n_3-1}x \\
&= y^2(xy^2)^{p-1}(xy)^{-n_1}(C^{-1})y(xy)^{-n_2-2}(xy^2)(xy)^{-n_3-1}x \\
&\cong C^{-1}y^2(xy^2)^{p-1}(xy)^{-n_1-1}(xy^2)(xy)^{-n_2-2}(xy^2)(xy)^{-n_3-1}x \\
&= C^{-1}y^2\sigma_2^{p-1}\sigma_1^{n_1+1}\sigma_2\sigma_1^{n_2+2}\sigma_2\sigma_1^{n_3+1}x
\end{aligned}
$$

Thus we get that:

$$
\begin{aligned}
k_i &= -1 \\
&= -\#\left\{\text{induced products } \sigma_2^{n_j}\sigma_1^{n_{j+1}} \text{ of negative syllables of } P_iN_i\right\}.
\end{aligned}
$$

The Algorithm for Type (4a):

$$\begin{aligned}
P_iN_i &= \sigma_2^p\sigma_1^{n_1}\sigma_2^{n_2}\cdots\sigma_1^{n_{2m-1}}\sigma_2^{n_{2m}} \\
&= (xy^2)^p(xy)^{-n_1}(yx)^{-n_2}\cdots(xy)^{-n_{2m-1}}(yx)^{-n_{2m}} \\
&= (xy^2)^p(xy)^{-n_1-1}(xy^2)(xy)^{-n_2-1}(x^2)y\cdots \\
&\quad \cdots(x^2)y(xy)^{-n_{2m-1}-2}(xy^2)(xy)^{-n_{2m}-1}x \\
&= (xy^2)^p(xy)^{-n_1-1}(xy^2)(xy)^{-n_2-1}(C^{-1})y\cdots \\
&\quad \cdots(C^{-1})y(xy)^{-n_{2m-1}-2}(xy^2)(xy)^{-n_{2m}-1}x \\
&\cong (C^{-1})^{m-1}(xy^2)^p(xy)^{-n_1-1}(xy^2)(xy)^{-n_2-2}(xy^2)\cdots \\
&\quad \cdots(xy^2)(xy)^{-n_{2m-1}-2}(xy^2)(xy)^{-n_{2m}-1}x \\
&= (C^{-1})^{m-1}\sigma_2^p\sigma_1^{n_1+1}\sigma_2\sigma_1^{n_2+2}\sigma_2\cdots\sigma_2\sigma_1^{n_{2m-1}+2}\sigma_2\sigma_1^{n_{2m}+1}x
\end{aligned}$$

Thus we get that:

$$\begin{aligned}
k_i &= -(m-1) \\
&= -\#\left\{\text{induced products } \sigma_2^{n_j}\sigma_1^{n_{j+1}} \text{ of negative syllables of } P_iN_i\right\}.
\end{aligned}$$

The Algorithm for Type (4b):

$$\begin{aligned}
P_iN_i &= \sigma_1^p\sigma_2^{n_1}\sigma_1^{n_2}\cdots\sigma_2^{n_{2m-1}}\sigma_1^{n_{2m}} \\
&= (y^2x)^p(yx)^{-n_1}(xy)^{-n_2}\cdots(yx)^{-n_{2m-1}}(xy)^{-n_{2m}} \\
&= y^2(xy^2)^{p-1}(xy)^{-n_1}(x^2)y(xy)^{-n_2-2}(xy^2)\cdots \\
&\quad \cdots(xy^2)(xy)^{-n_{2m-1}-1}(x^2)y(xy)^{-n_{2m}-1}
\end{aligned}$$

$$
\begin{aligned}
&= y^2(xy^2)^{p-1}(xy)^{-n_1}(C^{-1})y(xy)^{-n_2-2}(xy^2)\cdots \\
&\quad \cdots(xy^2)(xy)^{-n_{2m-1}-1}(C^{-1})y(xy)^{-n_{2m}-1} \\
&\cong (C^{-1})^m y^2(xy^2)^{p-1}(xy)^{-n_1-1}(xy^2)(xy)^{-n_2-2}(xy^2)\cdots \\
&\quad \cdots(xy^2)(xy)^{-n_{2m-1}-2}(xy^2)(xy)^{-n_{2m}-1} \\
&= (C^{-1})^m y^2\sigma_2^{p-1}\sigma_1^{n_1+1}\sigma_2\sigma_1^{n_2+2}\sigma_2\cdots\sigma_2\sigma_1^{n_{2m-1}+2}\sigma_2\sigma_1^{n_{2m}+1}
\end{aligned}
$$

Thus we get that:

$$
\begin{aligned}
k_i &= -m \\
&= -\#\left\{\text{induced products } \sigma_2^{n_j}\sigma_1^{n_{j+1}} \text{ of negative syllables of } P_iN_i\right\}.
\end{aligned}
$$

The Algorithm for Type (5a):

$$
\begin{aligned}
P_iN_i &= \sigma_2^p\sigma_1^{n_1}\sigma_2^{n_2}\cdots\sigma_1^{n_{2m-1}}\sigma_2^{n_{2m}}\sigma_1^{n_{2m+1}} \\
&= (xy^2)^p(xy)^{-n_1}(yx)^{-n_2}\cdots(xy)^{-n_{2m-1}}(yx)^{-n_{2m}}(xy)^{-n_{2m+1}} \\
&= (xy^2)^p(xy)^{-n_1-1}(xy^2)(xy)^{-n_2-1}(x^2)y\cdots \\
&\quad \cdots(x^2)y(xy)^{-n_{2m-1}-2}(xy^2)(xy)^{-n_{2m}-1}(x^2)y(xy)^{-n_{2m+1}-1} \\
&= (xy^2)^p(xy)^{-n_1-1}(xy^2)(xy)^{-n_2-1}(C^{-1})y\cdots \\
&\quad \cdots(C^{-1})y(xy)^{-n_{2m-1}-2}(xy^2)(xy)^{-n_{2m}-1}(C^{-1})y(xy)^{-n_{2m+1}-1} \\
&\cong (C^{-1})^m(xy^2)^p(xy)^{-n_1-1}(xy^2)(xy)^{-n_2-2}(xy^2)\cdots \\
&\quad \cdots(xy^2)(xy)^{-n_{2m-1}-2}(xy^2)(xy)^{-n_{2m}-2}(xy^2)(xy)^{-n_{2m+1}-1} \\
&= (C^{-1})^m\sigma_2^p\sigma_1^{n_1+1}\sigma_2\sigma_1^{n_2+2}\sigma_2\cdots\sigma_2\sigma_1^{n_{2m-1}+2}\sigma_2\sigma_1^{n_{2m}+2}\sigma_2\sigma_1^{n_{2m+1}+1}
\end{aligned}
$$

Thus we get that:

$$\begin{aligned} k_i &= -m \\ &= -\#\left\{\text{induced products } \sigma_2^{n_j}\sigma_1^{n_{j+1}} \text{ of negative syllables of } P_iN_i\right\}. \end{aligned}$$

The Algorithm for Type (5b):

$$\begin{aligned} P_iN_i &= \sigma_1^p\sigma_2^{n_1}\sigma_1^{n_2}\cdots\sigma_2^{n_{2m-1}}\sigma_1^{n_{2m}}\sigma_2^{n_{2m+1}} \\ &= (y^2x)^p(yx)^{-n_1}(xy)^{-n_2}\cdots(yx)^{-n_{2m-1}}(xy)^{-n_{2m}}(yx)^{-n_{2m+1}} \\ &= y^2(xy^2)^{p-1}(xy)^{-n_1}(x^2)y(xy)^{-n_2-2}(xy^2)\cdots \\ &\quad \cdots(xy^2)(xy)^{-n_{2m-1}-1}(x^2)y(xy)^{-n_{2m}-2}(xy^2)(xy)^{-n_{2m+1}-1}x \\ &= y^2(xy^2)^{p-1}(xy)^{-n_1}(C^{-1})y(xy)^{-n_2-2}(xy^2)\cdots \\ &\quad \cdots(xy^2)(xy)^{-n_{2m-1}-1}(C^{-1})y(xy)^{-n_{2m}-2}(xy^2)(xy)^{-n_{2m+1}-1}x \\ &\cong (C^{-1})^m y^2(xy^2)^{p-1}(xy)^{-n_1-1}(xy^2)(xy)^{-n_2-2}(xy^2)\cdots \\ &\quad \cdots(xy^2)(xy)^{-n_{2m-1}-2}(xy^2)(xy)^{-n_{2m}-2}(xy^2)(xy)^{-n_{2m+1}-1}x \\ &= (C^{-1})^m y^2\sigma_2^{p-1}\sigma_1^{n_1+1}\sigma_2\sigma_1^{n_2+2}\sigma_2\cdots\sigma_2\sigma_1^{n_{2m-1}+2}\sigma_2\sigma_1^{n_{2m}+2}\sigma_2\sigma_1^{n_{2m+1}+1}x \end{aligned}$$

Thus we get that:

$$\begin{aligned} k_i &= -m \\ &= -\#\left\{\text{induced products } \sigma_2^{n_j}\sigma_1^{n_{j+1}} \text{ of negative syllables of } P_iN_i\right\}. \end{aligned}$$

It is very important to notice that, in all the the cases above, the application of the Schreier

Normal Form Algorithm to each of the induced subword types P_iN_i does **not** ever require cyclic permutation. This is very important because the goal is to juxtapose the normal forms of the induced subwords P_iN_i and claim that this gives, after some minor modifications, the normal form of the full braid word β. To summarize, below is the list of normal forms of the induced subwords P_iN_i of β (as computed above).

List of Normal Forms of Induced Subwords P_iN_i of β:

(1a) $\sigma_2^p\sigma_1^{n_1}$

(1b) $\mathbf{y^2}\sigma_2^{p-1}\sigma_1^{n_1}\mathbf{x}$

(2a) $\sigma_2^p\sigma_1^{n_1+1}\sigma_2\sigma_1^{n_2+1}\mathbf{x}$

(2b) $C^{-1}\mathbf{y^2}\sigma_2^{p-1}\sigma_1^{n_1+1}\sigma_2\sigma_1^{n_2+1}$

(3a) $C^{-1}\sigma_2^p\sigma_1^{n_1+1}\sigma_2\sigma_1^{n_2+2}\sigma_2\sigma_1^{n_3+1}$

(3b) $C^{-1}\mathbf{y^2}\sigma_2^{p-1}\sigma_1^{n_1+1}\sigma_2\sigma_1^{n_2+2}\sigma_2\sigma_1^{-n_3-1}\mathbf{x}$

(4a) $(C^{-1})^{m-1}\sigma_2^p\sigma_1^{n_1+1}\sigma_2\sigma_1^{n_2+2}\sigma_2\cdots\sigma_2\sigma_1^{n_{2m-1}+2}\sigma_2\sigma_1^{n_{2m}+1}\mathbf{x}$, where $m \geq 2$

(4b) $(C^{-1})^m\mathbf{y^2}\sigma_2^{p-1}\sigma_1^{n_1+1}\sigma_2\sigma_1^{n_2+2}\sigma_2\cdots\sigma_2\sigma_1^{n_{2m-1}+2}\sigma_2\sigma_1^{n_{2m}+1}$, where $m \geq 2$

(5a) $(C^{-1})^m\sigma_2^p\sigma_1^{n_1+1}\sigma_2\sigma_1^{n_2+2}\sigma_2\cdots$
$\cdots\sigma_2\sigma_1^{n_{2m-1}+2}\sigma_2\sigma_1^{n_{2m}+2}\sigma_2\sigma_1^{n_{2m+1}+1}$, where $m \geq 2$

(5b) $(C^{-1})^m\mathbf{y^2}\sigma_2^{p-1}\sigma_1^{n_1+1}\sigma_2\sigma_1^{n_2+2}\sigma_2\cdots$
$\cdots\sigma_2\sigma_1^{n_{2m-1}+2}\sigma_2\sigma_1^{n_{2m}+2}\sigma_2\sigma_1^{n_{2m+1}+1}\mathbf{x}$, where $m \geq 2$

Let us now consider which types of induced subwords $P_{i+1}N_{i+1}$ can (cyclically) follow a given induced subword P_iN_i. Since β is assumed to be cyclically reduced into syllables and

since the the induced subwords P_iN_i contain unbroken syllables of β, then we get that:

- Induced subwords of Types (1), (3), and (5) can be followed by any of the five subwords, so long as they are of the same subtype.
- Induced subwords of Types (2) and (4) can be followed by any of the five subwords, so long as they are of different subtype.

See the "List of Types of Induced Subwords P_iN_i of β" to verify these claims. As an example, we have that an induced subword of Type (1a) can be followed by an induced subword of Type (2a) but can **not** be followed by a subword of Type (2b). On the other hand, an induced subword of Type (2a) can be followed by an induced subword of Type (5b) but can **not** be followed by a subword of Type (5a).

Recall that $C \in Z(B_3)$ commutes with the generators of B_3. Thus, when juxtaposing the normal form of P_iN_i with the normal form of $P_{i+1}N_{i+1}$, we may move the factor $C^{k_{i+1}}$ out of the way, moving it from between the normal forms to the beginning of the normal form of P_iN_i. This fact will be utilized below.

Looking now at the "List of Normal Forms of Induced Subwords P_iN_i of β", notice that half of the normal forms may potentially contain the variable $\mathbf{x}$ at the end of the word and half of the normal forms may contain the expression $\mathbf{y^2}\sigma_2^{p-1}$ at the beginning of the word (immediately after the C^{k_i} term that will be moved out of the way). We can now see that juxtaposing the normal form of P_iN_i with that of $P_{i+1}N_{i+1}$ either:

(1) involves neither $\mathbf{x}$ at the end of the normal form of P_iN_i nor $\mathbf{y^2}$ at the beginning of the normal form of $P_{i+1}N_{i+1}$, or

(2) involves (after moving $C^{k_{i+1}}$ out of the way) both an $\mathbf{x}$ at the end of the normal form of P_iN_i and a $\mathbf{y^2}\sigma_2^{p-1}$ at the beginning of the normal form of $P_{i+1}N_{i+1}$.

Consequently, upon juxtaposing the normal forms of all of the induced subwords together, we see that all factors $\mathbf{x}$ and $\mathbf{y^2}\sigma_2^{p-1}$ in the list of normal forms combine to form

$$\mathbf{xy^2}\sigma_2^{p-1} = \boldsymbol{\sigma_2}\sigma_2^{p-1} = \sigma_2^p.$$

Note, in particular, that juxtaposing the normal form of P_iN_i with that of $P_{i+1}N_{i+1}$ does **not** create any new nontrivial powers of C. Therefore, since C commutes with the generators of B_3, then we may group all C^{k_i} terms together at the beginning of the normal form braid word. We also have that juxtaposing the normal form of P_iN_i with that of $P_{i+1}N_{i+1}$ does **not** create any new induced products $\sigma_2^{n_j}\sigma_1^{n_{j+1}}$ of negative syllables. Thus, we can add the local number $-k_i$ of induced products $\sigma_2^{n_{j,i}}\sigma_1^{n_{j+1,i}}$ of negative syllables in the P_iN_i together to get the global number of such subwords. With this information, we are now able to conclude that:

$$\begin{aligned} k &= \sum_{i=1}^{t} k_i \\ &= \sum_{i=1}^{t} -\#\left\{\text{induced products } \sigma_2^{n_{j,i}}\sigma_1^{n_{j+1,i}} \text{ of negative syllables of } P_iN_i, \text{ where } n_j, n_{j+1} \leq -3\right\} \\ &= -\#\left\{\text{induced products } \sigma_2^{n_2}\sigma_1^{n_1} \text{ of negative syllables of } \beta, \text{ where } n_1, n_2 \leq -3\right\}. \end{aligned}$$

This gives the first desired result, that the parameter k from the Schreier normal form β' can

be seen in the original braid β. To conclude the proof, we need to relate the global parameter s from the Schreier normal form to local versions of the parameter s. Let s_i denote the local version of the parameter s, which comes from the normal form for the subword P_iN_i and will be more precisely defined below.

Look again at the "List of Normal Forms of Induced Subwords P_iN_i of β". Recall that juxtaposing the normal forms to create a braid word groups together the $\mathbf{x}$ and $\mathbf{y^2}$ factors in the normal forms in such a way that they are absorbed into a trivial or positive syllable σ_2^{p-1} to form σ_2^p. Also recall that we will collect together all individual powers of C from each P_iN_i normal form and use commutativity to form a single power of C at the beginning of the normal form braid word. Thus, after juxtaposition of the normal forms of the P_iN_i, what results is a braid word that looks like $C^kW_1 \cdots W_t$, where k is an integer and W_i is an alternating word that is positive in σ_2, negative in σ_1, begins with a σ_2 syllable, and ends with a σ_1 syllable. By cyclic permutation and the commutativity of C, we get that this braid word is equivalent to the generic normal form of β.

Given an alternating subword $W_i = \sigma_2^{p_{1,i}}\sigma_1^{n_{1,i}} \cdots \sigma_2^{p_{q,i}}\sigma_1^{n_{q,i}}$ as described above, we define $s_i = q$. To provide an example, for the normal form:

$$C^{-1}\sigma_2^p\sigma_1^{n_1+1}\sigma_2\sigma_1^{n_2+2}\sigma_2\sigma_1^{n_3+2}\sigma_2\sigma_1^{n_4+1}\mathbf{x}$$

of Type (4a), we have that $s_i = 4$. Consider the product:

$$W_iW_{i+1} = (\sigma_2^{p_{1,i}}[\sigma_1^{n_{1,i}} \cdots \sigma_2^{p_{q,i}}\sigma_1^{n_{q,i}}) \cdot (\sigma_2^{p_{1,i+1}}]\sigma_1^{n_{1,i+1}} \cdots \sigma_2^{p_{q,i+1}}\sigma_1^{n_{q,i+1}}).$$

Note that the subword $[\sigma_1^{n_{1,i}} \cdots \sigma_2^{p_{q,i}} \sigma_1^{n_{q,i}} \cdot \sigma_2^{p_{1,i+1}}]$ looks like the alternating part of a generic braid word. From this perspective of (cyclically) borrowing the first syllable of the next subword, the local parameter s_i makes sense as being the local version of the global parameter s.

Returning to the above application of the Schreier Normal Form Algorithm to each subtype of induced subword P_iN_i, it can be seen that the number of negative syllables in P_iN_i is equal to s_i for the normal form of P_iN_i. Therefore, combining this fact with what we have learned above about how the juxtaposition works, we are now able to conclude that:

$$\begin{aligned} t^-(D) &= \#\{\text{negative syllables in } \beta\} \\ &= \sum_{i=1}^{t} \#\{\text{negative syllables in } P_iN_i\} \\ &= \sum_{i=1}^{t} s_i \\ &= s. \end{aligned}$$

□

Chapter 7

Volume Bounds for Hybrid Braid-Plats

After studying both closures of braids and plat closures of braids, we would now like to join these families together by considering links that have both closed braid and plat closure aspects. Such links were studied by Birman and Kanenobu in [2]. Specifically, we will use our volume bounds for plat closures and volume bounds for negative closed braids (studied in Section 9.1 of [11]) to obtain volume bounds for this new family of links, which we will call *hybrid braid-plats*.

7.1 Background on Hybrid Braid-Plats

Definition 7.1.1. Let $\beta = \sigma_{m_1}^{r_1} \cdots \sigma_{m_l}^{r_l} \in B_n$, where $1 \leq m_1, \ldots, m_l \leq n-1$, denote an n-braid diagram. From this braid diagram, we form a *hybrid braid-plat diagram* $D(K)$ by closing up the first $2p$ strands of the braid in the sense of plat closure and closing up the remaining $n-2p$ strands in the sense of braid closure.

For a schematic depiction of a hybrid braid-plat, see Figure 7.1. For an example of the all-A state H_A of a hybrid braid-plat $D(K)$, see Figure 7.2. Also, it may be useful to return to

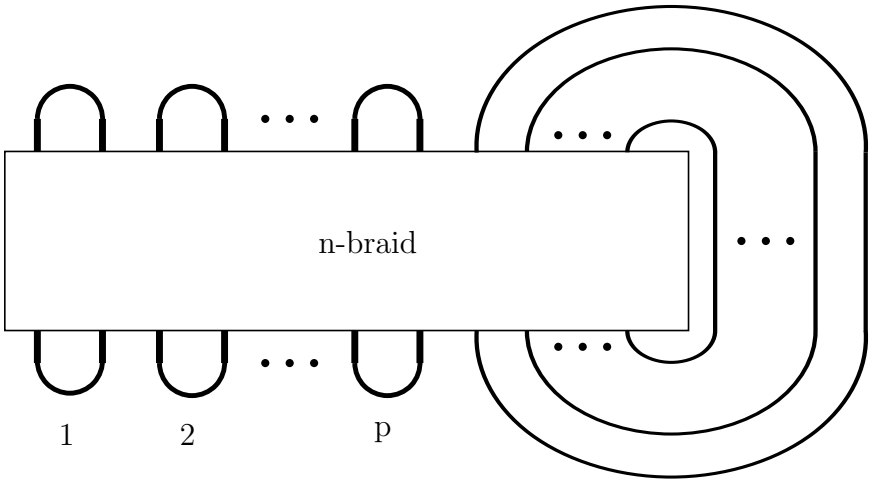

Figure 7.1: A schematic depiction of a hybrid braid-plat diagram $D(K)$.

Section 4.1 to recall both notation and the types of braids used to form the plat closures of this work.

Assumption: To strategically separate the plat information from the braid information in a hybrid braid-plat, we will need to place some restrictions on the occurrence of the generator σ_{2p} in the braid word $\beta \in B_n$. Specifically we will assume that:

(1) σ_{2p} can only occur in the braid word with positive exponents, and that

(2) a syllable in the letter σ_{2p} can only occur at most once after each braid subword $\beta_o^j = \sigma_1^{r_1^j}\sigma_3^{r_3^j}\cdots\sigma_{2p-1}^{r_{2p-1}^j}$ of the plat portion of the diagram.

Definition 7.1.2. We will call the column of positive crossings corresponding to the occurrences of σ_{2p} in β the *transitional crossing column*, and shall denote the number of (positive) twist regions in the transitional crossing column by $t(T)$.

Definition 7.1.3. Call a hybrid braid-plat *separable* if it satisfies Condition (1) and Condition (2) above.

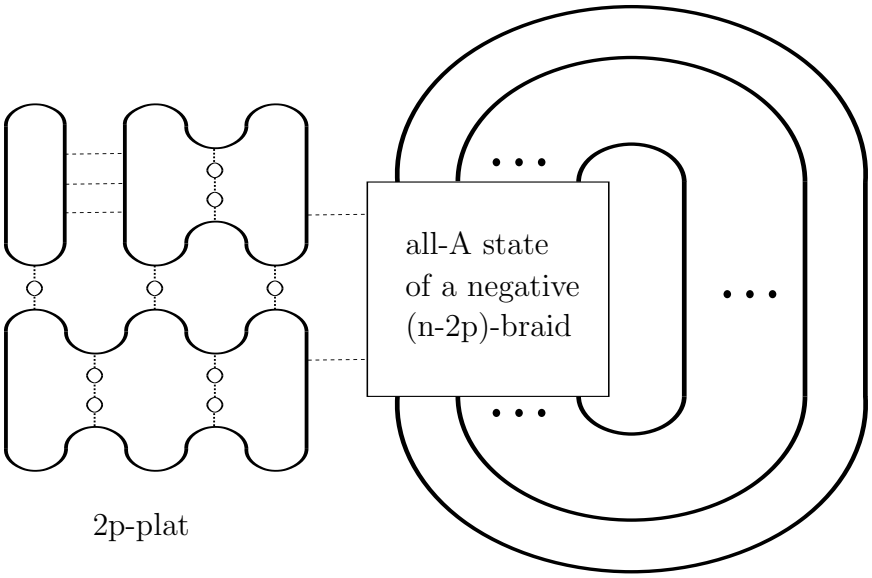

Figure 7.2: An example of the all-A state of a hybrid braid-plat.

With this new notation and terminology, we may now view the hybrid braid-plat diagram $D(K)$ as decomposed into a *plat part*, a transitional crossing column, and a *braid part*. The reason for the restriction placed on σ_{2p} is to ensure that the reduced all-A graph $\mathbb{G}'_A$ will contain a plat part reduced all-A graph and a braid part reduced all-A graph that do not share vertices and are only connected to each other via edges coming from the transitional crossing column. Consequently, we will be able to use prior work on volume bounds for closed braids and plat closures to obtain volume bounds for hybrid braid-plats.

Notation: Denote the subdiagram coming from the braid part of $D(K)$ by D_B and denote the subdiagram coming from the plat part of $D(K)$ by D_P.

Notation: Denote the reduced all-A graph of the hybrid braid-plat diagram $D(K)$ by $\mathbb{G}'_A(H)$, the reduced all-A graph of the braid part of $D(K)$ by $\mathbb{G}'_A(B)$, and the reduced all-A graph of the plat part of $D(K)$ by $\mathbb{G}'_A(P)$.

7.2 The Foundational Theorem for Hybrid Braid-Plats

In what follows, we will use the assumption (from Section 9.1 of [11]) that each (negative) twist region of the braid part contains at least three crossings. Letting r_j denote the exponent of an arbitrary generator σ_j in the braid part of $D(K)$, we may rewrite this assumption as $r_j \leq -3$.

Theorem 7.2.1. *Let $D(K)$ be a separable hybrid braid-plat diagram coming from a braid $\beta \in B_n$ with plat closure on the first $2p$ strands and braid closure on the last $n-2p$ strands. Furthermore, assume that $D(K)$ satisfies the following conditions:*

(1a) For a negative plat part, we have that $a_{i,j} \leq -3$ in odd-numbered rows and $a_{i,j} \leq -2$ in even-numbered rows.

(1b) For a mixed-sign plat part, we have that $a_{i,j} \leq -3$ or $a_{i,j} \geq 1$ in odd-numbered rows and $a_{i,j} \leq -2$ in even-numbered rows.

(2) For all plat parts, we have that $k \geq 1$, that $p \geq 3$, and that $t(D_P) \geq 2$.

(3) For all (negative) braid parts, we have that the restriction of β to $\sigma_{2p+1}, \ldots, \sigma_n$ is a nice braid, that $r_j \leq -3$ for all $2p+1 \leq j \leq n$, and that $t(D_B) \geq 2$.

(4) For the transitional crossing column, we have that $t(T) \geq 2$.

Then $D(K)$ is a connected, prime, A-adequate link diagram that satisfies the TELC and contains $t(D) \geq 6$ twist regions. Furthermore, we have that K is hyperbolic.

Proof. Since the plat part satisfies $a_{i,j} \neq 0$ for all i and j and since the braid part satisfies $|r_j| \geq 1$ for all $2p+1 \leq j \leq n$, then we have that $D(K)$ is a connected link diagram.

Since:

(1) $a_{i,j} \neq 0$ for all i and j,

(2) $k \geq 1$,

(3) $p \geq 3$,

(4) $t(T) \geq 2$, and

(5) the restriction of β to $\sigma_{2p+1}, \ldots, \sigma_n$ is a nice braid,

then we have that $D(K)$ is a prime link diagram. The first three assumptions guarantee (as shown in the proof of Theorem 4.2.1) that the plat part of the diagram will be prime. The assumption that $t(T) \geq 2$ prevents nugatory crossings from occurring between the plat part of $D(K)$ and the braid part of $D(K)$. The last assumption guarantees, by Proposition 5.4.1, that the braid part of the diagram is prime. Finally, by looking globally at the link diagram, it can be seen by inspection that the entire diagram $D(K)$ is prime.

Since:

(1) $a_{i,j} \leq -2$ or $a_{i,j} \geq 1$ in odd-numbered rows,

(2) the twist regions in the transitional crossing column are positive, and

(3) $r_j \leq -2$ for all $2p+1 \leq j \leq n$,

then we have that $D(K)$ is an A-adequate link diagram. The first assumption guarantees (as shown in the proof of Theorem 4.2.1 for negative plats and the proof of Theorem 4.4.1 for mixed-sign plats) that the plat part of the diagram is A-adequate. The second assumption guarantees that the corresponding horizontal A-segments of H_A connect pairs of distinct

all-A circles. Finally, the last assumption and Lemma 9.8 of [11] guarantee that the braid part of the diagram is A-adequate. Thus, since we have inspected the A-segments of the braid part, plat part, and transitional crossing column, then we may globally conclude that the entire hybrid braid-plat diagram $D(K)$ is A-adequate.

Since:

(1) $a_{i,j} \leq -3$ or $a_{i,j} \geq 1$ in odd-numbered rows,

(2) $a_{i,j} \leq -2$ in even-numbered rows,

(3) $r_j \leq -3$ for all $2p+1 \leq j \leq n$, and

(4) $D(K)$ is a separable hybrid braid-plat,

then we have that $D(K)$ satisfies the TELC. As seen in the proofs of Theorem 4.2.1 and Theorem 4.4.1, the first two assumptions guarantee that the TELC is satisfied for the (negative or mixed-sign) plat part of the diagram. As seen in the proof of Lemma 9.9 of [11], the third assumption guarantees that the braid part of the diagram trivially satisfies the TELC. By the last assumption, each twist region of the transitional crossing column is a (positive) short twist region and, furthermore, each other circle of the all-A state of the plat part of $D(K)$ is incident to the horizontal A-segments from at most one short twist region resolution of the transitional crossing column. (See Figure 7.2 for an example.) Consequently, we now have that $D(K)$ globally satisfies the TELC.

Next, notice that the structure of our hybrid braid-plats gives:

$$t(D) = t(D_B) + t(D_P) + t(T) \tag{7.1}$$

Since $t(D_B) \geq 2$, $t(D_P) \geq 2$, and $t(T) \geq 2$, then $t(D) \geq 6$. Hence, by what was shown above and by Proposition 2.2.1, we have that K is hyperbolic.

□

7.3 Computation of $-\chi(\mathbb{G}'_A(H))$

Lemma 7.3.1. *Given a separable hybrid braid-plat diagram $D(K)$, we have that:*

$$-\chi(\mathbb{G}'_A(H)) = -\chi(\mathbb{G}'_A(B)) - \chi(\mathbb{G}'_A(P)) + t(T).$$

Proof. By definition of $-\chi(\mathbb{G}'_A(H))$ and by Remark 2.1.2, we have that:

$$\begin{aligned} -\chi(\mathbb{G}'_A(H)) &= e(\mathbb{G}'_A(H)) - v(\mathbb{G}'_A(H)) \\ &= e(\mathbb{G}'_A(H)) - \#\left\{\text{all} - \text{A state circles}\right\}. \end{aligned}$$

Since $D(K)$ is separable, then each (positive) short twist region of the transitional crossing column corresponds to a single edge of $\mathbb{G}'_A(H)$ and, furthermore, the edges of $\mathbb{G}'_A(H)$ coming from the transitional crossing column are the only edges that join $\mathbb{G}'_A(B)$ to $\mathbb{G}'_A(P)$. Let $e(T') = t(T)$ denote the number of edges of $\mathbb{G}'_A(H)$ coming from the transitional crossing column. Putting everything together we get:

$$
\begin{aligned}
-\chi(\mathbb{G}'_A(H)) &= e(\mathbb{G}'_A(H)) - \#\{\text{all} - \text{A state circles}\} \\
&= \left[e(\mathbb{G}'_A(B)) + e(\mathbb{G}'_A(P)) + e(T')\right] - \left[v(\mathbb{G}'_A(B)) + v(\mathbb{G}'_A(P))\right] \\
&= -\chi(\mathbb{G}'_A(B)) - \chi(\mathbb{G}'_A(P)) + t(T).
\end{aligned}
$$

□

We now present a lemma from [11] that will be needed in this work:

Lemma 7.3.2 ([11], Lemma 9.1)**.** *In the notation of this work, we have that:*

$$-\chi(G'_A(B)) \geq \frac{2t(D_B)}{3}.$$

7.4 Volume Bounds in Terms of $t(D)$ and in Terms of the Colored Jones Polynomial

We now find volume bounds for the separable hybrid braid-plats considered in this work. Specifically, we first express these bounds in terms of the twist number $t(D)$ and, second, express these bounds in terms of the stable penultimate coefficient β'_K of the colored Jones polynomial.

Theorem 7.4.1. *For $D(K)$ a separable hybrid braid-plat diagram that satisfies the assumptions of Theorem 7.2.1 and that contains a negative plat part, we have that the complement of K satisfies the following volume bounds:*

$$\frac{2v_8}{3} \cdot (t(D) - 1) + v_8 \leq \mathrm{vol}(S^3 \backslash K) < 10v_3 \cdot (t(D) - 1)\,.$$

Similarly, for $D(K)$ a separable hybrid braid-plat diagram that satisfies the assumptions of Theorem 7.2.1, that contains a mixed-sign plat part, and that has mixed-sign plat part with at least as many negative twist regions as positive twist regions, we have that the complement of K satisfies the following volume bounds:

$$\frac{v_8}{3} \cdot (t(D) - 1) + \frac{4v_8}{3} \leq \mathrm{vol}(S^3 \backslash K) < 10v_3 \cdot (t(D) - 1)\,.$$

Theorem 7.4.2. *For $D(K)$ a separable hybrid braid-plat diagram that satisfies the assumptions of Theorem 7.2.1 and that contains a negative plat part, we have that the complement of K satisfies the following volume bounds:*

$$v_8 \cdot \left(\left|\beta'_K\right| - 1\right) \leq \mathrm{vol}(S^3 \backslash K) < 15v_3 \cdot (\left|\beta'_K\right| - 1) - 15v_3.$$

Similarly, for $D(K)$ a separable hybrid braid-plat diagram that satisfies the assumptions of Theorem 7.2.1, that contains a mixed-sign plat part, and that has mixed-sign plat part with at least as many negative twist regions as positive twist regions, we have that the complement of K satisfies the following volume bounds:

$$v_8 \cdot \left(\left|\beta'_K\right| - 1\right) \leq \mathrm{vol}(S^3 \backslash K) < 30v_3 \cdot (\left|\beta'_K\right| - 1) - 40v_3.$$

Combined Proof of Both Theorems. We will separate into negative plat part and mixed-sign plat part cases.

Case 1: Suppose that the plat part of $D(K)$ comes from a negative plat diagram. Recall that we have previously shown in Inequality 4.1 of the proof of Theorem 4.2.1 (in slightly different notation) that:

$$-\chi(G'_A(P)) \geq \frac{4}{5} \cdot (t(D_P) - 1) + \frac{1}{5}.$$

Then, by respectively applying Lemma 7.3.1, Lemma 7.3.2, the above inequality, Equation 7.1, and the assumptions that $t(D_P) \geq 2$ and $t(T) \geq 2$, we get:

$$\begin{aligned}
-\chi(G'_A(H)) = & -\chi(\mathbb{G}'_A(B)) - \chi(\mathbb{G}'_A(P)) + t(T) \\
& \geq \frac{2t(D_B)}{3} + \frac{4}{5} \cdot (t(D_P) - 1) + \frac{1}{5} + t(T) \\
& = \frac{10t(D_B) + 12t(D_P) - 9 + 15t(T)}{15} \\
& = \frac{10\left[t(D_B) + t(D_P) + t(T)\right] + 2t(D_P) + 5t(T) - 9}{15} \\
& = \frac{10t(D) + 2t(D_P) + 5t(T) - 9}{15} \\
& \geq \frac{2t(D) + 1}{3} \\
& = \frac{2}{3} \cdot (t(D) - 1) + 1. \qquad (7.2)
\end{aligned}$$

Since $D(K)$ satisfies the assumptions of Theorem 7.2.1, then we may apply Theorem 2.2.2 to get:

$$\frac{2v_8}{3} \cdot (t(D) - 1) + v_8 \leq \text{vol}(S^3 \backslash K) < 10v_3 \cdot (t(D) - 1)\,.$$

Transitioning to the colored Jones polynomial setting, note that Theorem 3.5.1 gives the desired lower bound on volume. Combining Theorem 2.3.1 with Inequality 7.2 gives:

$$\left|\beta'_K\right| - 1 = -\chi(G'_A(H)) \geq \frac{2}{3} \cdot (t(D) - 1) + 1.$$

Hence:

$$t(D) - 1 \leq \frac{3}{2} \cdot (\left|\beta'_K\right| - 1) - \frac{3}{2},$$

which implies that:

$$10v_3 \cdot (t(D) - 1) \leq 15v_3 \cdot (\left|\beta'_K\right| - 1) - 15v_3,$$

which gives the desired upper bound on volume.

Case 2: Suppose that the plat part of $D(K)$ comes from a mixed-sign plat diagram with at least as many negative twist regions as positive twist regions. Recall that we have previously shown in Inequality 4.3 of the proof of Theorem 4.4.1 (in slightly different notation) that:

$$-\chi(G'_A(P)) \geq \frac{1}{3} \cdot (t(D) - 1) - \frac{2}{3}.$$

Then, by respectively applying Lemma 7.3.1, Lemma 7.3.2, the above inequality, Equation 7.1, and the assumptions that $t(D_B) \geq 2$ and $t(T) \geq 2$, we get:

$$\begin{aligned}
-\chi(G'_A(H)) = \quad & -\chi(\mathbb{G}'_A(B)) - \chi(\mathbb{G}'_A(P)) + t(T) \\
\geq \quad & \frac{2t(D_B)}{3} + \frac{1}{3} \cdot (t(D_P) - 1) - \frac{2}{3} + t(T) \\
= \quad & \frac{2t(D_B) + t(D_P) - 3 + 3t(T)}{3} \\
= \quad & \frac{[t(D_B) + t(D_P) + t(T)] + t(D_B) + 2t(T) - 3}{3} \\
= \quad & \frac{t(D) + t(D_B) + 2t(T) - 3}{3} \\
\geq \quad & \frac{t(D) + 3}{3} \\
= \quad & \frac{1}{3} \cdot (t(D) - 1) + \frac{4}{3}. \qquad (7.3)
\end{aligned}$$

Since $D(K)$ satisfies the assumptions of Theorem 7.2.1, then we may apply Theorem 2.2.2 to get:

$$\frac{v_8}{3} \cdot (t(D) - 1) + \frac{4v_8}{3} \leq \mathrm{vol}(S^3 \backslash K) < 10v_3 \cdot (t(D) - 1)\,.$$

Transitioning to the colored Jones polynomial setting, note that Theorem 3.5.1 gives the desired lower bound on volume. Combining Theorem 2.3.1 with Inequality 7.3 gives:

$$\left|\beta'_K\right| - 1 = -\chi(G'_A(H)) \geq \frac{1}{3} \cdot (t(D) - 1) + \frac{4}{3}.$$

Hence:

$$t(D) - 1 \leq 3 \cdot (\left|\beta'_K\right| - 1) - 4,$$

which implies that:

$$10v_3 \cdot (t(D) - 1) \leq 30v_3 \cdot (\left|\beta'_K\right| - 1) - 40v_3,$$

which gives the desired upper bound on volume.

□

Remark 7.4.1. It should be noted that similar methods can be used to obtain volume bounds for hybrid braid-plats where the (closed) braid part comes from the closed braids considered in this work.

BIBLIOGRAPHY

BIBLIOGRAPHY

[1] Ian Agol, Peter A. Storm, and William P. Thurston. Lower bounds on volumes of hyperbolic Haken 3-manifolds. *J. Amer. Math. Soc.*, 20(4):1053–1077, 2007. With an appendix by Nathan Dunfield.

[2] Joan S. Birman and Taizo Kanenobu. Jones' braid-plat formula and a new surgery triple. *Proc. Amer. Math. Soc.*, 102(3):687–695, 1988.

[3] Joan S. Birman and William W. Menasco. Studying links via closed braids. III. Classifying links which are closed 3-braids. *Pacific J. Math.*, 161(1):25–113, 1993.

[4] Gary Chartrand and Ping Zhang. *A First Course in Graph Theory*. Dover Publications, 2012.

[5] Oliver T. Dasbach, David Futer, Efstratia Kalfagianni, Xiao-Song Lin, and Neal W. Stoltzfus. The Jones polynomial and graphs on surfaces. *J. Combin. Theory Ser. B*, 98(2):384–399, 2008.

[6] Oliver T. Dasbach and Xiao-Song Lin. On the head and the tail of the colored Jones polynomial. *Compos. Math.*, 142(5):1332–1342, 2006.

[7] Tudor Dimofte and Sergei Gukov. Quantum field theory and the volume conjecture. In *Interactions between hyperbolic geometry, quantum topology and number theory*, volume 541 of *Contemp. Math.*, pages 41–67. Amer. Math. Soc., Providence, RI, 2011.

[8] David Futer and François Guéritaud. On canonical triangulations of once-punctured torus bundles and two-bridge link complements. *Geom. Topol.*, 10:1239–1284, 2006.

[9] David Futer, Efstratia Kalfagianni, and Jessica Purcell. Hyperbolic semi-adequate links. Arxiv:1311.3008v1.

[10] David Futer, Efstratia Kalfagianni, and Jessica Purcell. Jones polynomials, volume, and essential knot surfaces: a survey. In: Proceedings of Knots in Poland III, Banach Center Publications, to appear, arXiv:1110.6388v2.

[11] David Futer, Efstratia Kalfagianni, and Jessica Purcell. *Guts of surfaces and the colored Jones polynomial*, volume 2069 of *Lecture Notes in Mathematics*. Springer, Heidelberg, 2013.

[12] David Futer, Efstratia Kalfagianni, and Jessica S. Purcell. Cusp areas of Farey manifolds and applications to knot theory. *Int. Math. Res. Not. IMRN*, 2010(23):4434–4497, 2010.

[13] Allen Hatcher. Notes on basic 3-manifold topology. www.math.cornell.edu/hatcher/3M/3Mdownloads.html.

[14] William H. Jaco and Peter B. Shalen. Seifert fibered spaces in 3-manifolds. *Mem. Amer. Math. Soc.*, 21(220):viii+192, 1979.

[15] Klaus Johannson. *Homotopy equivalences of* 3*-manifolds with boundaries*, volume 761 of *Lecture Notes in Mathematics*. Springer, Berlin, 1979.

[16] V. F. R. Jones. Hecke algebra representations of braid groups and link polynomials. *Ann. of Math. (2)*, 126(2):335–388, 1987.

[17] Vaughan F. R. Jones. A polynomial invariant for knots via von Neumann algebras [MR0766964 (86e:57006)]. In *Fields Medallists' lectures*, volume 5 of *World Sci. Ser. 20th Century Math.*, pages 448–458. World Sci. Publ., River Edge, NJ, 1997.

[18] Marc Lackenby. The volume of hyperbolic alternating link complements. *Proc. London Math. Soc. (3)*, 88(1):204–224, 2004. With an appendix by Ian Agol and Dylan Thurston.

[19] W. B. Raymond Lickorish. *An introduction to knot theory*, volume 175 of *Graduate Texts in Mathematics*. Springer-Verlag, New York, 1997.

[20] G. D. Mostow. Quasi-conformal mappings in n-space and the rigidity of hyperbolic space forms. *Inst. Hautes Études Sci. Publ. Math.*, (34):53–104, 1968.

[21] Hitoshi Murakami. An introduction to the volume conjecture. In *Interactions between hyperbolic geometry, quantum topology and number theory*, volume 541 of *Contemp. Math.*, pages 1–40. Amer. Math. Soc., Providence, RI, 2011.

[22] Makoto Ozawa. Essential state surfaces for knots and links. *J. Aust. Math. Soc.*, 91(3):391–404, 2011.

[23] Gopal Prasad. Strong rigidity of $\mathbf{Q}$-rank 1 lattices. *Invent. Math.*, 21:255–286, 1973.

[24] Kurt Reidemeister. Elementare Begründung der Knotentheorie. *Abh. Math. Sem. Univ. Hamburg*, 5(1):24–32, 1927.

[25] Otto Schreier. Über die gruppen $A^a B^b = 1$. *Abh. Math. Sem. Univ. Hamburg*, 3(1):167–169, 1924.

[26] Alexander Stoimenow. Coefficients and non-triviality of the Jones polynomial. *J. Reine Angew. Math.*, 657:1–55, 2011.

[27] William P. Thurston. Three-dimensional manifolds, Kleinian groups and hyperbolic geometry. *Bull. Amer. Math. Soc. (N.S.)*, 6(3):357–381, 1982.

[28] Vladimir Turaev. *Quantum invariants of knots and 3-manifolds*, volume 18. De Gruyter Studies in Mathematics, New York, 2010.